

Air-Sea Interactions in Earth-System Modelling

Role of Ocean Waves in an Earth-System Model.

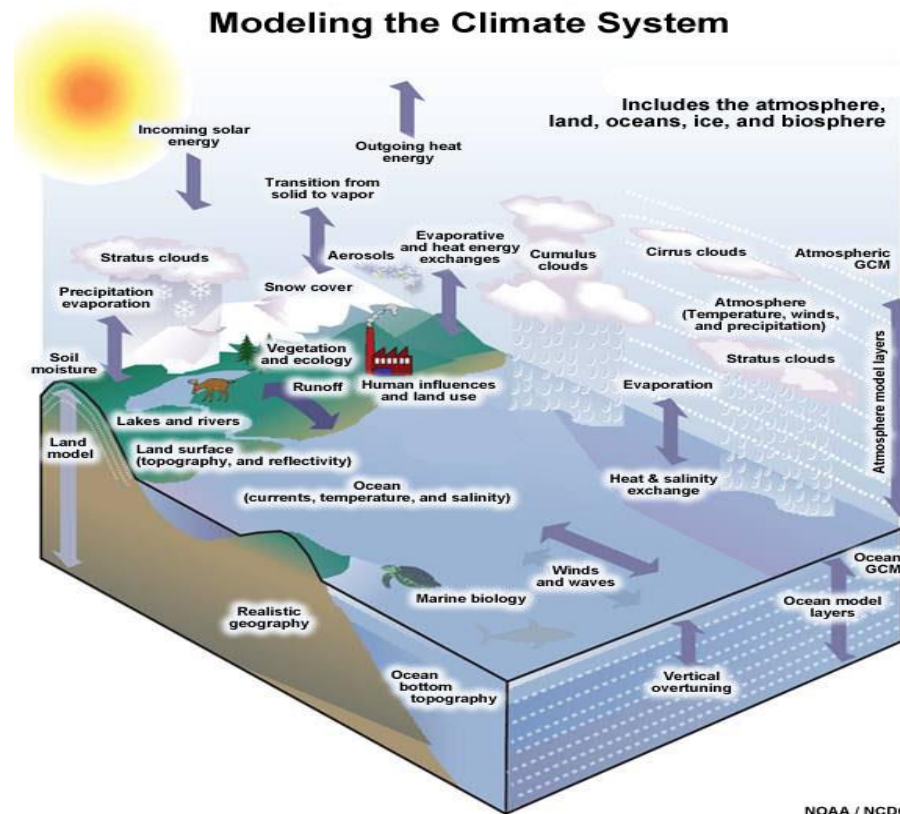
Jean-Raymond Bidlot
Coupled Processes Team

ECMWF

jean.bidlot@ecmwf.int

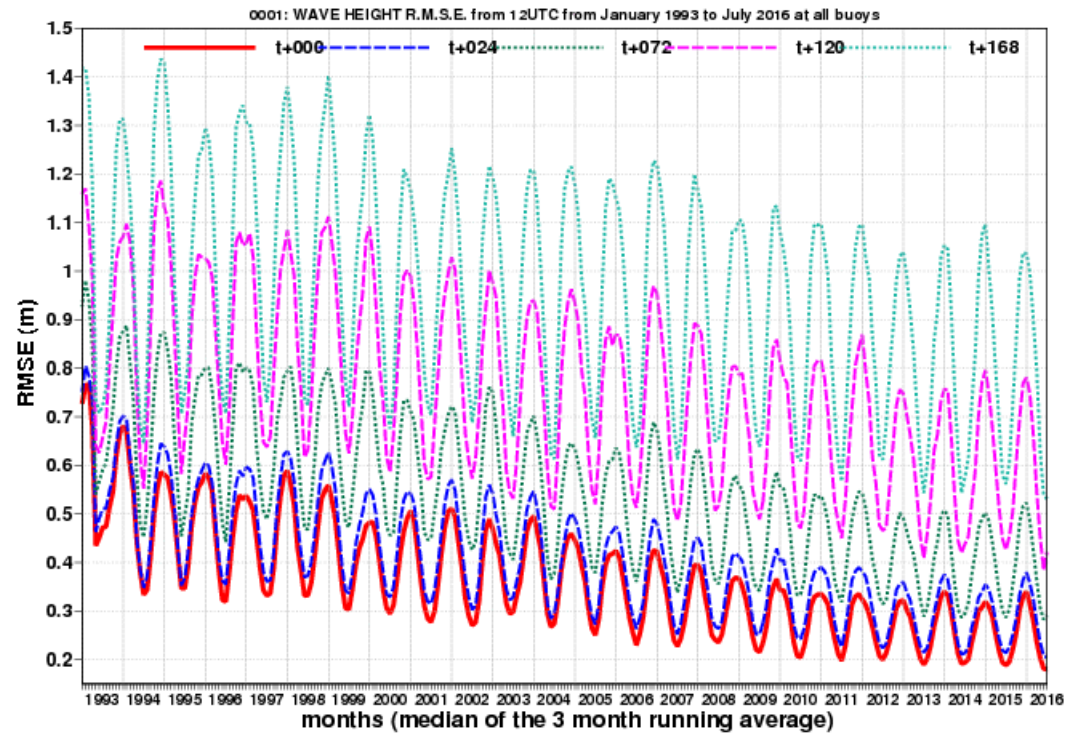
Outline

- - Wave modelling and its role in air-sea interaction.
- - Towards an Earth-System model at ECMWF.



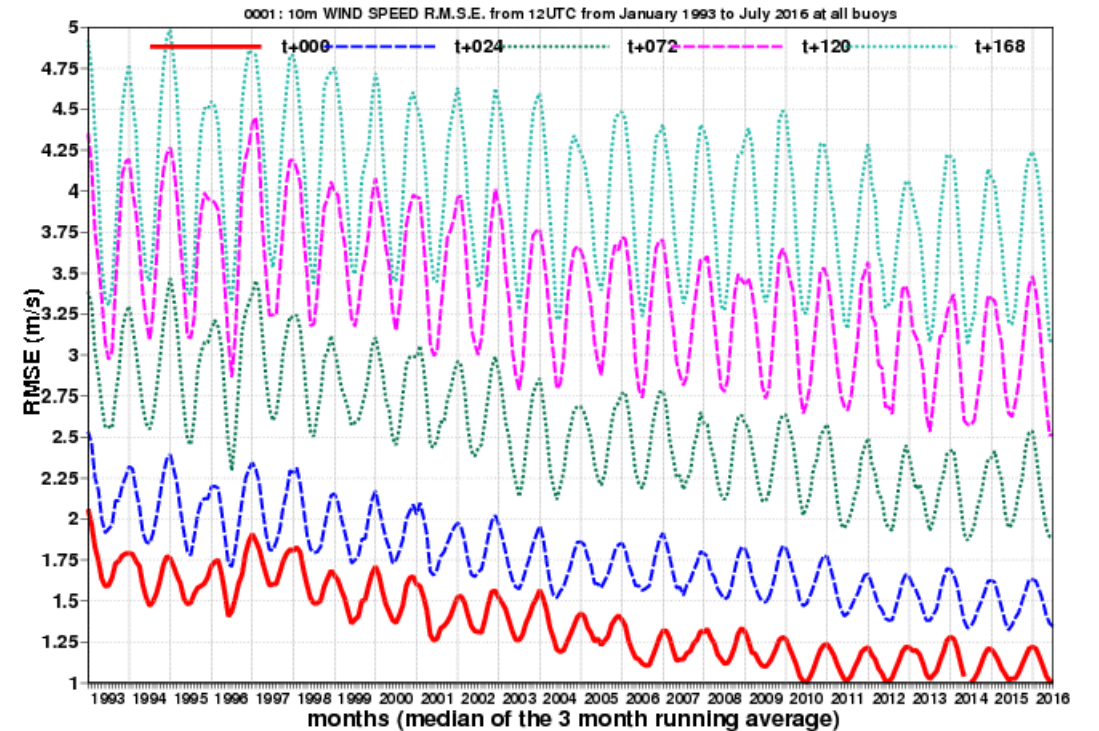
Introduction:

Comparison of ECMWF analysis and forecasts against buoy data (RMSE)



Significant wave height (SWH)

7 day FC
5 day FC
3 day FC
1 day FC
analysis

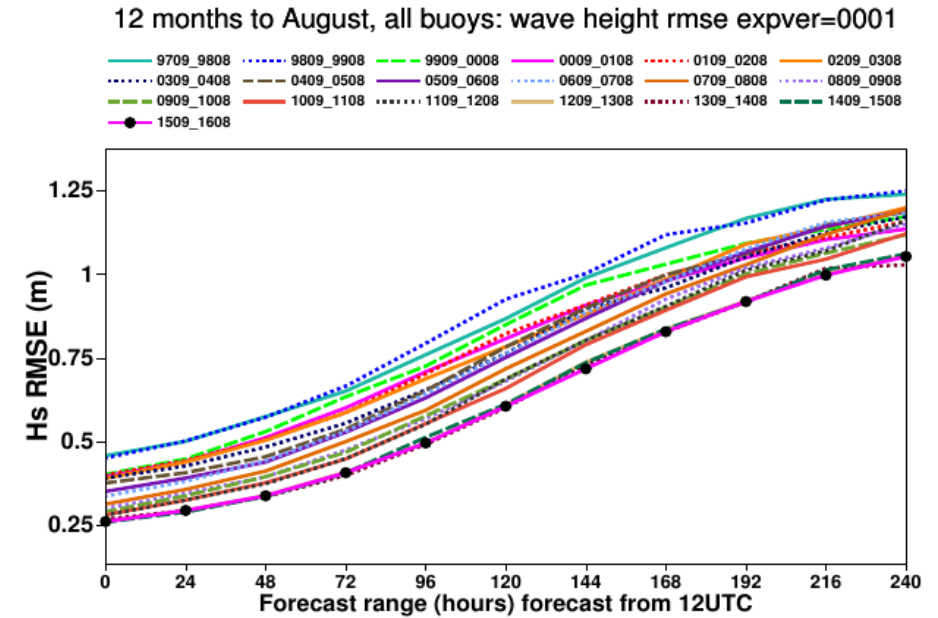


10m wind speed

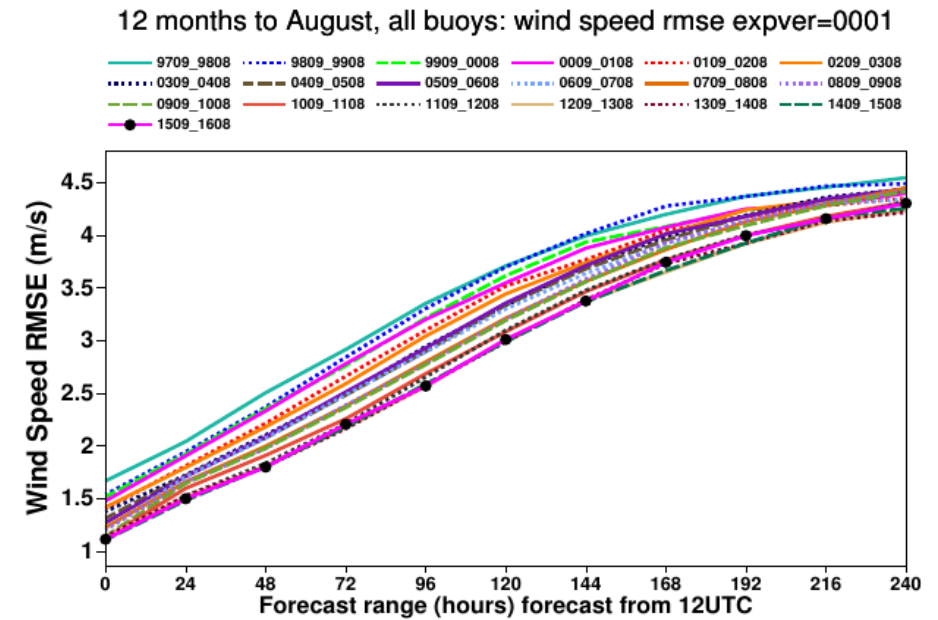
Can it be maintained?

Significant wave height (SWH)

Comparison against
buoy data
yearly statistics
since 1997



10m wind speed



ECMWF global forecast models for medium range forecasts

High resolution / Ensemble systems

Atmospheric model TCo1279/TCo639*
~9km/~18km

* Resolution as of 8 March 2016

Wave model (ECWAM) 14km/28km*

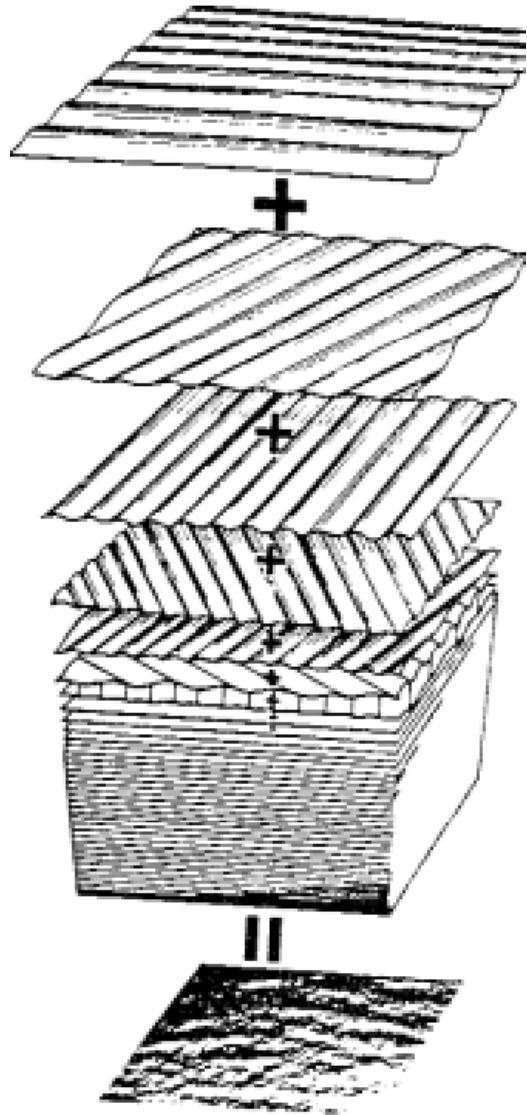
Ocean model (NEMO)

Ice model (LIM2)

ORCA1_Z42
1° in the horizontal
42 vertical levels

Twice per day, ECMWF run a high resolution forecast model up to 10 days ahead. It also runs the lower resolution system (51 forecasts) up to day 15 in order to characterise the forecast uncertainty.

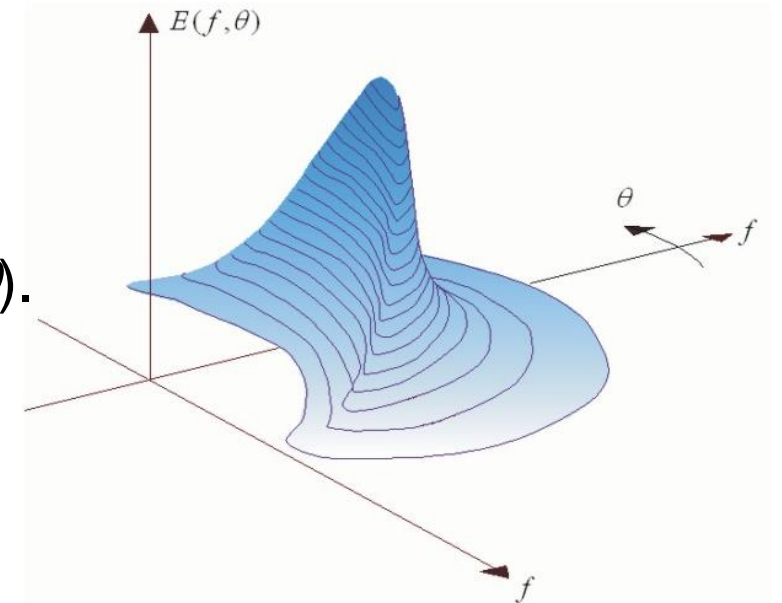
Ocean Wave Modelling: Wave Spectrum



The irregular water surface can be decomposed into a number of simple sinusoidal components with different frequencies (f) and propagation directions (θ).

The distribution of wave energy among those components is called: “wave energy spectrum”, $\rho_w g F(f, \theta)$.

water density: ρ_w and gravity: g



Ocean Wave Model

The 2-D spectrum follows from the energy balance equation (in its simplest form: deep water case):

$$\frac{\partial F}{\partial t} + \underbrace{\vec{V}_g \cdot \nabla F}_{\text{advection}} = \underbrace{S_{in}}_{\text{generation}} - \underbrace{S_{nl}}_{\text{redistribution}} + \underbrace{S_{diss}}_{\text{dissipation}}$$

Where the group velocity \mathbf{V}_g is derived from the dispersion relationship which relates frequency (f) and wave number (k) for a given water depth (D).

S_{in} : wind input source term (**generation**).

S_{nl} : non-linear 4-wave interaction (**redistribution**).

S_{diss} : dissipation term due to whitecapping (**dissipation**).

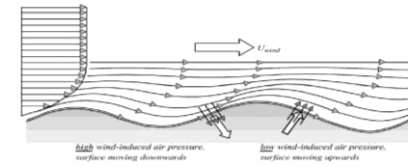


Figure 6.16. The wave-induced wind-pressure variation over a propagating harmonic wave.

the wave grows by this mechanism, the mechanism become: the wave can therefore grow faster, which in turn makes the mechanism effective, etc.

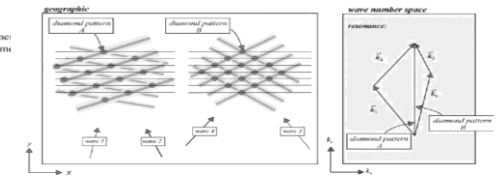
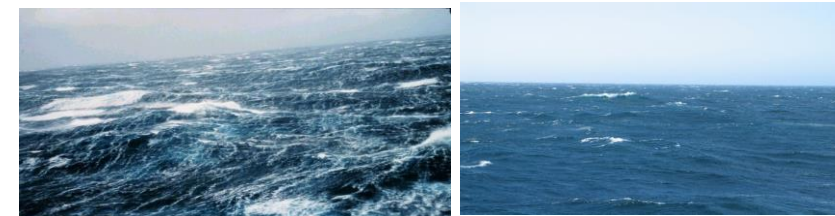


Figure 6.20. Quadruplet wave-wave interactions (realisable in deep water). Two pairs of wave components can create two diamond patterns with identical wave lengths and directions and therefore identical wave numbers. When the four waves are superimposed (not shown here), they can thus resonate. The wave-number vectors of the four wave components are shown in the right-hand panel in wave-number space with $\vec{k}_1 + \vec{k}_2 = \vec{k}_3 + \vec{k}_4$.



Wind Input and its interaction

Following Miles (1957), S_{in} depends on the surface stress $\tau = \rho_a u_*^2$ and is proportional to the wave spectrum:

$$S_{in} = \gamma F \quad \gamma \sim \frac{\rho_a}{\rho_w} \beta(z_0) \left(\frac{u_*}{c} \right)^2$$

with c the phase speed of the waves, ρ_a air density and ρ_w water density, and β is a function of z_0 the roughness length experienced by the airflow.

The wave growth by wind implies a momentum loss/drag of the airflow, in such a way that the drag is proportional to the steepness of the waves. As a consequence, for steep waves the roughness length z_0 is larger than for gentle waves.

In other words, there is a strong mutual interaction between wind and waves, where the strength of the interaction is determined by the wave-induced stress:

$$\tau_w = \frac{\rho_w}{\rho_a} g \int d\omega d\theta \frac{1}{c} S_{in} \quad \text{i.e. the momentum flux due the wind input}$$

Atmospheric model TCo1279/TCo639
9km/18km

Towards a coupled system

$$\tau = \rho_a u_*^2$$

$$U_{10} = \frac{u_*}{\kappa} \ln\left(\frac{10}{z_0}\right)$$

Neutral wind

Every IFS time step

Roughness

Charnock relation

$$z_0 = \frac{\alpha u_*^2}{g}$$

All configurations

Since 1998

Single executable

Wave model (ECWAM) 14km/28km

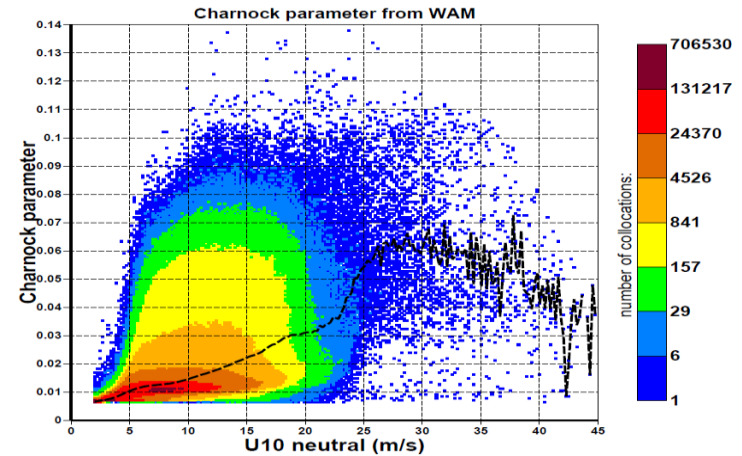
$$\alpha = \frac{\tilde{\alpha}}{\sqrt{1 - \frac{\tau_w}{\rho_a u_*^2}}}$$

If uncoupled:

$$\alpha = 0.018$$

$$\alpha = 0.10$$

$$\tau_w = \frac{\rho_w}{\rho_a} g \int d\omega d\theta \frac{1}{c} S_{in}$$

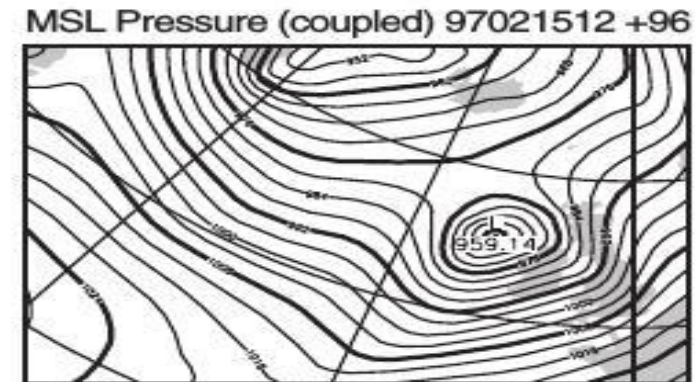
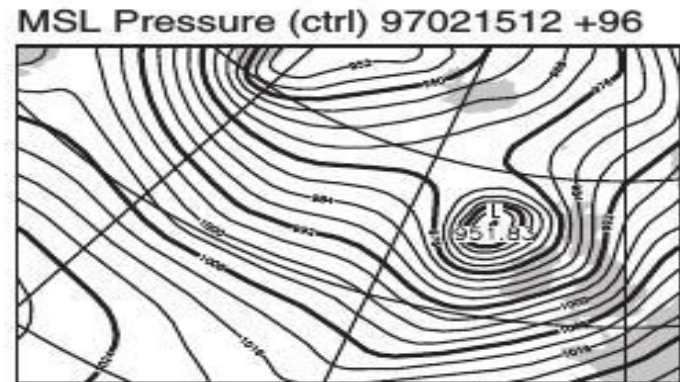


Forecast data from stream lwvv, class rd, expver gbl3, all WAM sea points from 20140702 00UTC, for steps from 3 to 168 by 3

Impact of sea state dependent momentum flux

Minimum pressure
952 hPa

uncoupled

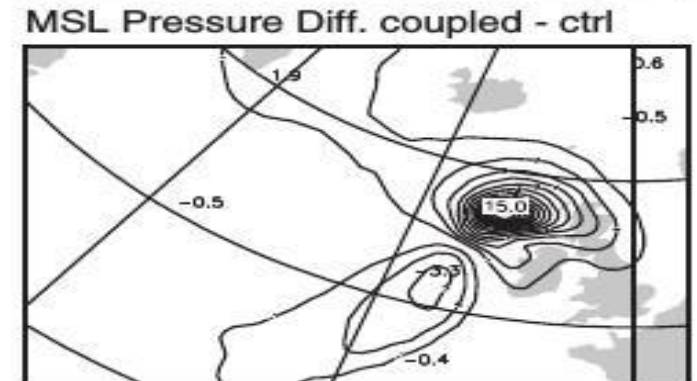
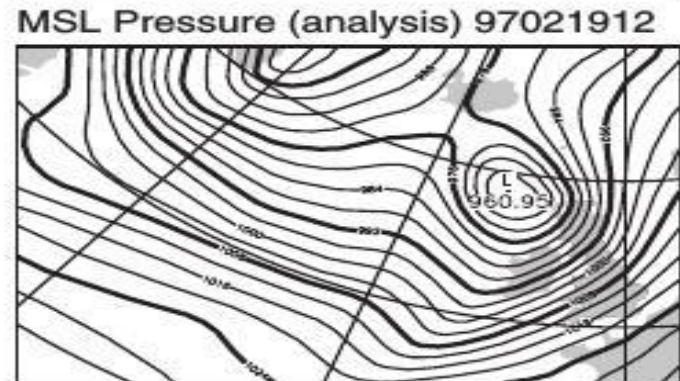


959 hPa

coupled

960 hPa

Verifying analysis



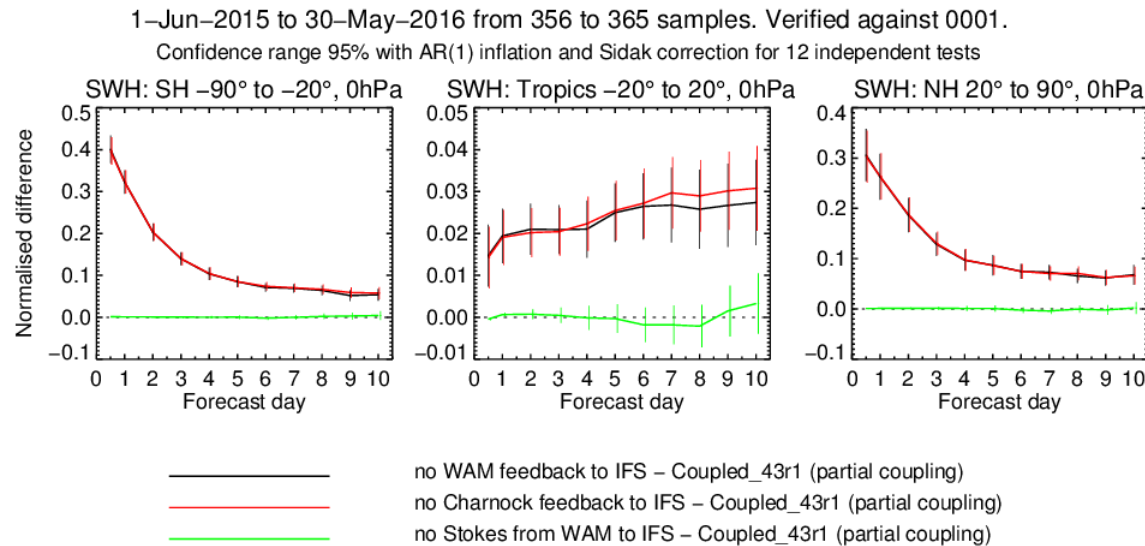
Comparison of 4-day forecast of surface pressure over the North Atlantic, valid for 19 February 1997. Version of coupled model is $T213/L31 - 0.5$ deg.

Janssen et al. 2002 and Janssen 2004

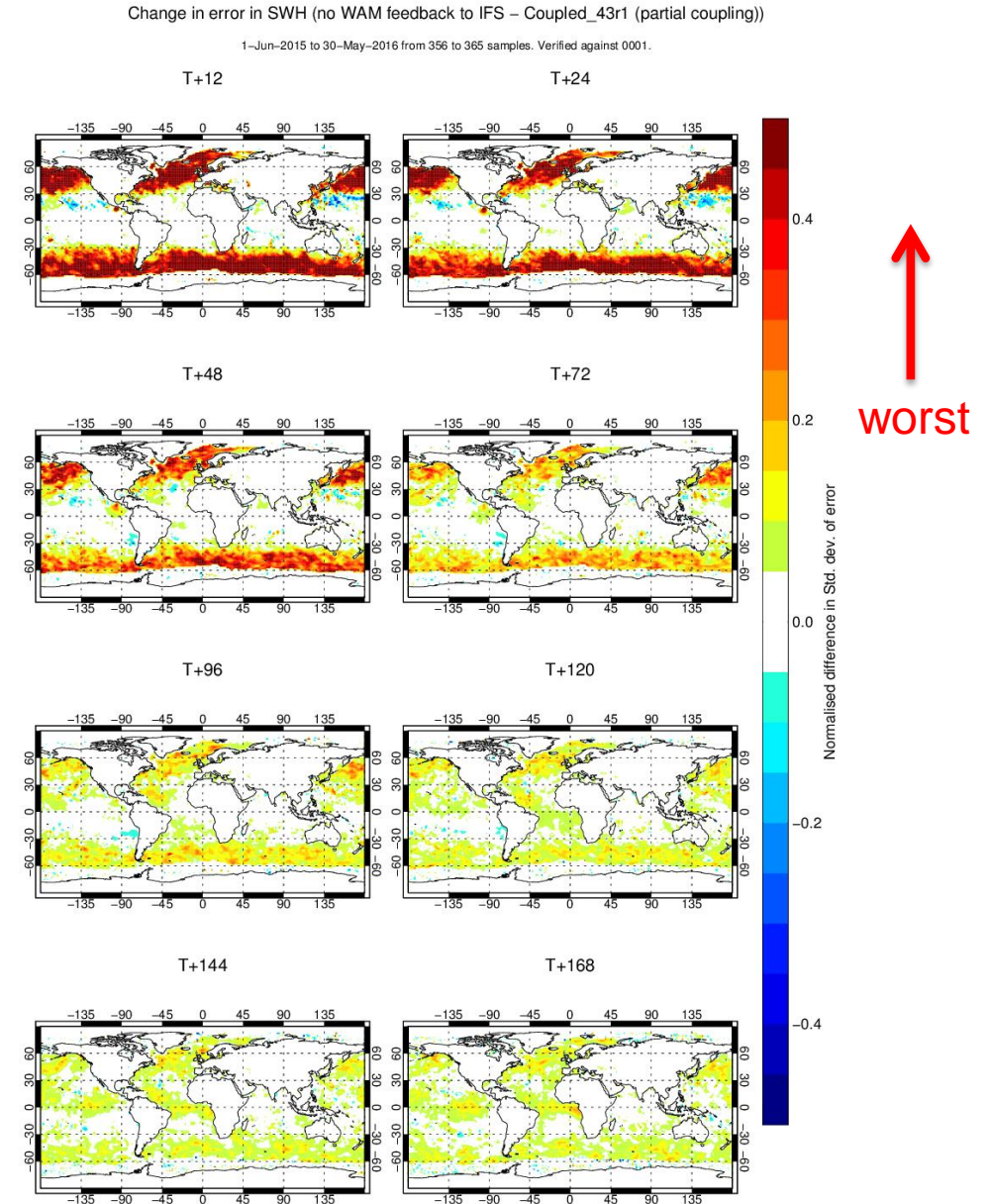
Sensitivity study: Impact of no waves feedback to the atmospheric model

We are currently performing sensitivity studies, running coupled* IFS-ECWAM-NEMO forecasts daily at Tco399 (~40km) resolution, with latest CY43R1, starting from operational analysis, from 1 June 2015 to 31 May 2016, 0 UTC. Scores are against operational analysis

Normalised difference in standard deviation of error for SWH



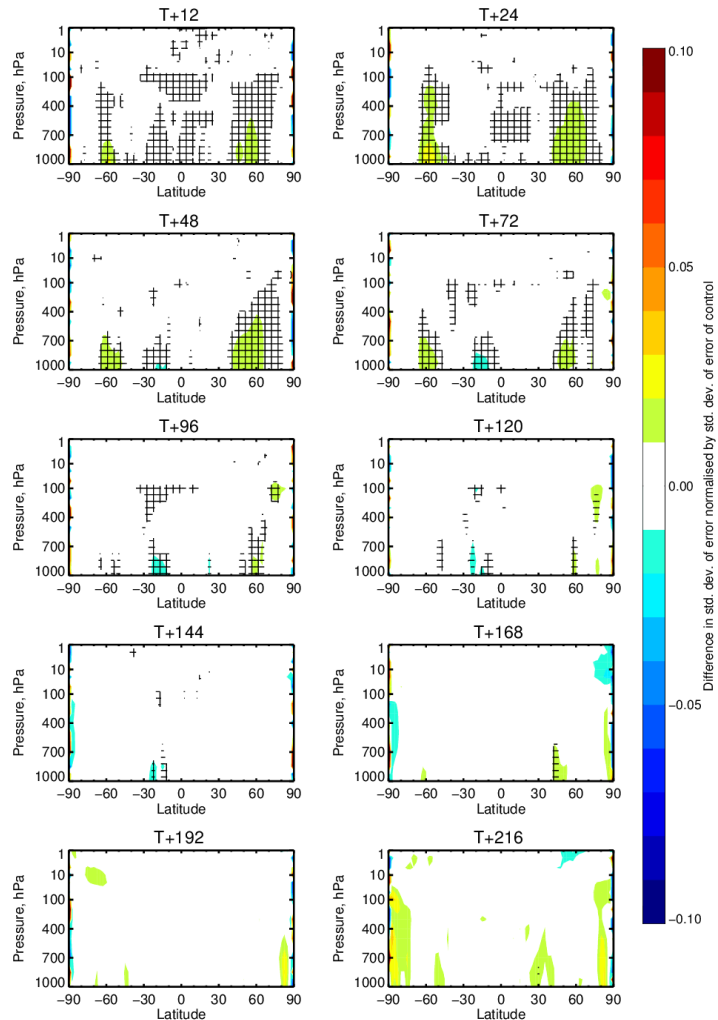
> 0
means
worst



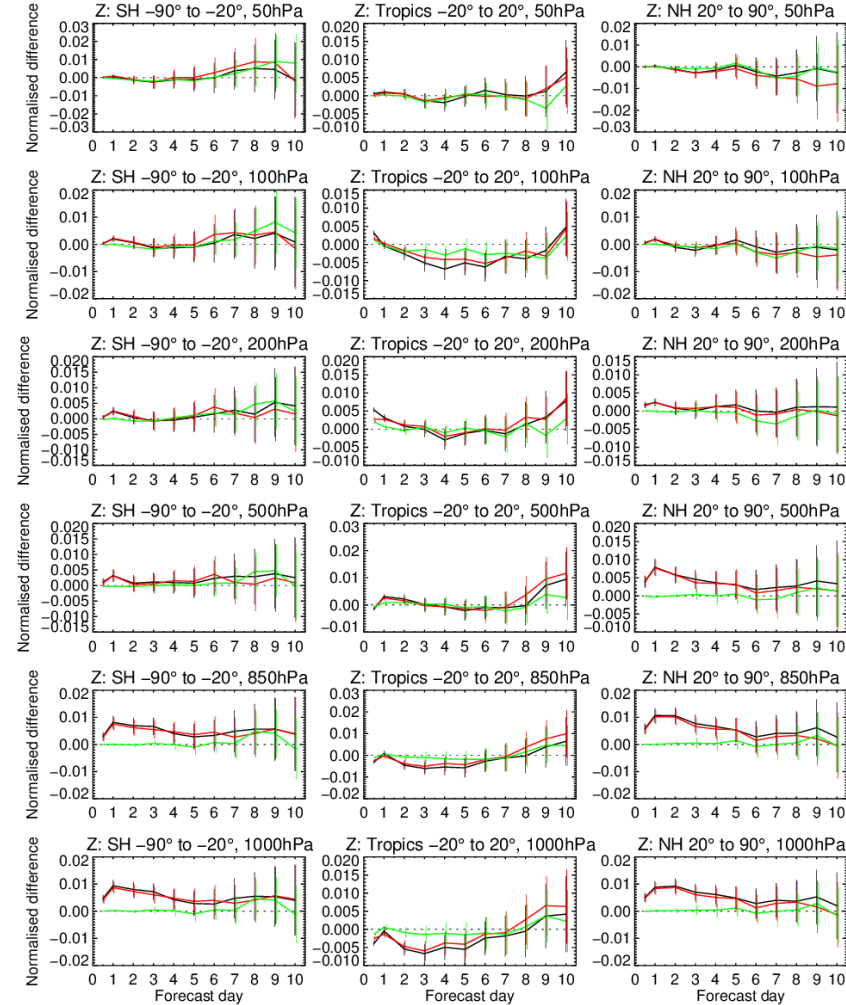
Sensitivity study: Impact of no waves feedback to the atmospheric model

Normalised difference in standard deviation of error for Z

Change in error in Z (no WAM feedback to IFS-Coupled_43r1 (partial coupling))
 1-Jun-2015 to 30-May-2016 from 356 to 365 samples. Cross-hatching indicates 95% confidence. Verified against 0001.



1-Jun-2015 to 30-May-2016 from 356 to 365 samples. Verified against 0001.
 Confidence range 95% with AR(1) inflation and Sidak correction for 12 independent tests

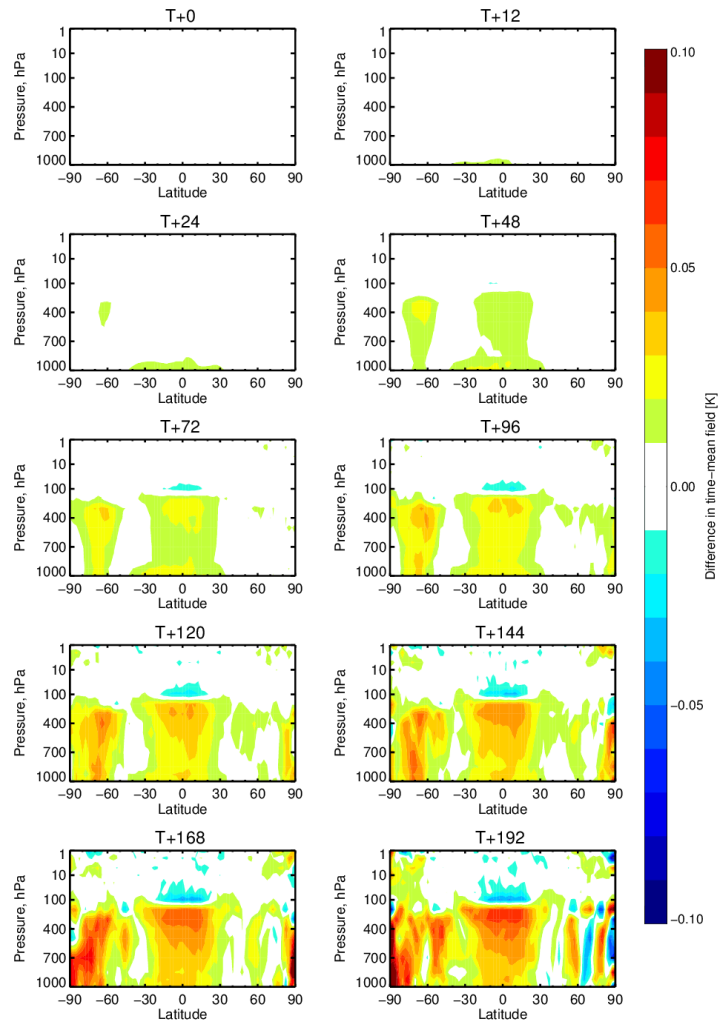


> 0
 means
 worst

Sensitivity study: Impact of no wave feedback to the atmosphere

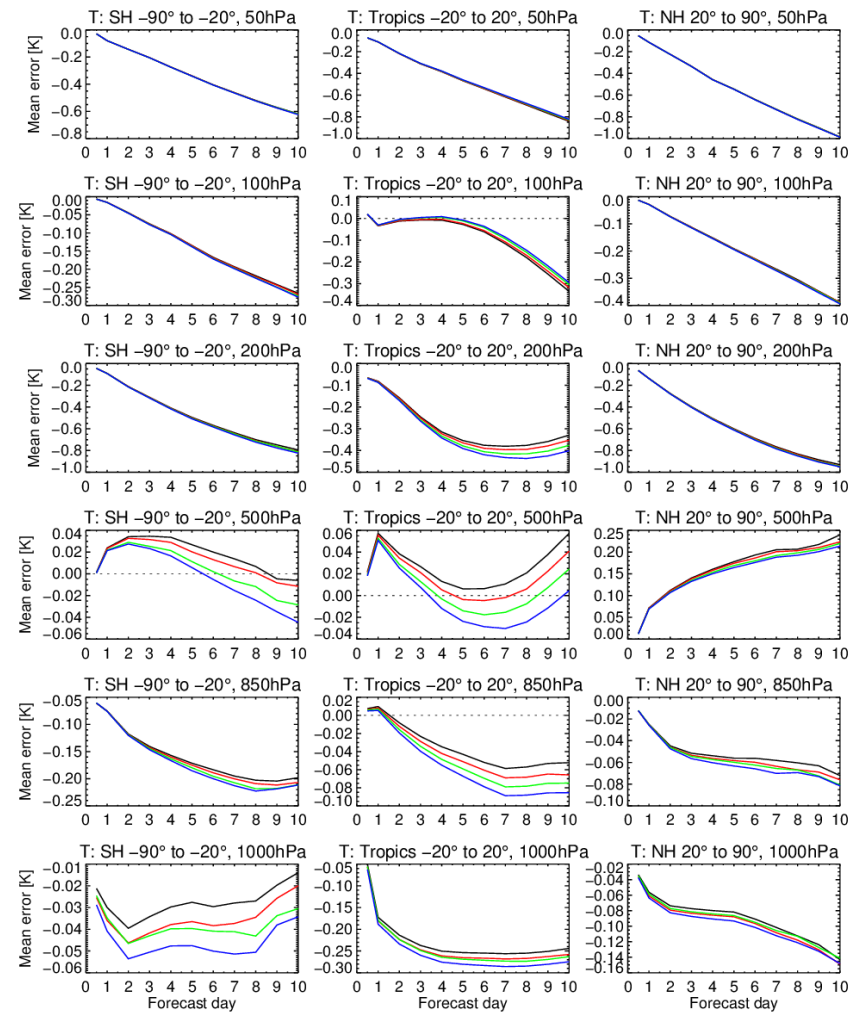
Difference in time-mean T (no WAM feedback to IFS-Coupled_43r1 (partial coupling))

11-Jun-2015 to 31-May-2016 from 356 to 356 analyses.



Mean forecast difference in T

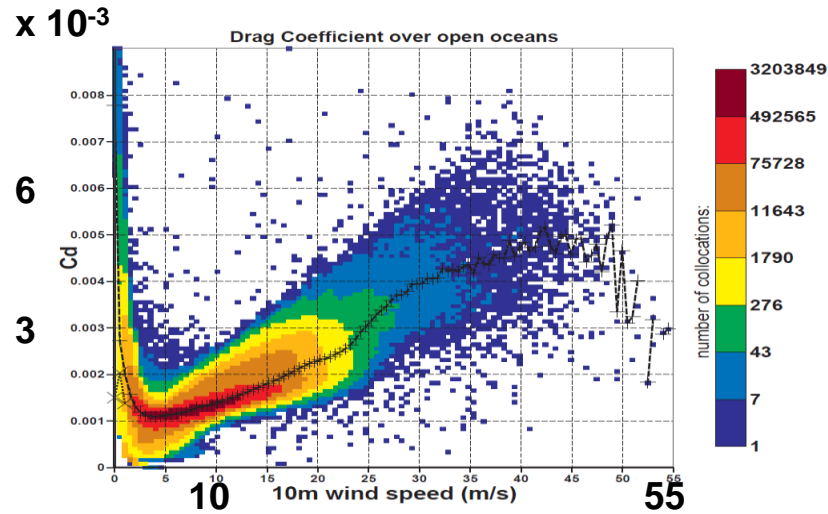
1-Jun-2015 to 30-May-2016 from 356 to 365 samples. Verified against 0001.



Mean forecast error for T

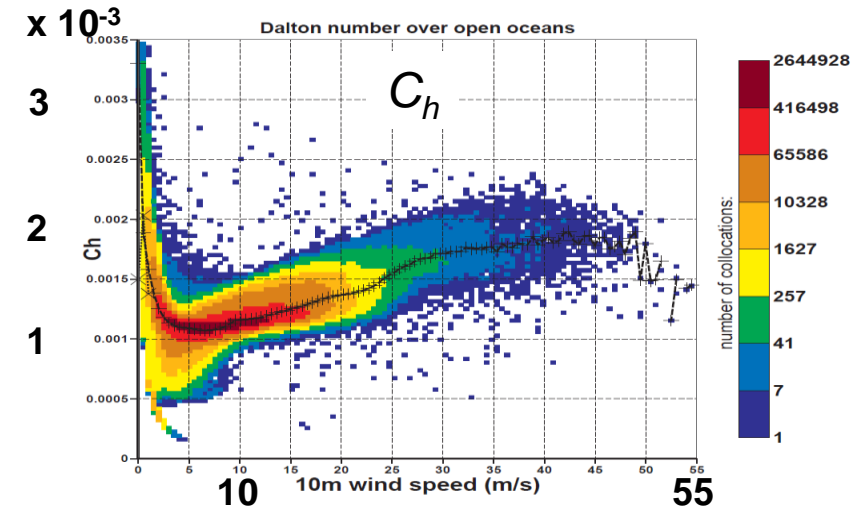
- no WAM feedback to IFS
- no Chamock feedback to IFS
- no Stokes from WAM to IFS
- Coupled_43r1 (partial coupling)

Sea state dependency on heat flux



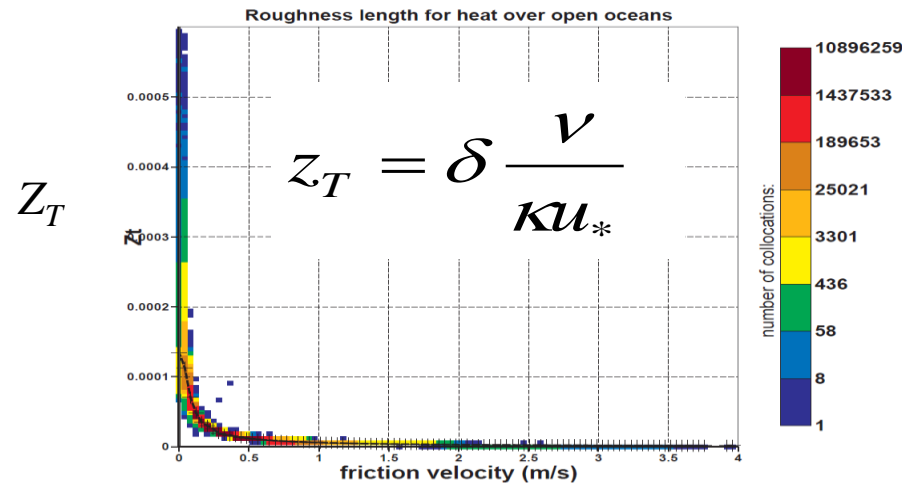
T1279 forecast
gbl3 from 20140702 step 0 to 168 by 3

Exchange coefficients
dependency on wind speed
Left: for momentum (C_d)
Right: for heat (C_h)
Forecast from 20140702
t=0 to 168 by 3
all grid points.



T1279 forecast
gbl3 from 20140702 step 0 to 168 by 3

C_d is sea state dependent



T1279 forecast
gbl3 from 20140702 step 0 to 168 by 3

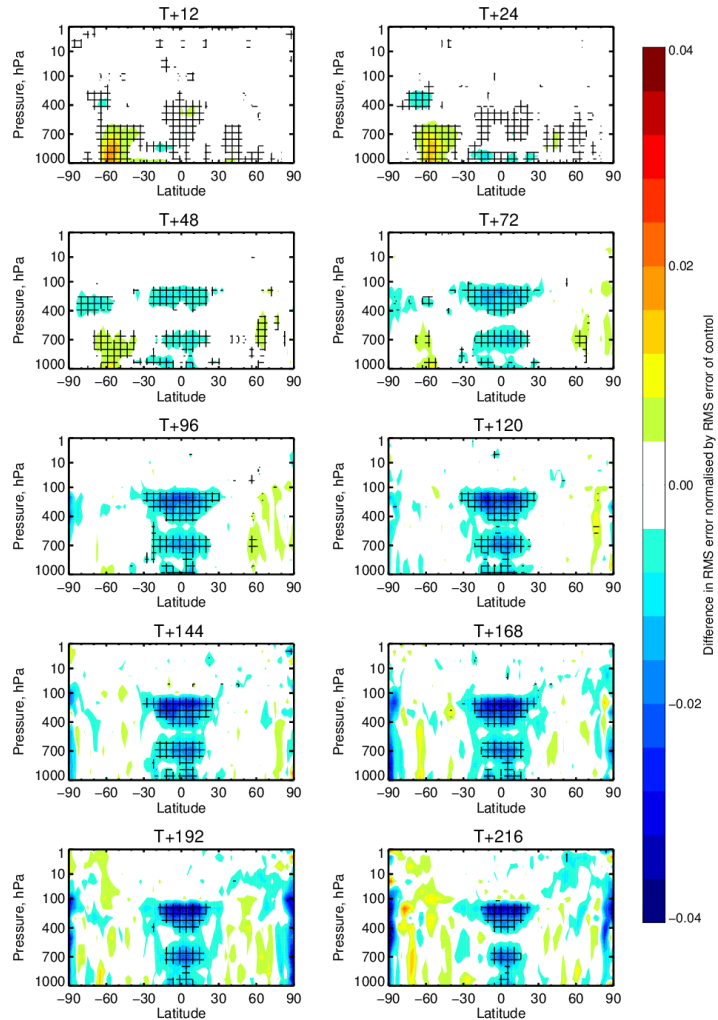
$$C_h = C_d^{1/2} \frac{\kappa}{\ln\left(\frac{10}{z_T}\right)}$$

Current operational system

Sensitivity study: Impact of no waves feedback to the atmospheric model

Normalised difference in RMSE for T

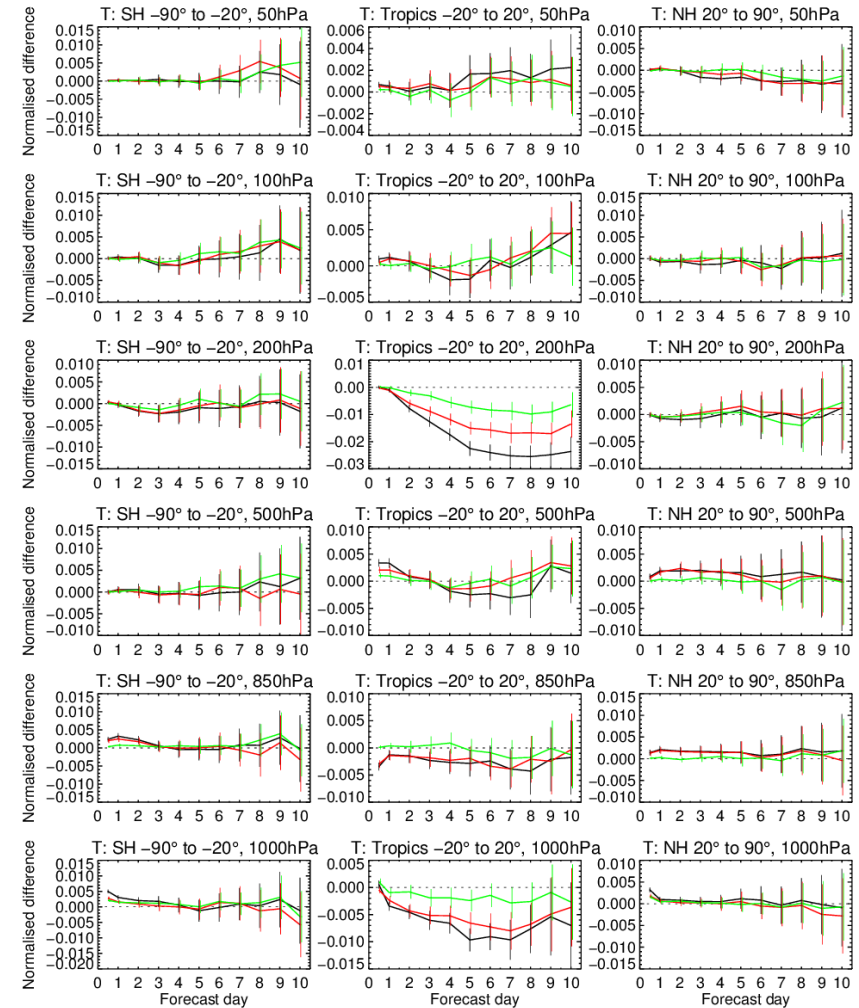
Change in error in T (no WAM feedback to IFS-Coupled_43r1 (partial coupling))
 1-Jun-2015 to 30-May-2016 from 356 to 365 samples. Cross-hatching indicates 95% confidence. Verified against 0001.



↑
worst

↓
better

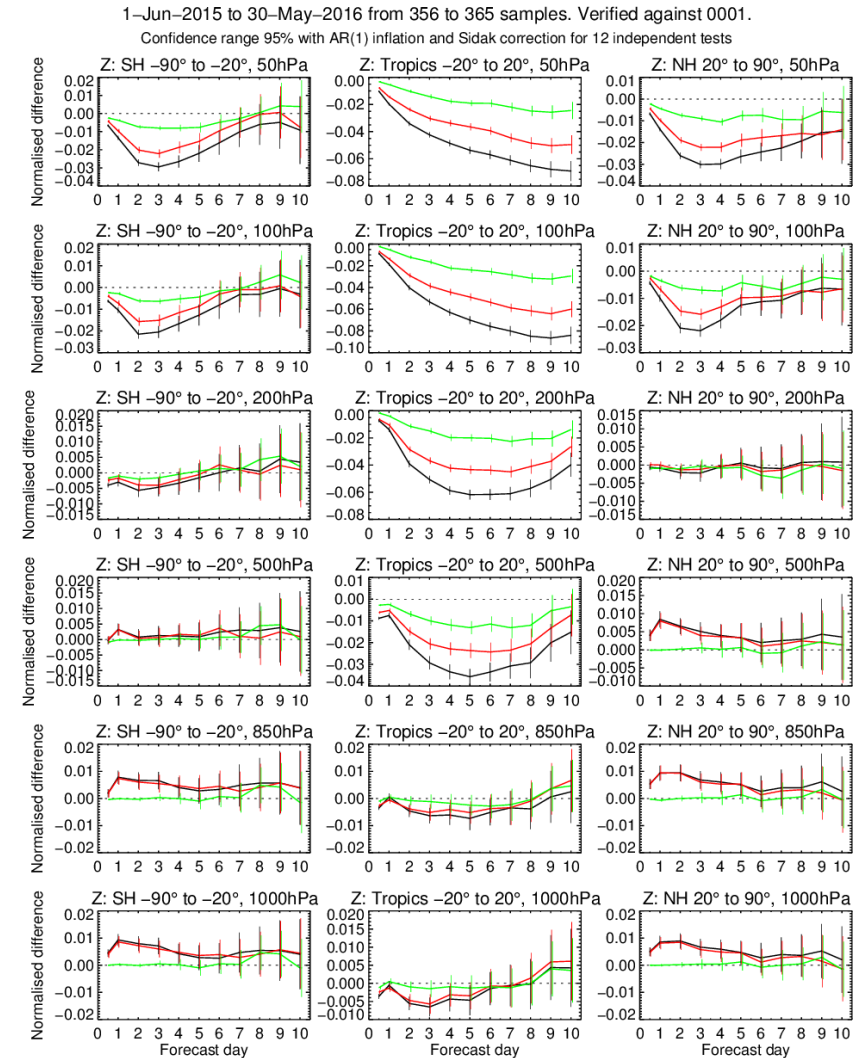
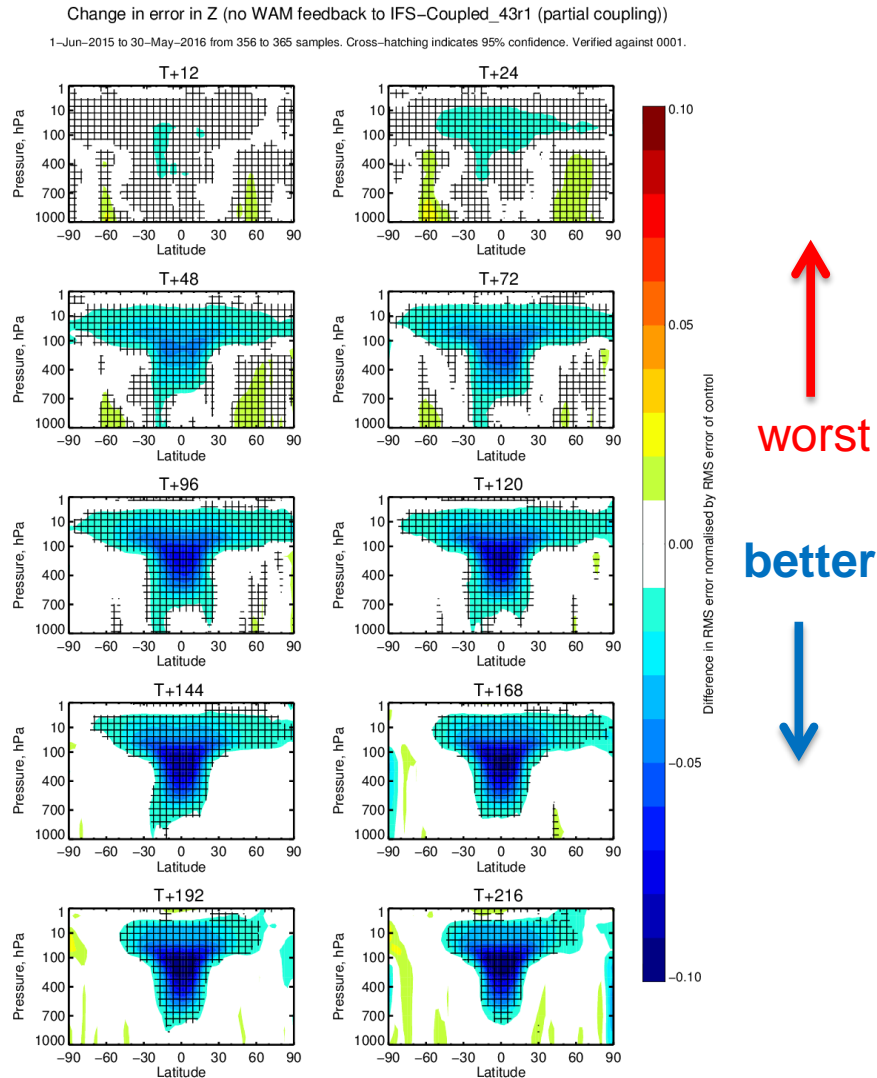
1-Jun-2015 to 30-May-2016 from 356 to 365 samples. Verified against 0001.
 Confidence range 95% with AR(1) inflation and Sidak correction for 12 independent tests



> 0
means
worst

Sensitivity study: Impact of no waves feedback to the atmospheric model

Normalised difference in RMSE for Z

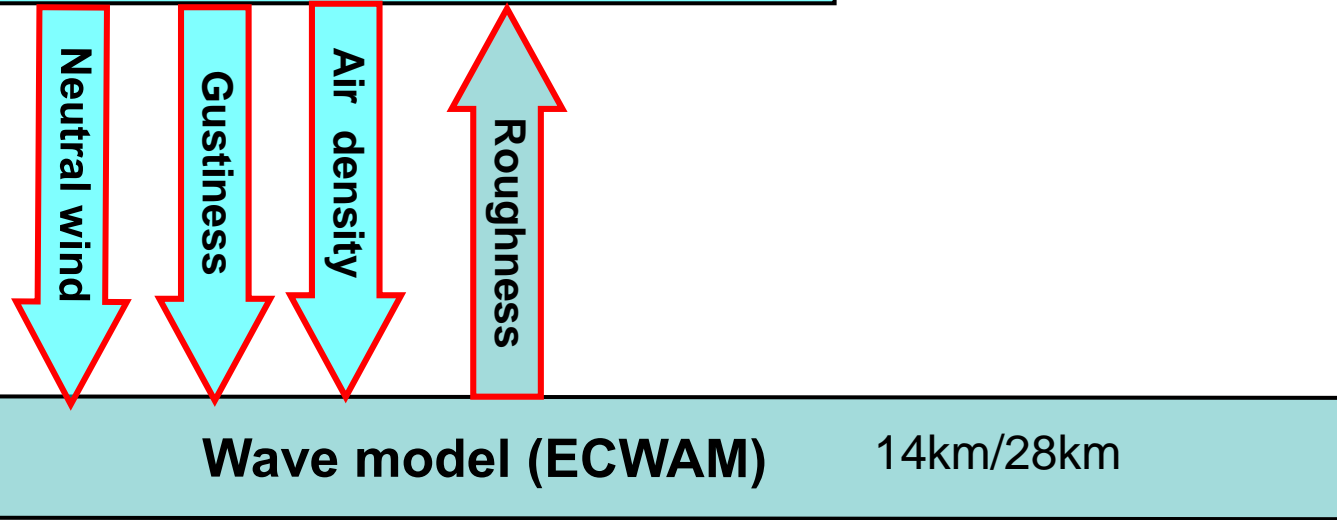


— no WAM feedback to IFS - Coupled_43r1 (partial coupling)
 — no Charnock feedback to IFS - Coupled_43r1 (partial coupling)
 — no Stokes from WAM to IFS - Coupled_43r1 (partial coupling)

> 0
means
worst

Atmospheric model TCo1279/TCo639
9km/18km

Towards a coupled system



All configurations

Since 2002

Gustiness parameterisation:

$$\gamma(u_*) = 0.5 (\gamma(\bar{u}_* + \sigma_*) + \gamma(\bar{u}_* - \sigma_*))$$

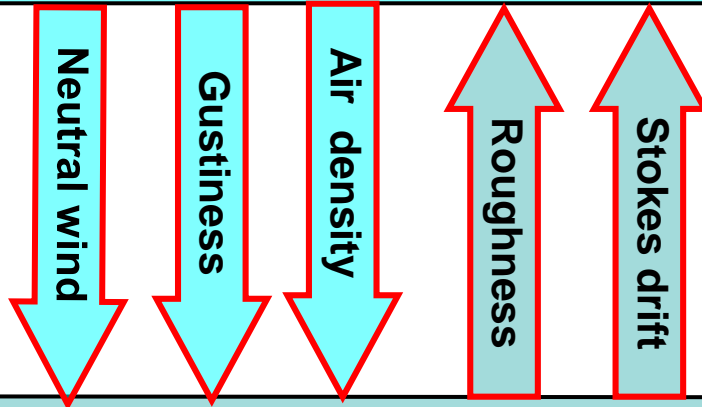
$$\sigma_* = \text{function} \left(\bar{u}_* \text{ and } \frac{z_i}{L} \right)$$

Air density effect:

$$\gamma \sim \frac{\rho_a}{\rho_w} \beta(z_0) \left(\frac{u_*}{c} \right)^2$$

z_i is the height of the lowest inversion,
L is the Monin-Obukhov length

Atmospheric model TCo1279/TCo639
9km/18km



Wave model (ECWAM) 14km/28km

Towards a coupled system

All configurations

Since 2010

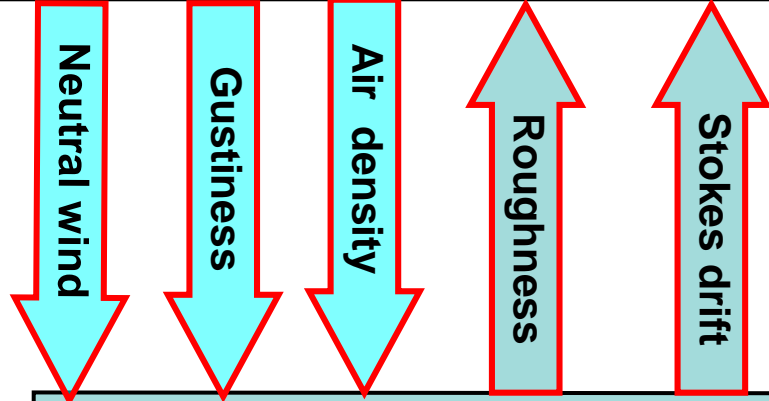
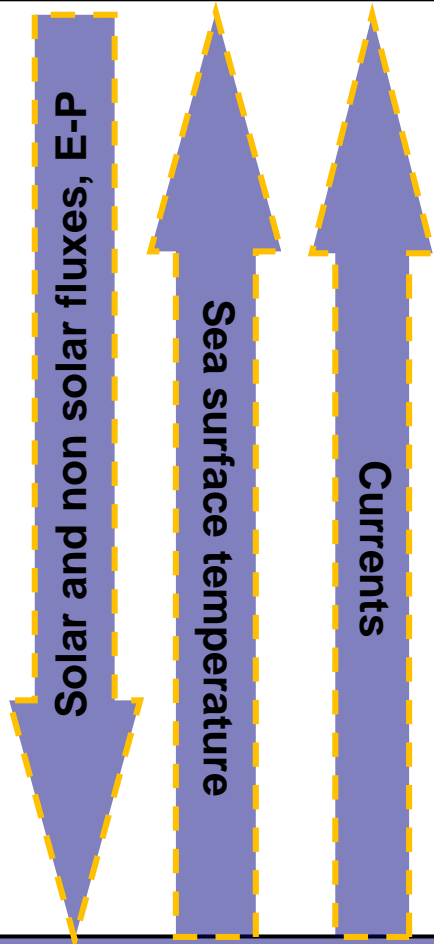
The surface Stokes drift is used to parameterise the wave induced mixing in the SST warm layer scheme in the IFS for the representation of the SST diurnal cycle (Takaya et al. 2010)

Stokes drift:

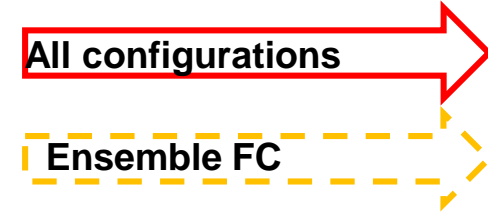
$$\mathbf{u}_s(z) = 4\pi \int_0^{2\pi} \int_0^{\infty} f \mathbf{k} e^{2kz} F(f, \theta) df d\theta$$

Atmospheric model TCo1279/TCo639
9km/18km

**Towards a fully coupled system
(currently only operational in EPS)**



Every IFS time step



Single executable

Wave model (ECWAM) 14km/28km

Every coupling time step (1 or 3 hours)

Wave effects?

- Ensemble systems only:**
- Medium range forecast
 - Monthly forecast
 - Seasonal forecast

Ocean model (NEMO)

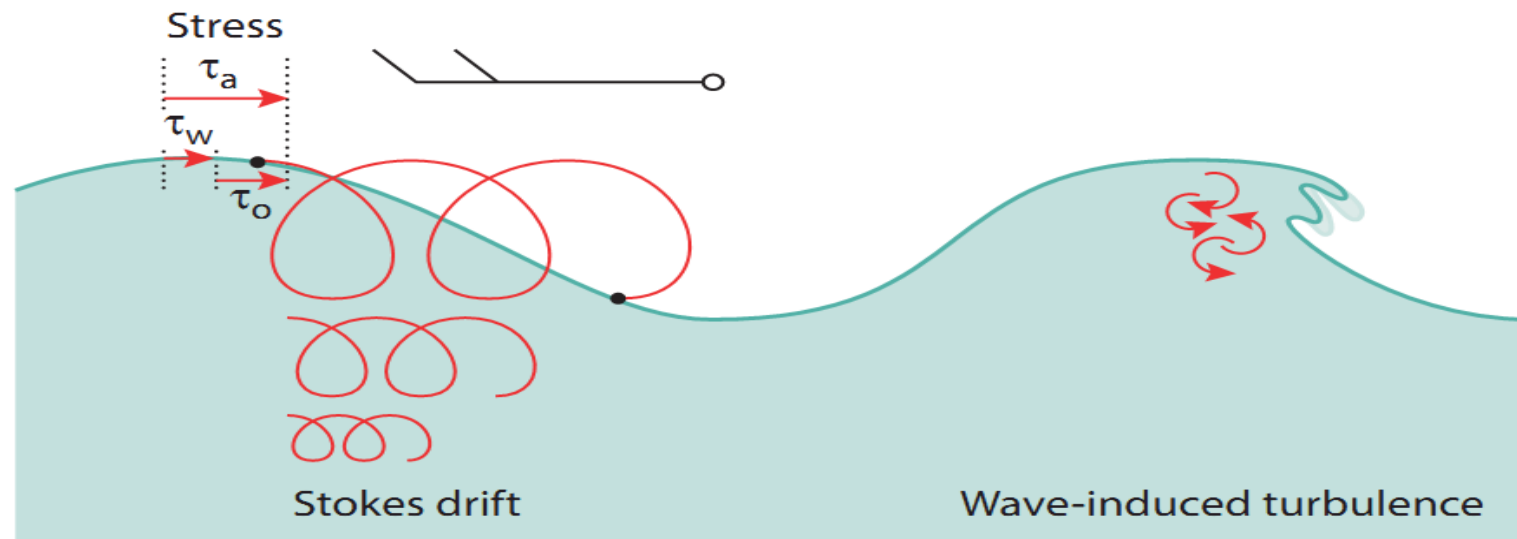
ORCA1_Z42

Wave effects in NEMO

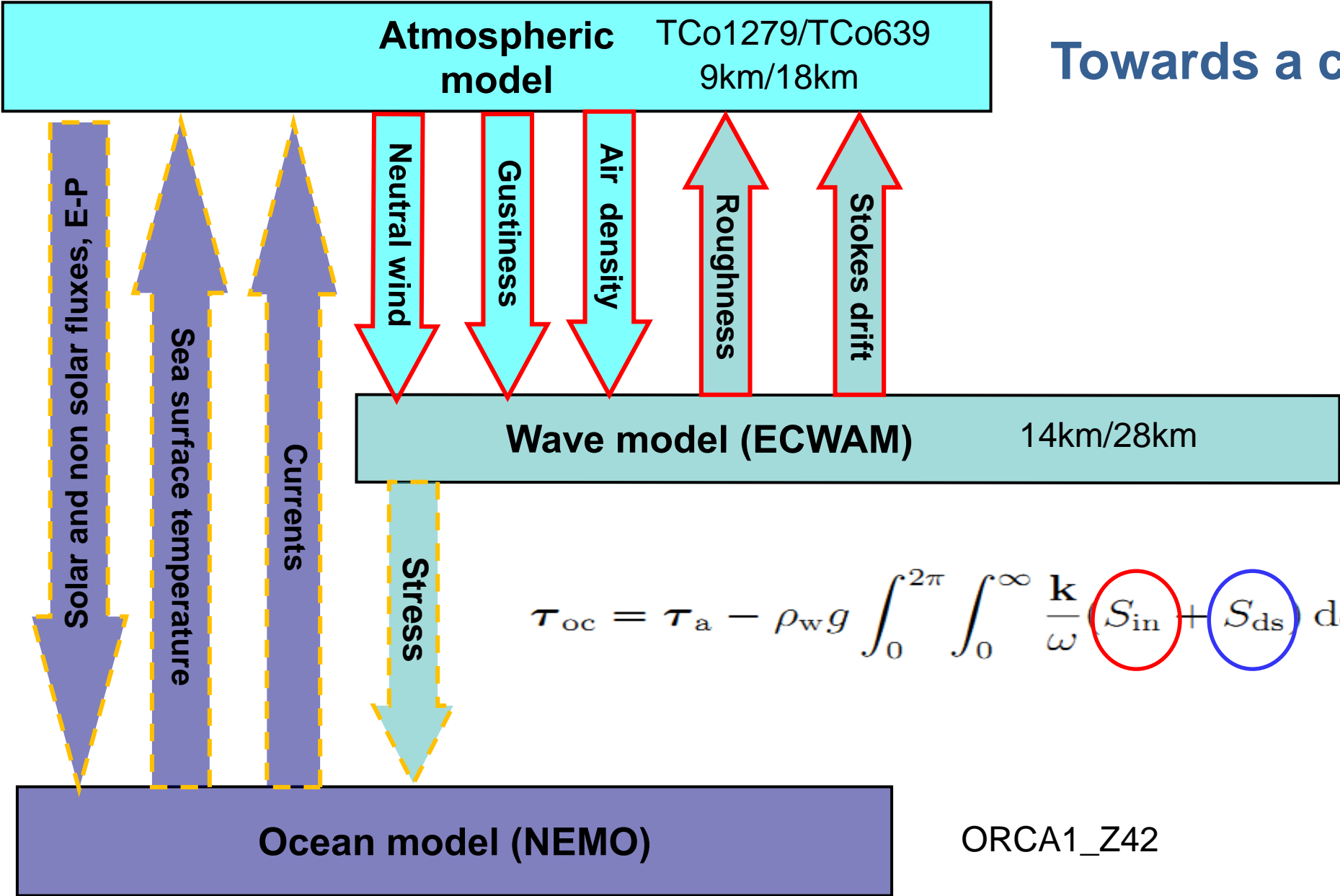
Stress: As waves grow under the influence of the wind, the waves absorb momentum (τ_w) which otherwise would have gone directly into the ocean (τ_0).

Stokes-Coriolis forcing: The Stokes drift sets up a current in the along-wave direction. Near the surface it can be substantial (~ 1 m/s). The Coriolis effect works on the Stokes drift and adds a new term to the momentum equations.

Mixing: Mixing: As waves break, turbulent kinetic energy is injected into the ocean mixed layer, significantly enhancing the mixing.



Towards a coupled system



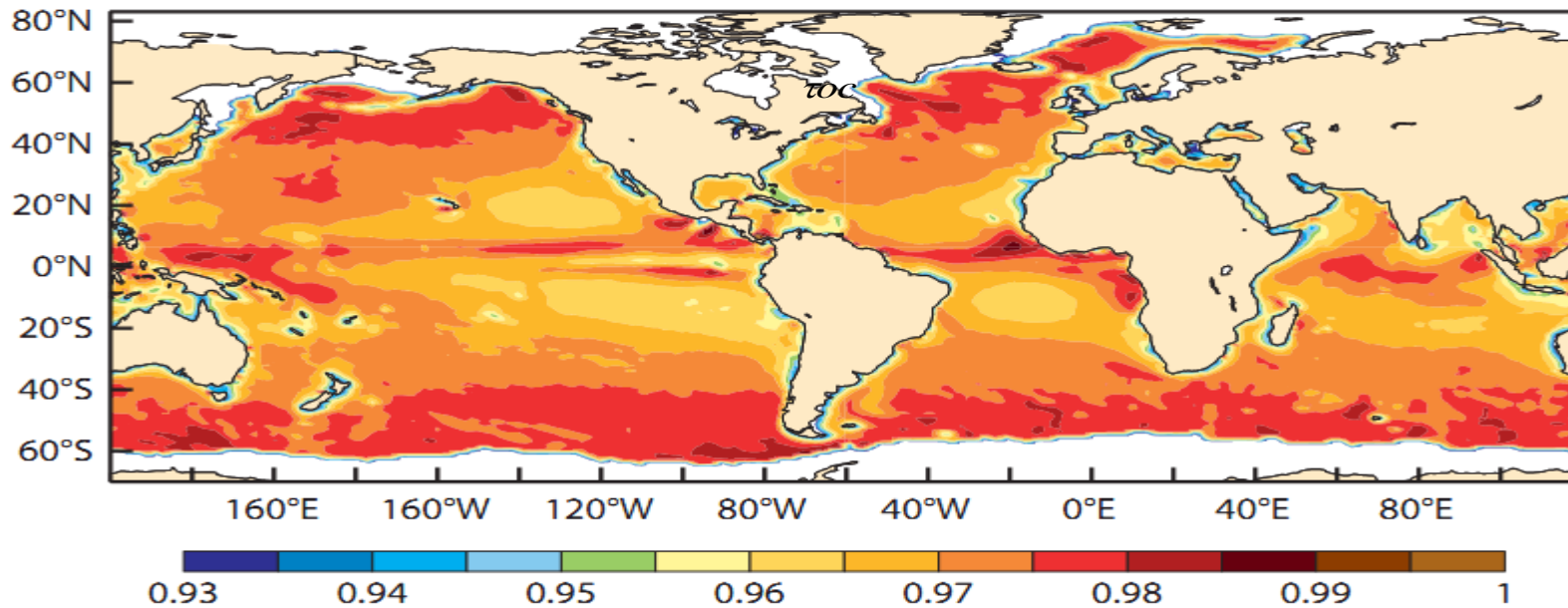
Single executable

$$\tau_{oc} = \tau_a - \rho_w g \int_0^{2\pi} \int_0^{\infty} \frac{k}{\omega} (S_{in} + S_{ds}) d\omega d\theta.$$

Wave effects in NEMO: sea state modulated surface stress

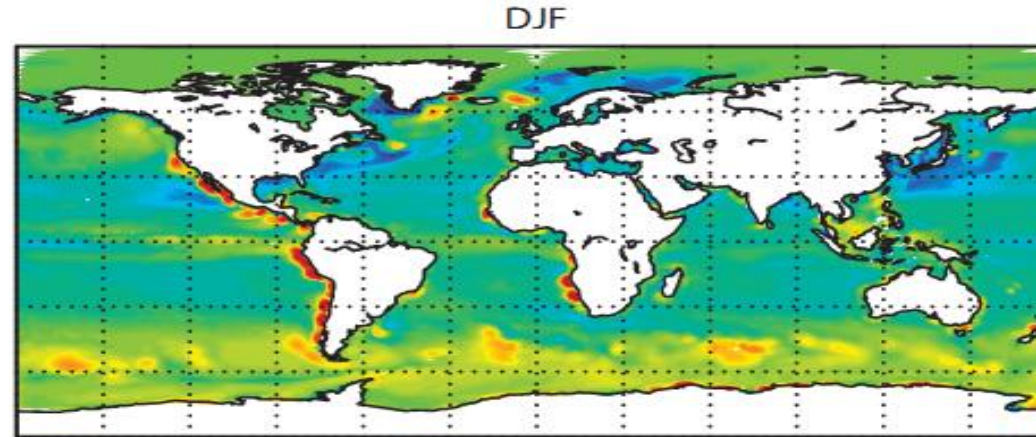
$$\tau_{oc} = \tau_a - \rho_w g \int_0^{2\pi} \int_0^{\infty} \frac{\mathbf{k}}{\omega} (S_{in} + S_{ds}) d\omega d\theta.$$

Normalised mean of the momentum flux into the ocean from ERA-Interim analysis
from 1 October 2010 to 30 September 2012

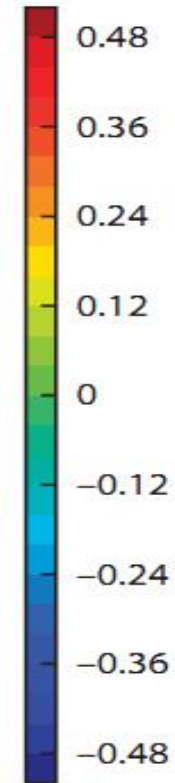
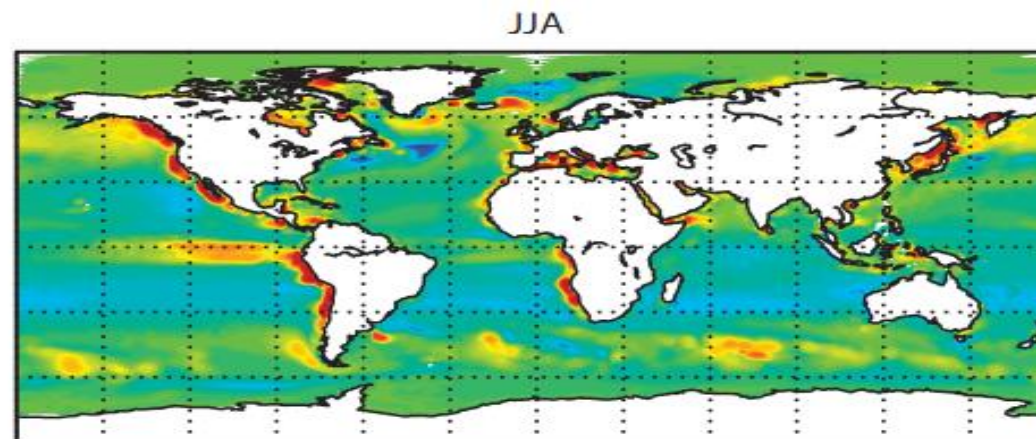


Wave effects in NEMO: sea state modulated surface stress

Boreal winter



Boreal summer



SST
mean difference

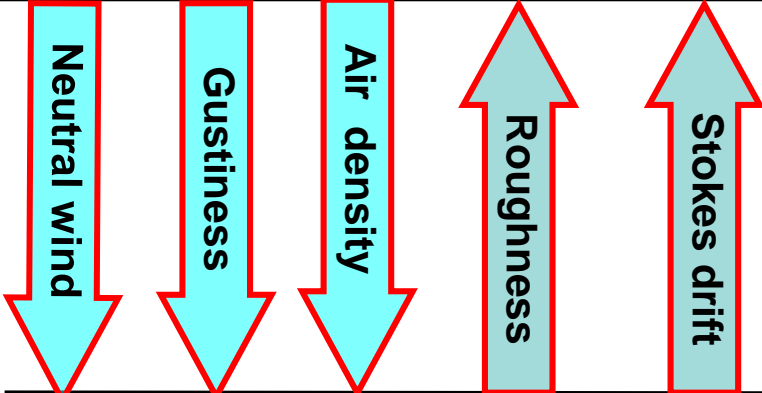
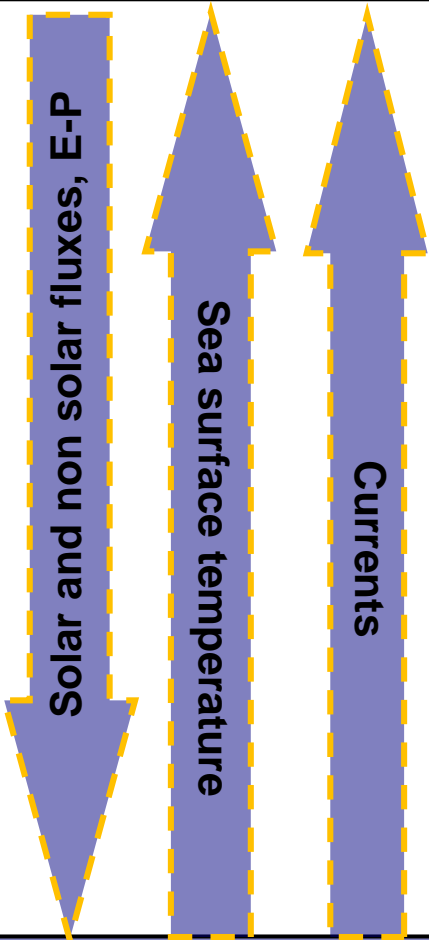
Results from standalone runs, forced by ERA-interim fluxes and sea state.
Averages are over a 20 year period

Atmospheric model TCo1279/TCo639
9km/18km

Towards a coupled system



Single executable



Wave model (ECWAM) 14km/28km



$$u_s(z) = 4\pi \int_0^{2\pi} \int_0^\infty f k e^{2kz} F(f, \theta) df d\theta$$

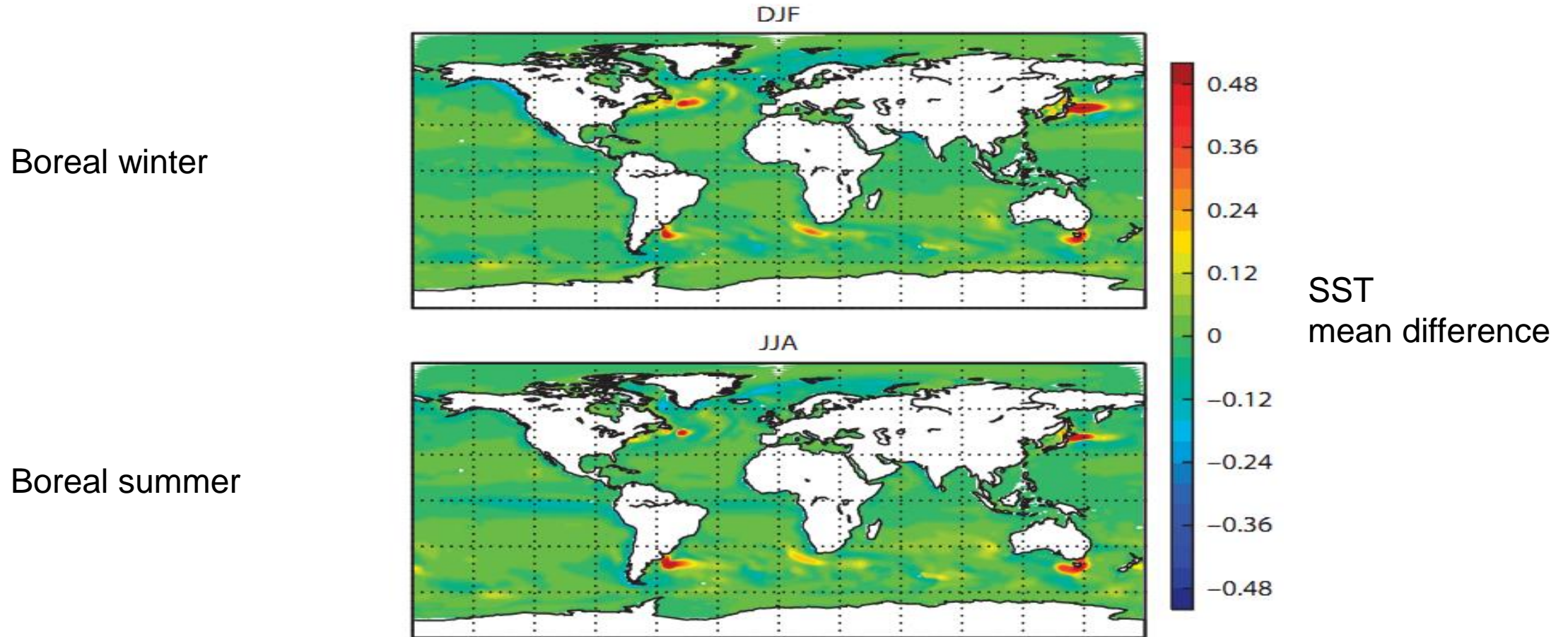
$$\frac{Du}{Dt} = -\frac{1}{\rho} \nabla p + (\mathbf{u} + \mathbf{u}_s) \times f \mathbf{e}_z + \frac{1}{\rho} \frac{\partial \tau}{\partial z}$$

Ocean model (NEMO)

ORCA1_Z42

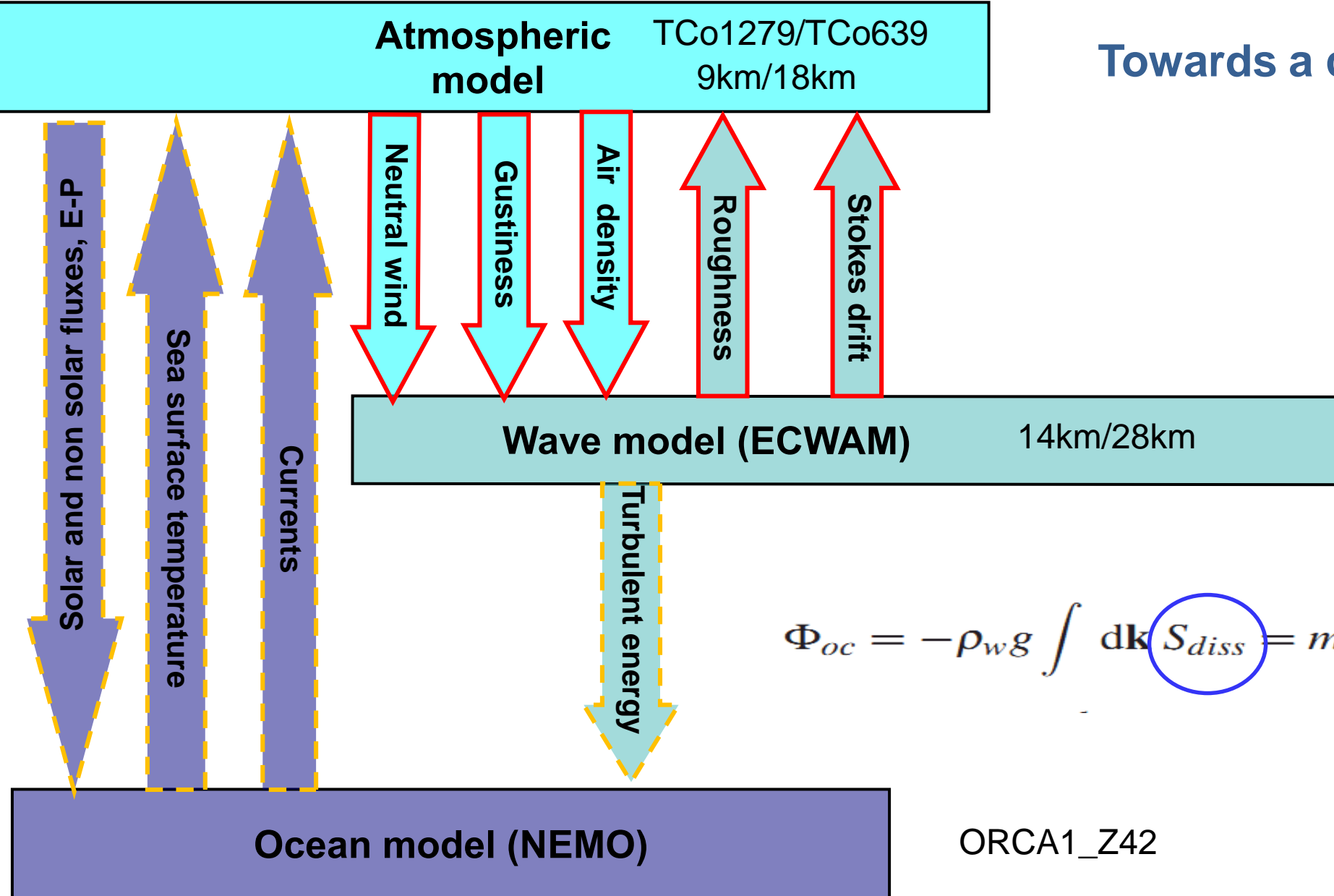
$U_s(z)$ vertical profile approximated using Breivik et al. 2014

Wave effects in NEMO: Stokes-Coriolis Forcing



Results from standalone runs, forced by ERA-interim fluxes and sea state.
Averages are over a 20 year period

Towards a coupled system



All configurations

Ensemble FC

Single executable

$$\Phi_{oc} = -\rho_w g \int dk S_{diss} = m\rho_a u_*^3$$

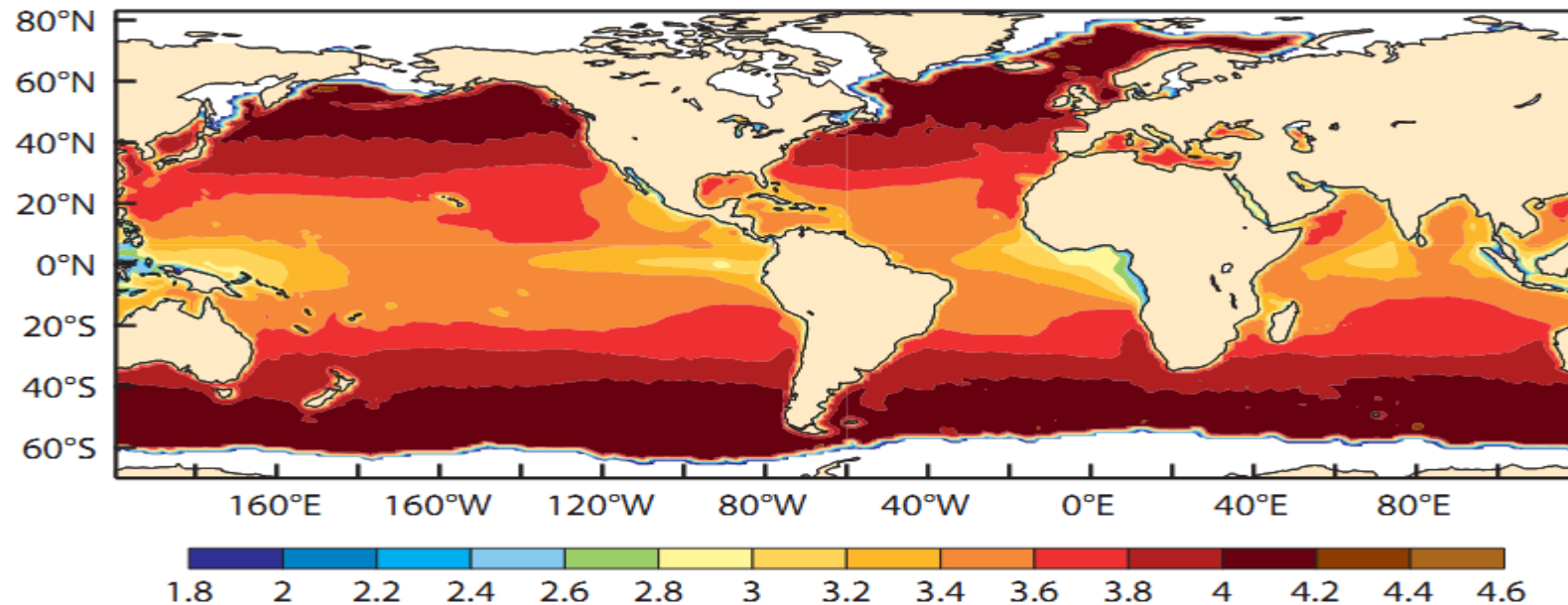
Wave effects in NEMO: input of turbulent kinetic energy

The turbulence modelling is based on an extension of the **Mellor-Yamada scheme** with sea state effects introduced following Craig and Banner (1994). Here, the turbulence is enhanced by means of the energy flux from waves to ocean column which follows from the dissipation term in the energy balance equation:

$$\Phi_{oc} = -\rho_w g \int dk S_{diss} = m \rho_a u_*^3.$$

Normalised mean of the energy flux into the ocean from ERA-Interim analysis
from 1 October 2010 to 30 September 2012

m:
NEMO
default
m=3.5



TKE EQUATION

If effects of advection are ignored, the turbulent kinetic energy (TKE) equation describes the rate of change of turbulent kinetic energy e due to processes such as shear production (including the shear in the Stokes drift), damping by buoyancy, vertical transport of TKE, and turbulent dissipation ε . It reads

$$\frac{\partial e}{\partial t} = \frac{\partial}{\partial z} \left(v_q \frac{\partial e}{\partial z} \right) + v_m S^2 + v_m S \frac{\partial U_S}{\partial z} - v_h N^2 - \varepsilon,$$

where $e = q^2/2$, with q the turbulent velocity, $S = \partial U / \partial z$ and $N^2 = g\rho_0^{-1} \partial \rho / \partial z$, with N the Brunt-Väisälä frequency. The eddy viscosities for momentum, heat, and TKE are denoted by v_m , v_h and v_q . E.g $v_m = l(z)q(z)S_M$ where $l(z)$ is the mixing length and S_M depends on stratification.

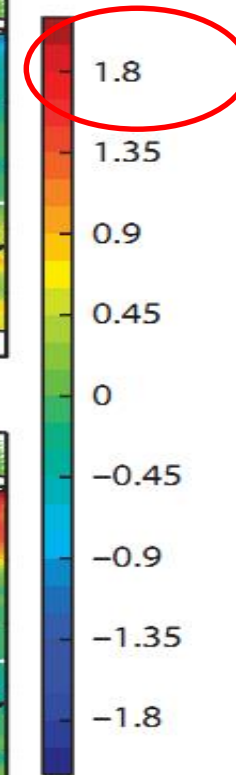
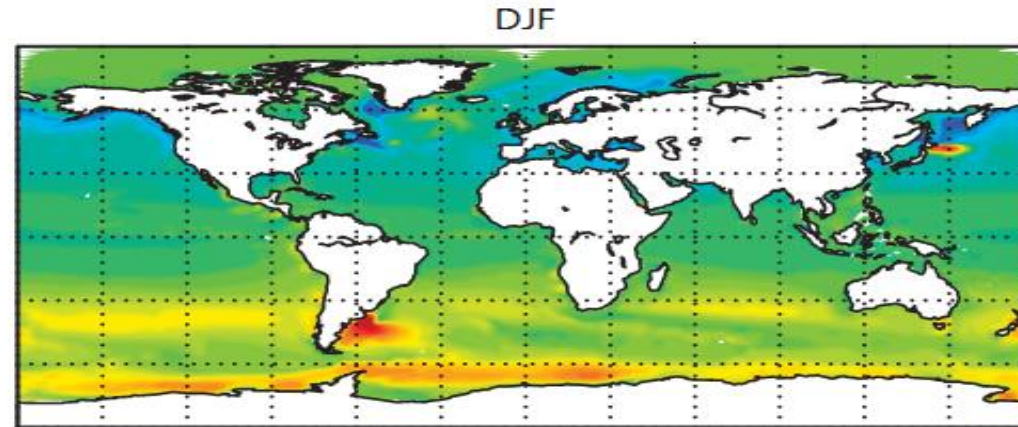
Wave-induced turbulence is introduced by the boundary condition:

$$\rho_w v_q \frac{\partial e}{\partial z} = \Phi_{oc}, \quad z = 0.$$

while effects of Langmuir turbulence are introduced by the term involving the shear in the Stokes-drift profile.

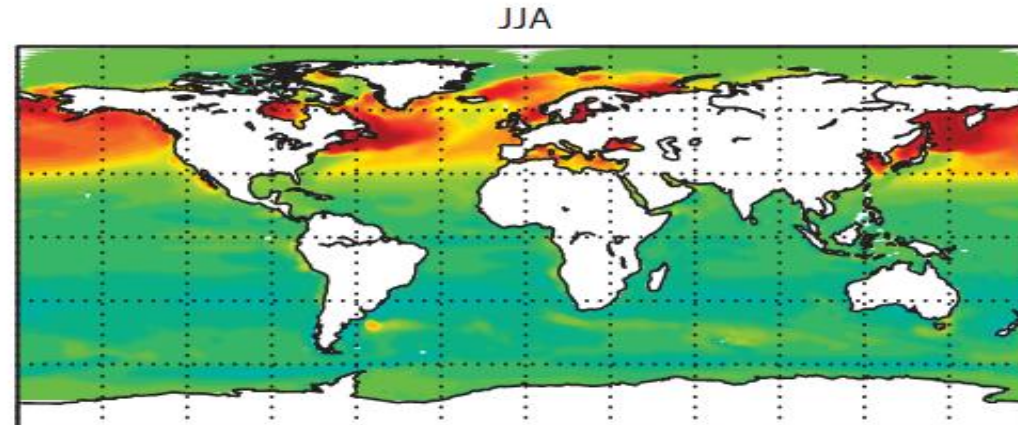
Wave effects in NEMO: input of turbulent kinetic energy

Boreal winter



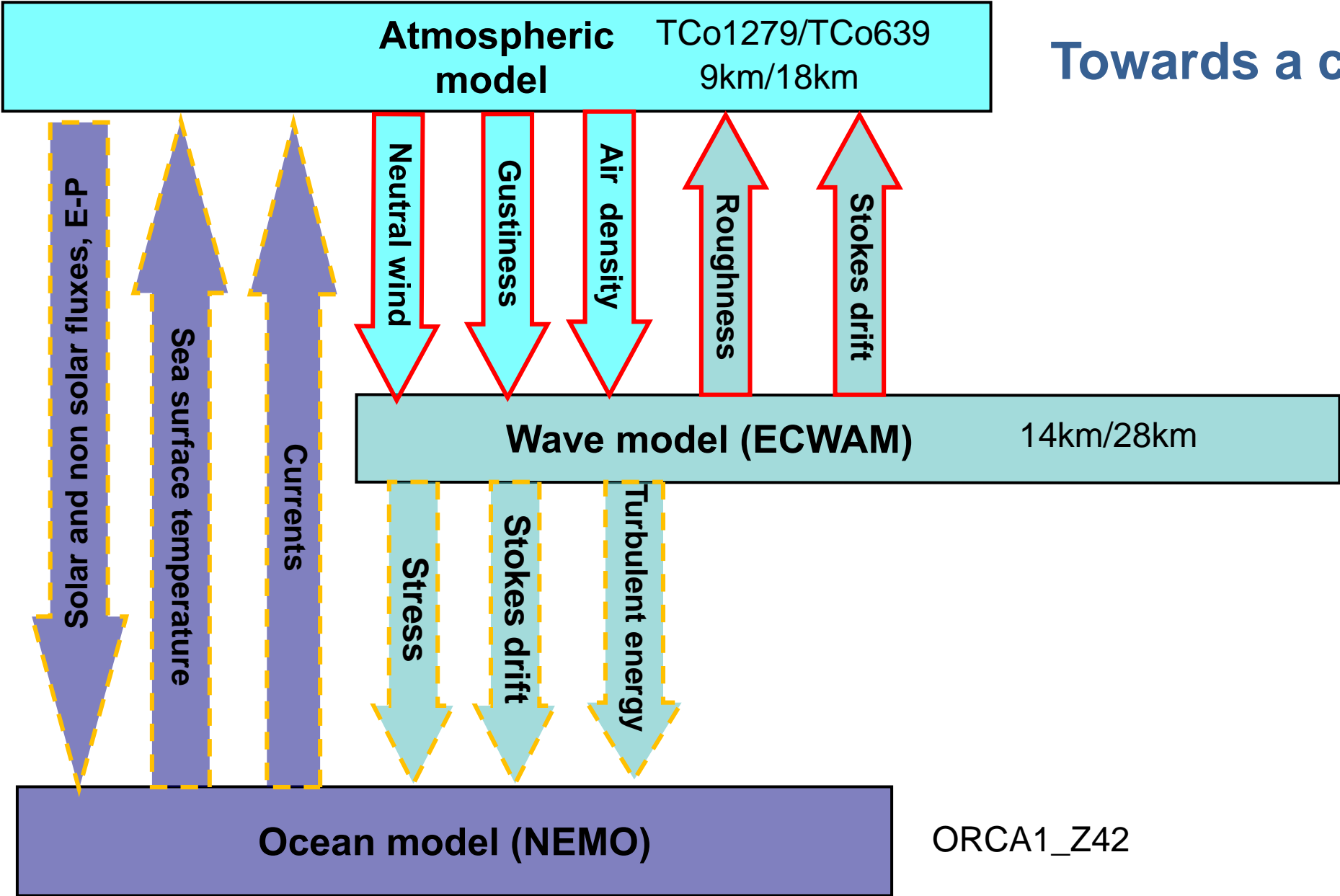
SST
mean difference

Boreal summer



Results from standalone runs, forced by ERA-interim fluxes and sea state.
Averages are over a 20 year period

Towards a coupled system



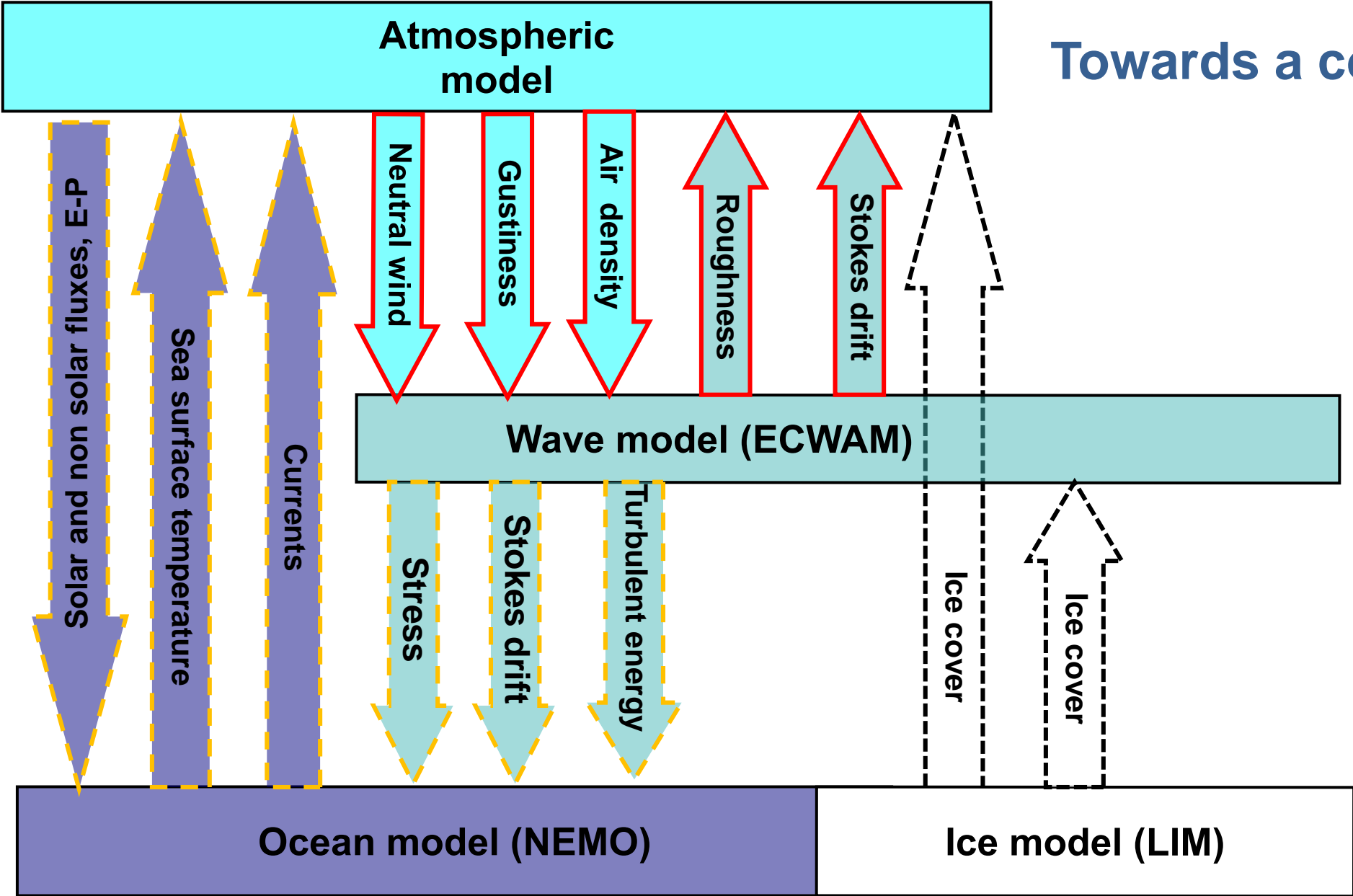
All configurations

Ensemble FC

Single executable

Operational from day 0 since 2013

Towards a coupled system



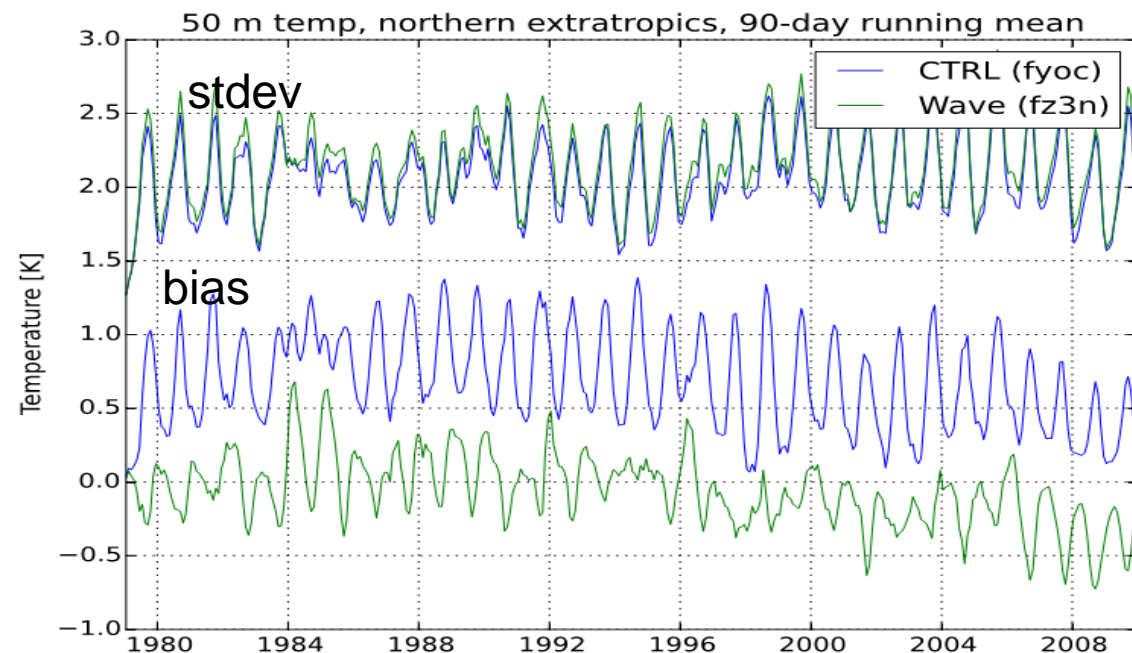
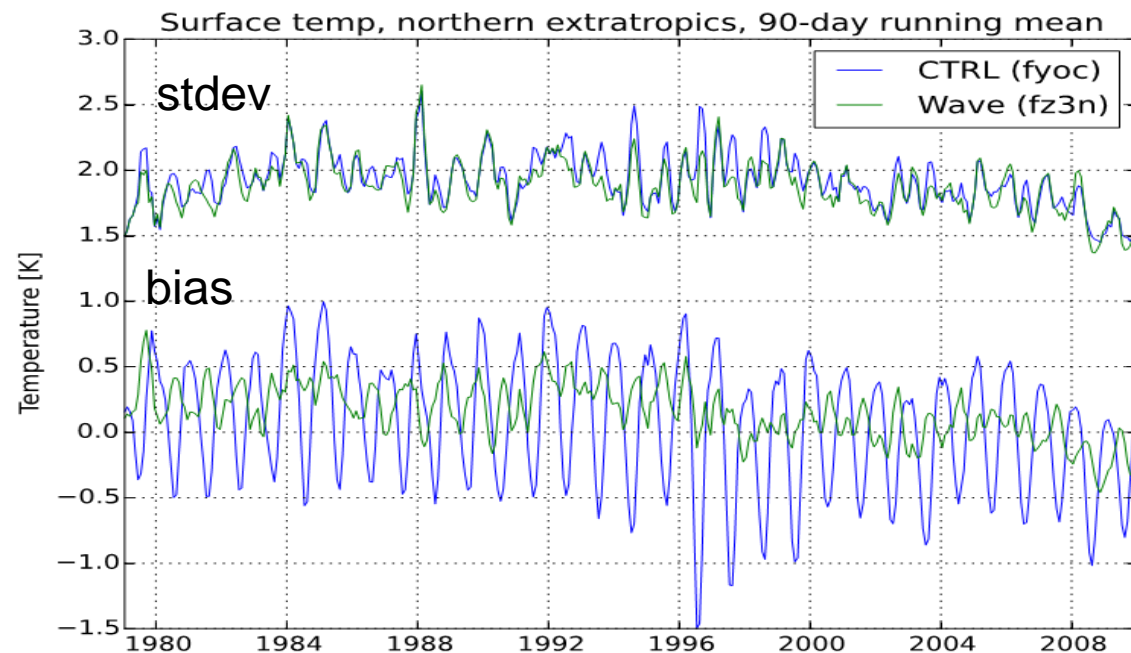
- All configurations
- Ensemble FC
- future operational

Single executable

Adding active sea ice model
 Implementation:
 CY43R1
 end 2016.

ORCA0.25°_Z75

Wave effects in NEMO



Comparison of surface (left) and 50 m depth (right) EN3 ocean temperature observations (Ingleby and Huddleston, 2007) in the northern extra-tropics in the CTRL run (blue) and a run with all three wave effects switched on (green).

The upper curves show the standard deviation while the lower curves represent the bias.

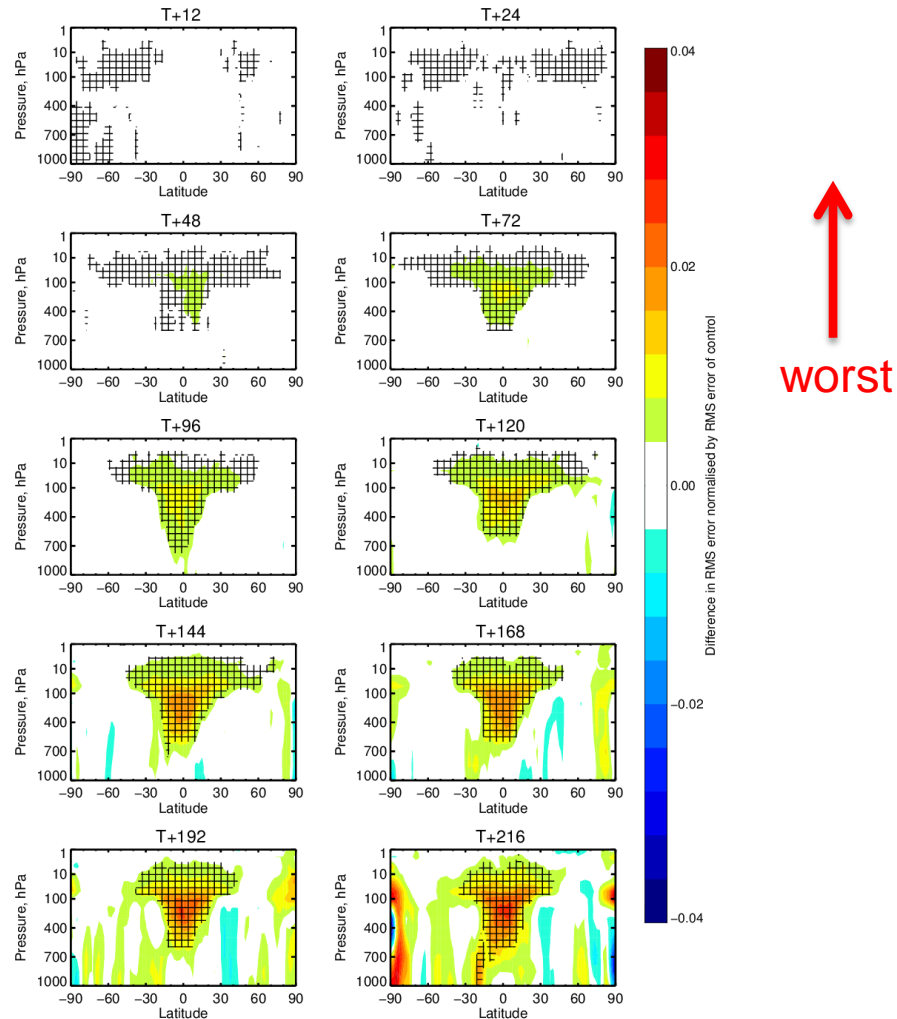
A 90-day running mean is employed.

Sensitivity study: no wave feedback to NEMO

Normalised difference in RMSE for Z

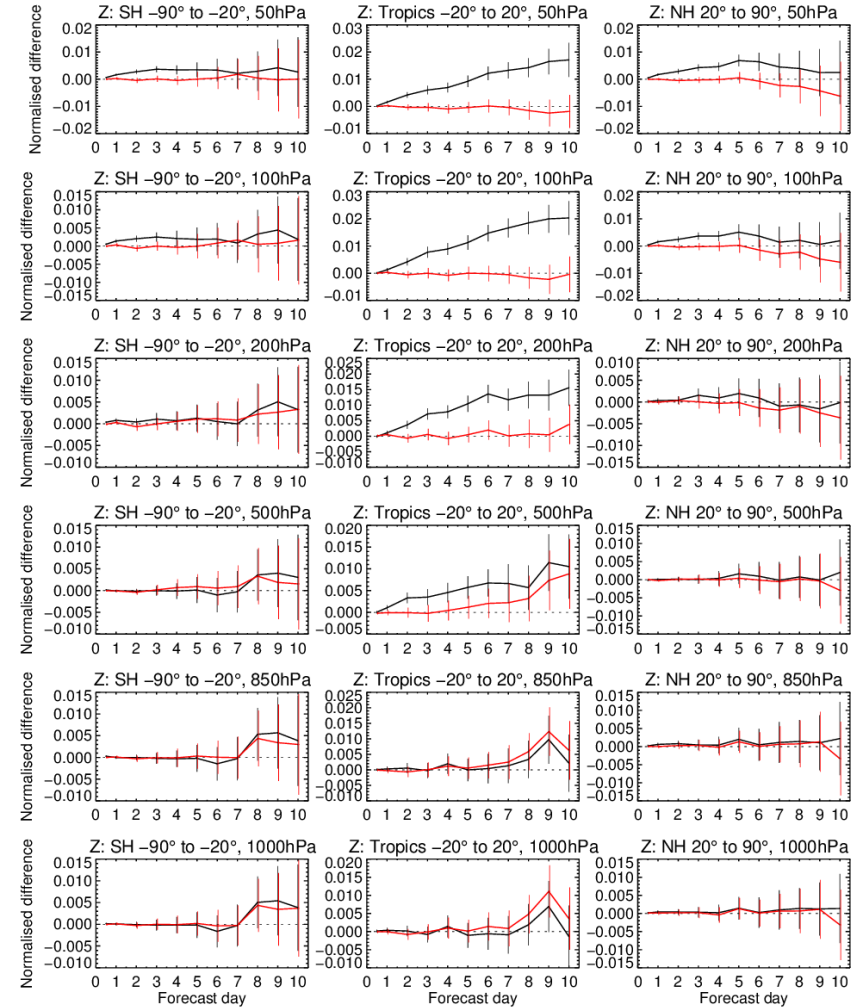
Change in error in Z (Partial Coupling no WAM feedback to NEMO-Coupled_43r1 (partial coupling))

1-Jun-2015 to 30-May-2016 from 356 to 365 samples. Cross-hatching indicates 95% confidence. Verified against 0001.



1-Jun-2015 to 30-May-2016 from 356 to 365 samples. Verified against 0001.

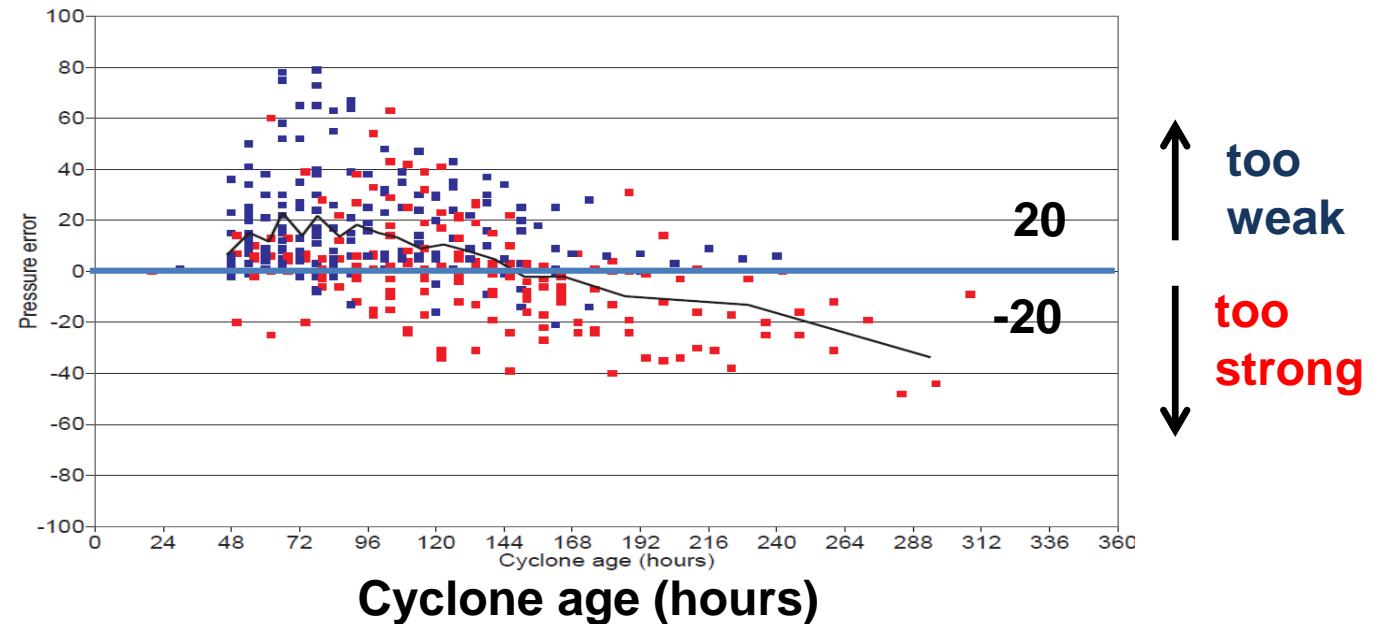
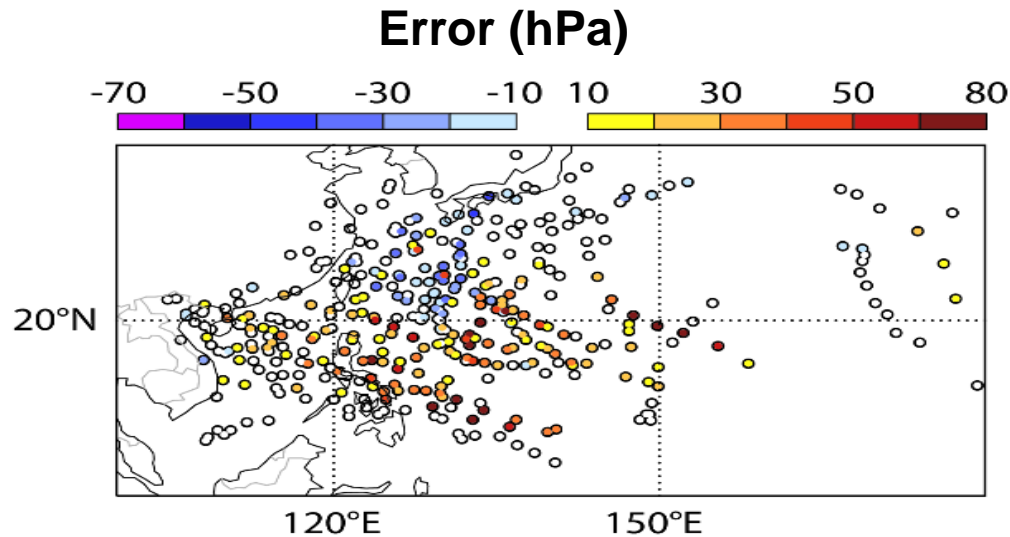
Confidence range 95% with AR(1) inflation and Sidak correction for 8 independent tests



> 0
means
worst

Impact of Coupling on tropical cyclone forecast:

Tropical cyclone **core pressure mean error** in the Western Pacific (hPa) of the operational high resolution system (HRES) in 2013-2014:



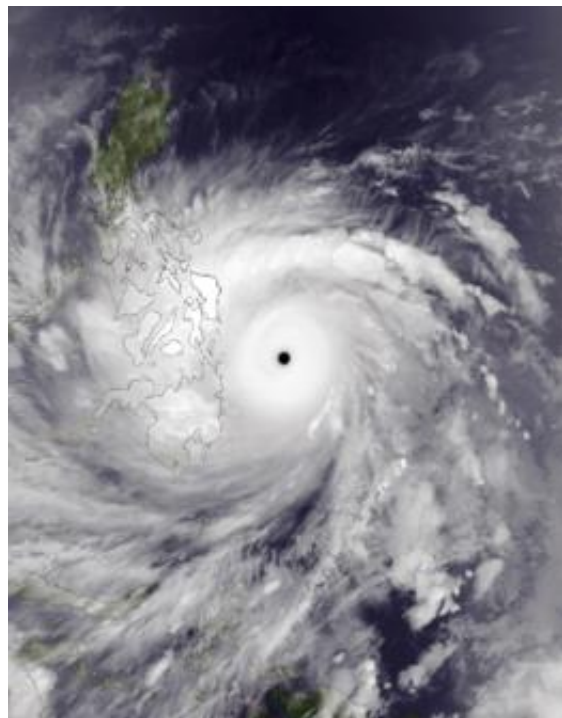
Red dots: north of 20°N

Blue dots: south of 20°N

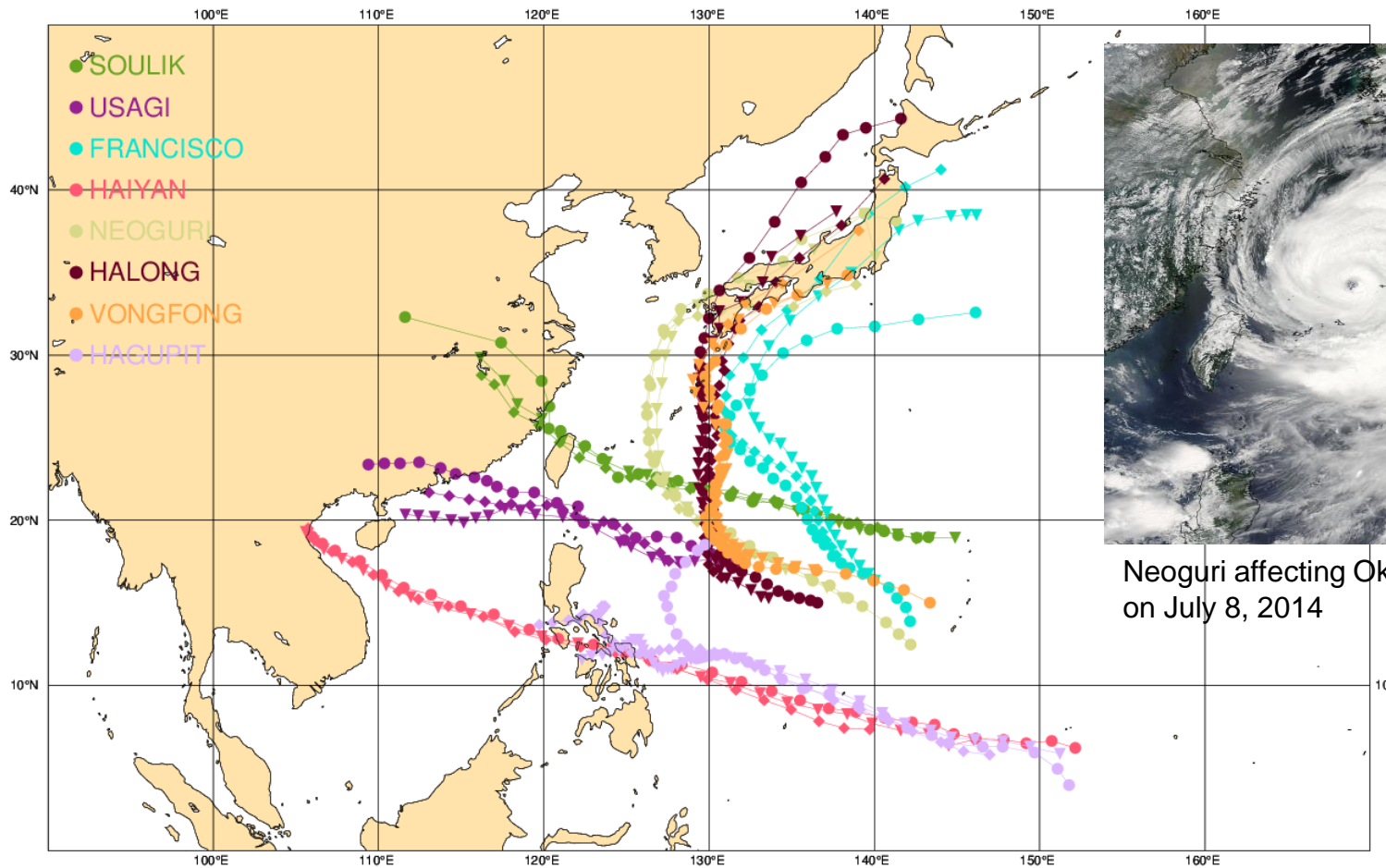
Rodwell et al., 2015: New Developments in the Diagnosis and Verification of High-Impact Weather Forecasts. ECMWF Technical Memorandum 759. <http://www.ecmwf.int/en/elibrary/technical-memoranda>

TCo1279+ORCA025 fully coupled

TCo1279/ORCA025 fully coupled



Typhoon Haiyan at peak intensity on November 7, 2013

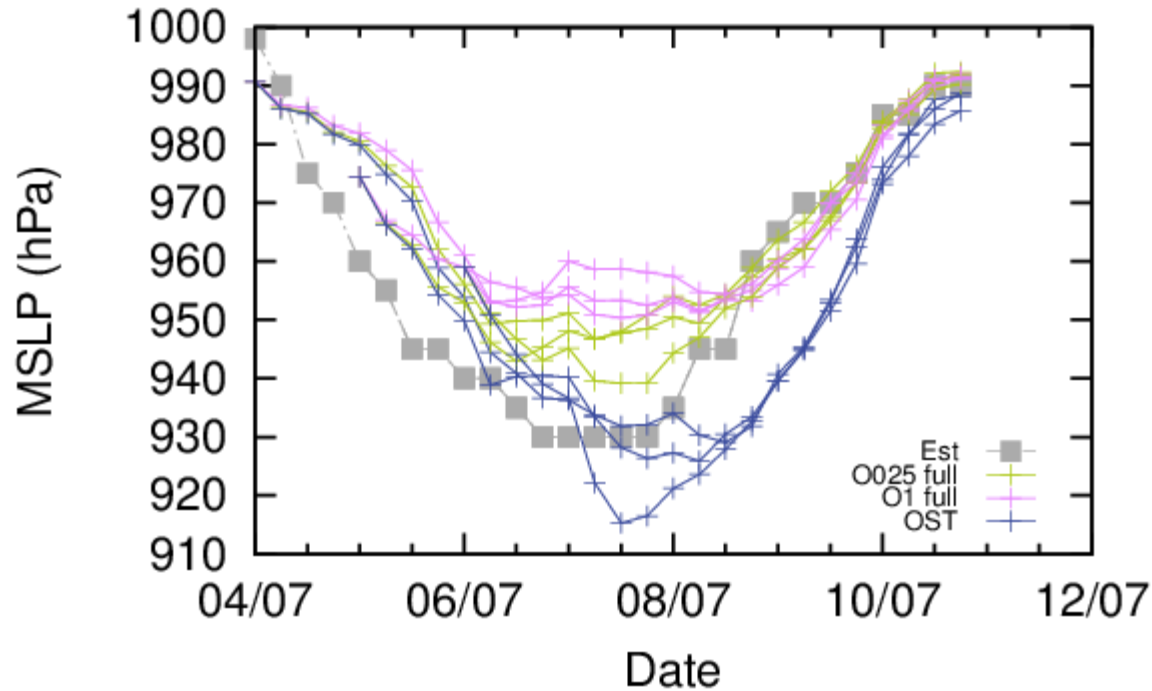


Neoguri affecting Okinawa on July 8, 2014

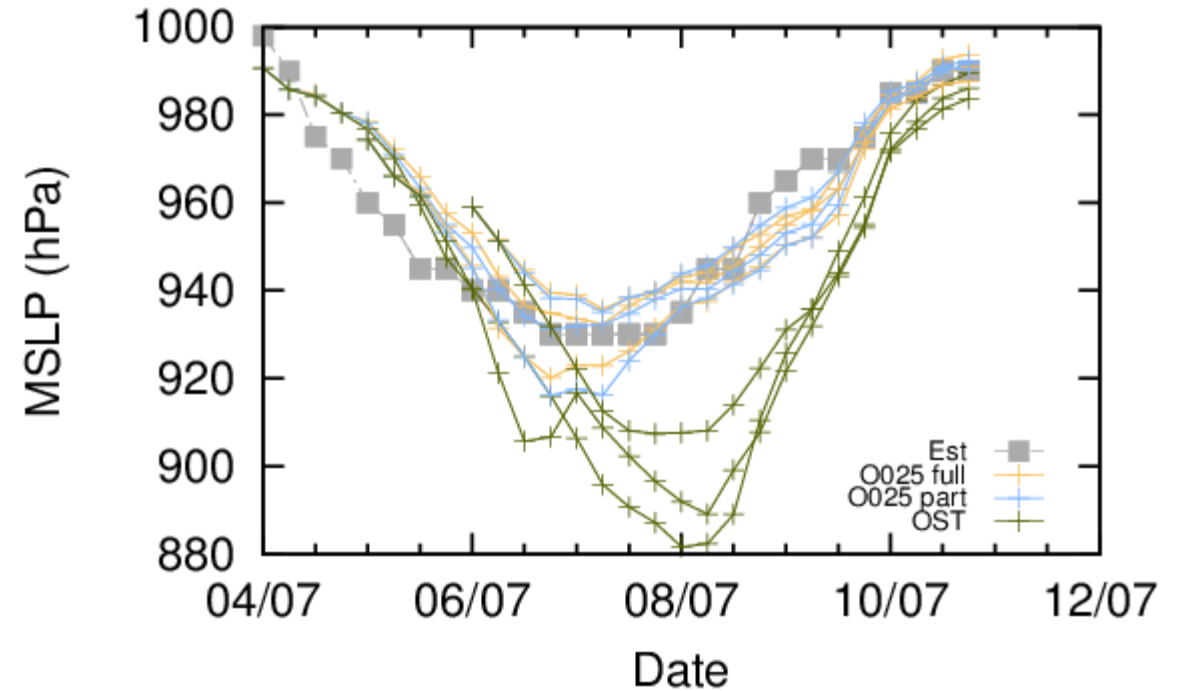
NEOGURI centre pressure, CY43R1 latest testing

NEOGURI

TL1279



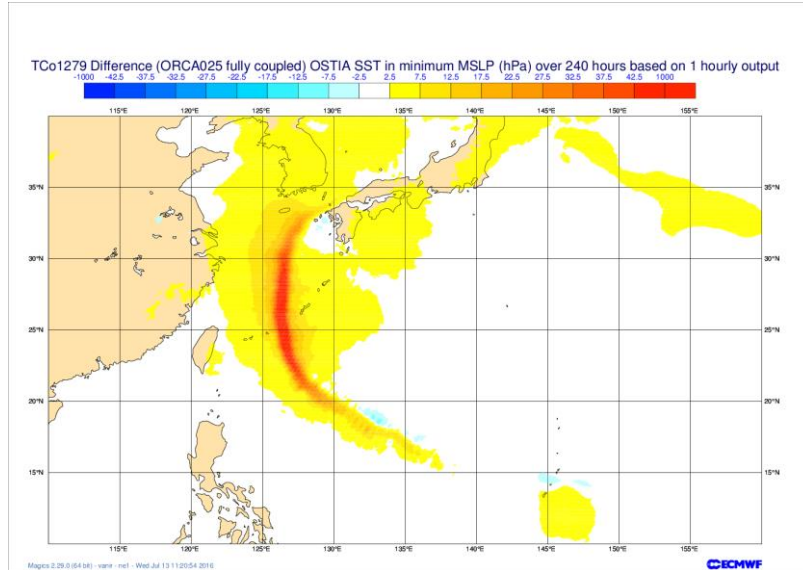
TCo1279



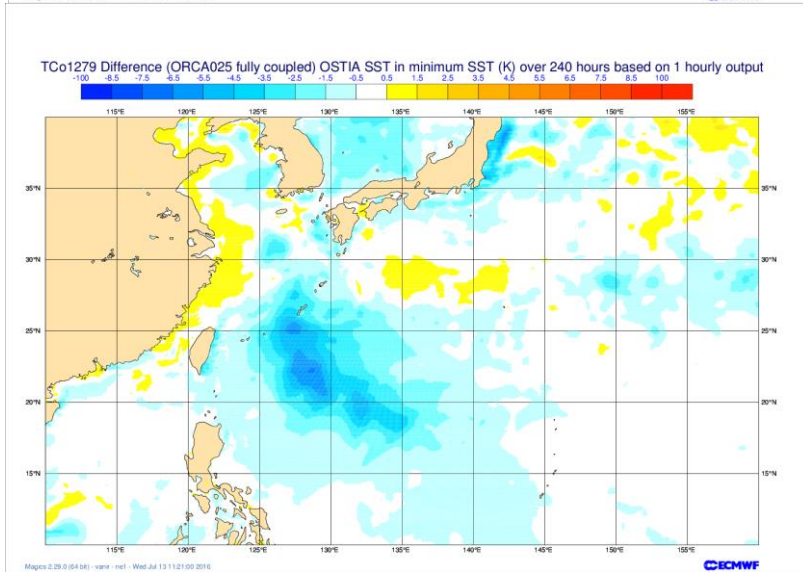
EST : estimated from observations
O025: ORCA0.25°_Z75
O1: ORCA1.0°_Z42
OST : prescribed OSTIA SST (uncoupled)

Differences between coupled and uncoupled for NEOGURI TCo1279 (CY43R1)

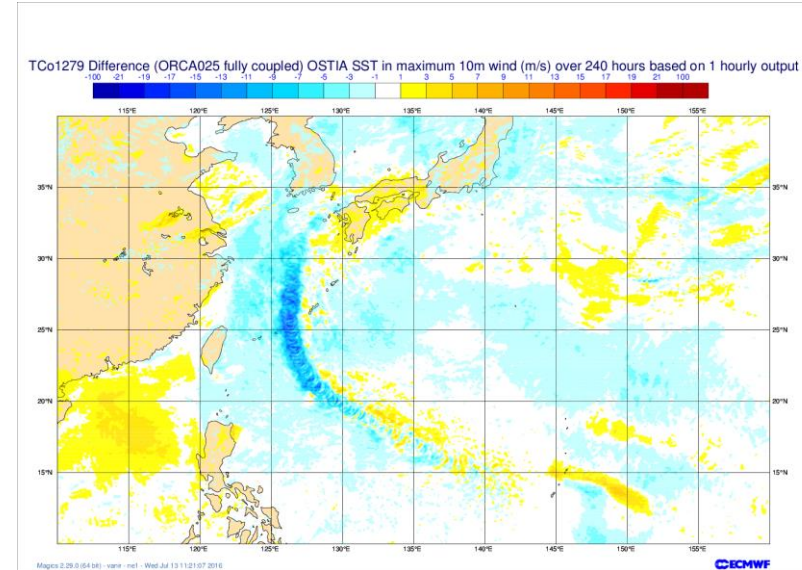
Difference in Minimum MSLP (hPa): Coupled minus operational



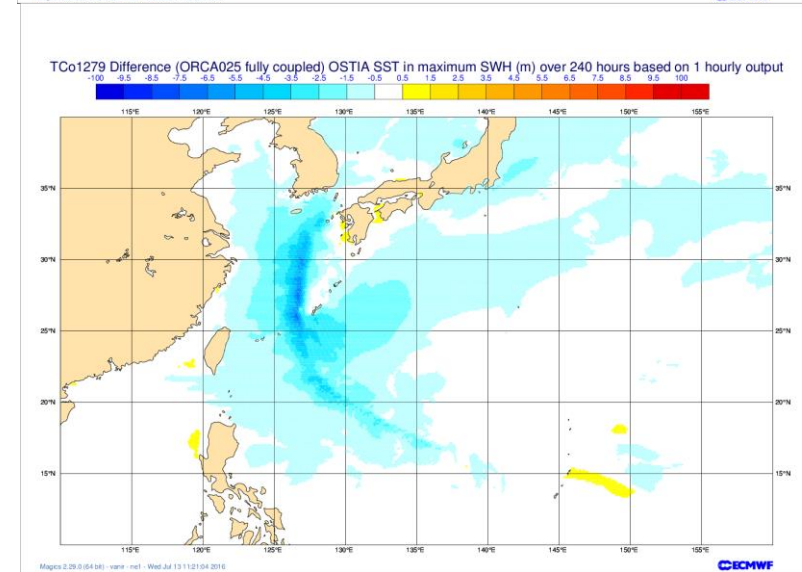
Difference in Minimum SST (K): Coupled minus uncoupled



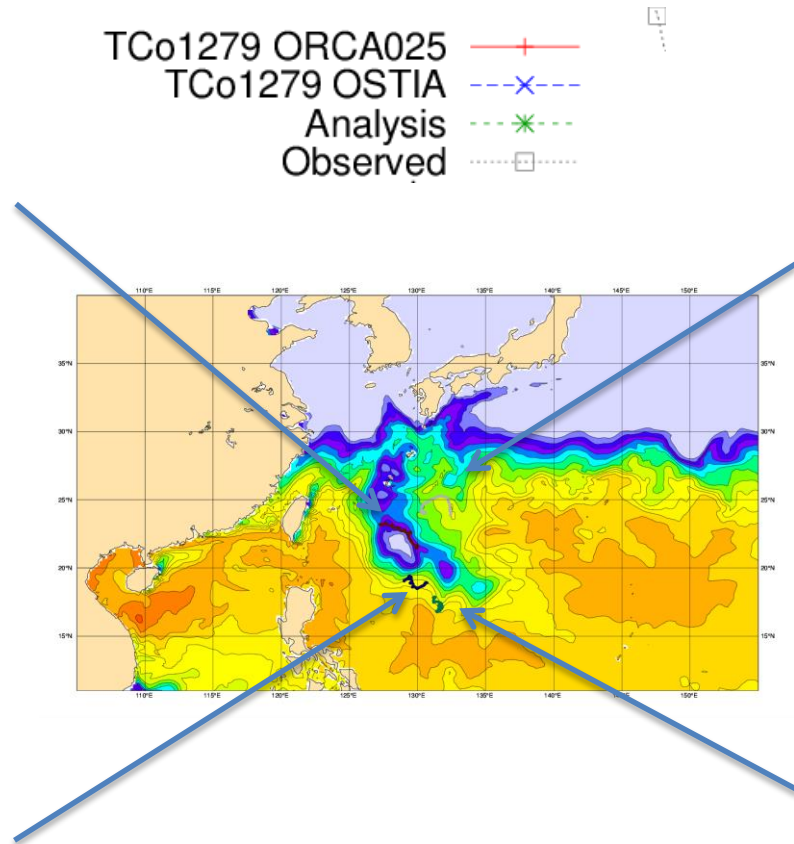
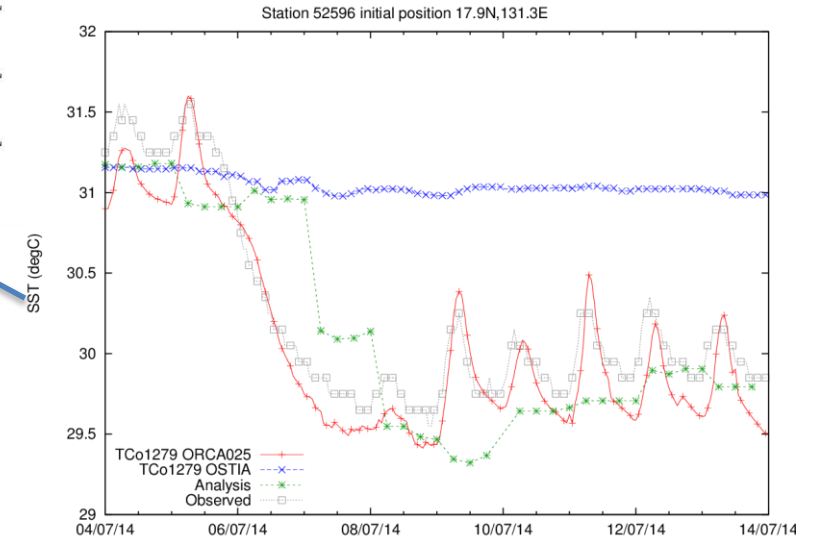
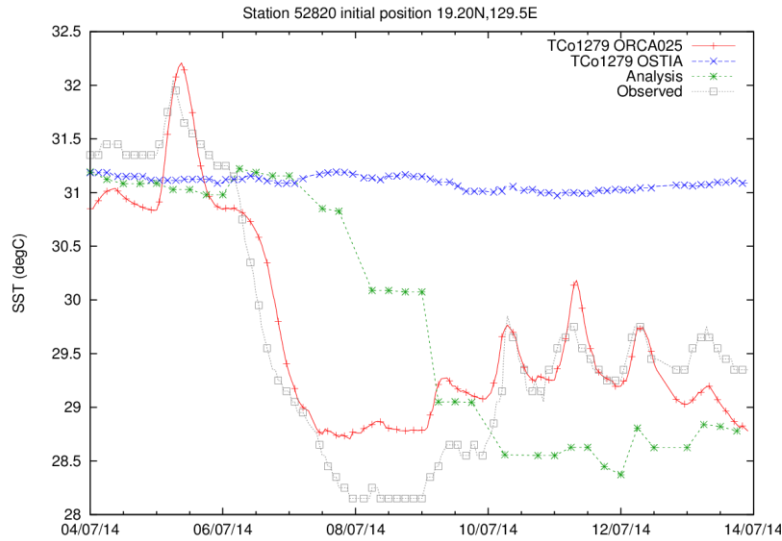
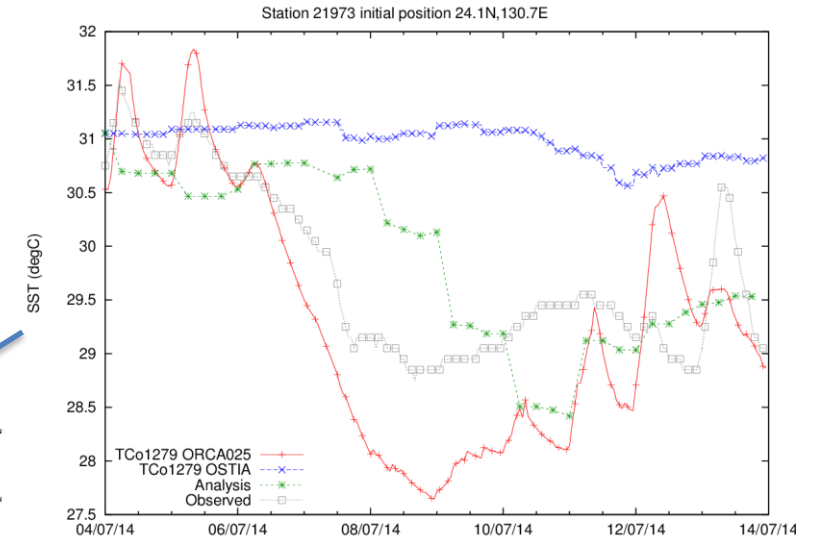
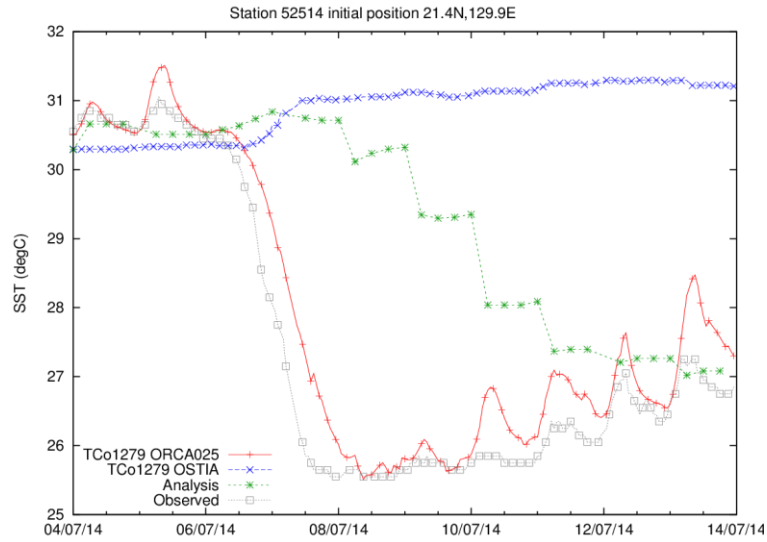
Difference in Maximum Wind speed (m/s): Coupled minus uncoupled



Difference in Maximum SWH (m): Coupled minus operational

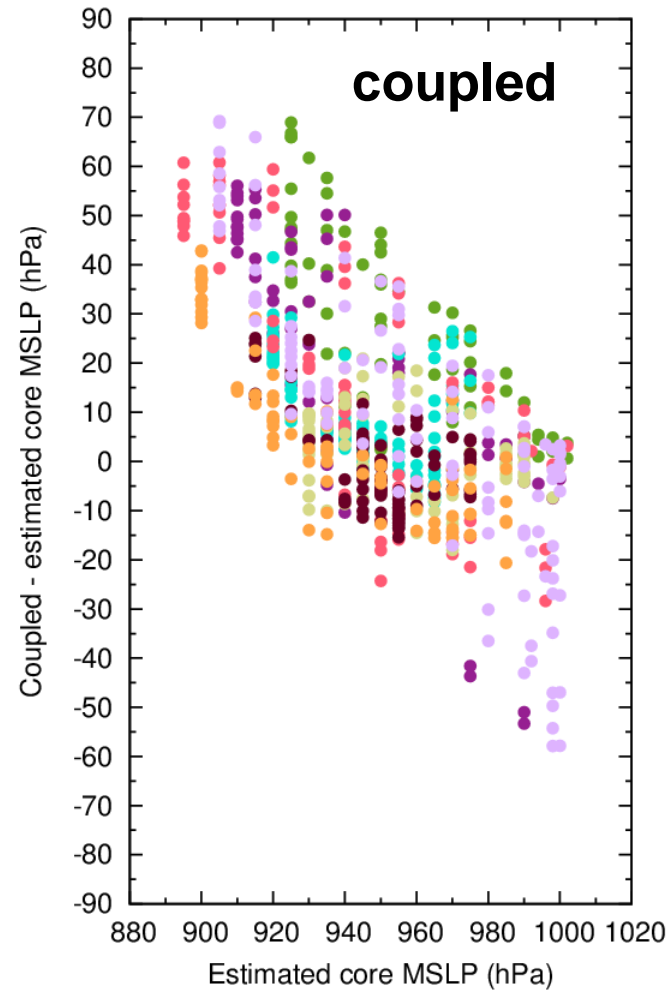
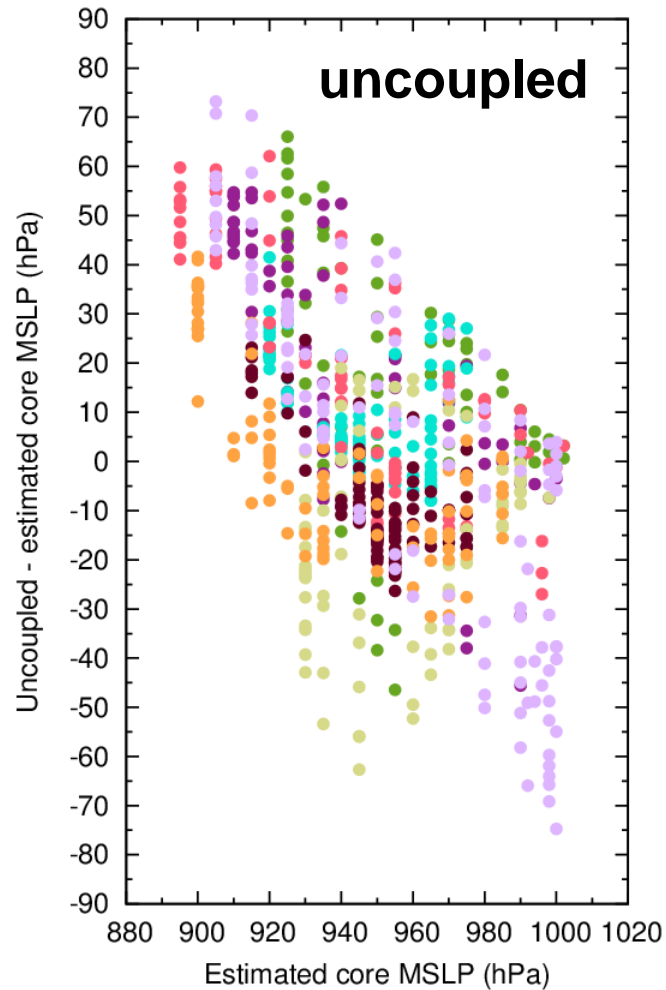


NEOGURI SST comparison with drifting buoys: TCo1279 full coupling (CY43R1).

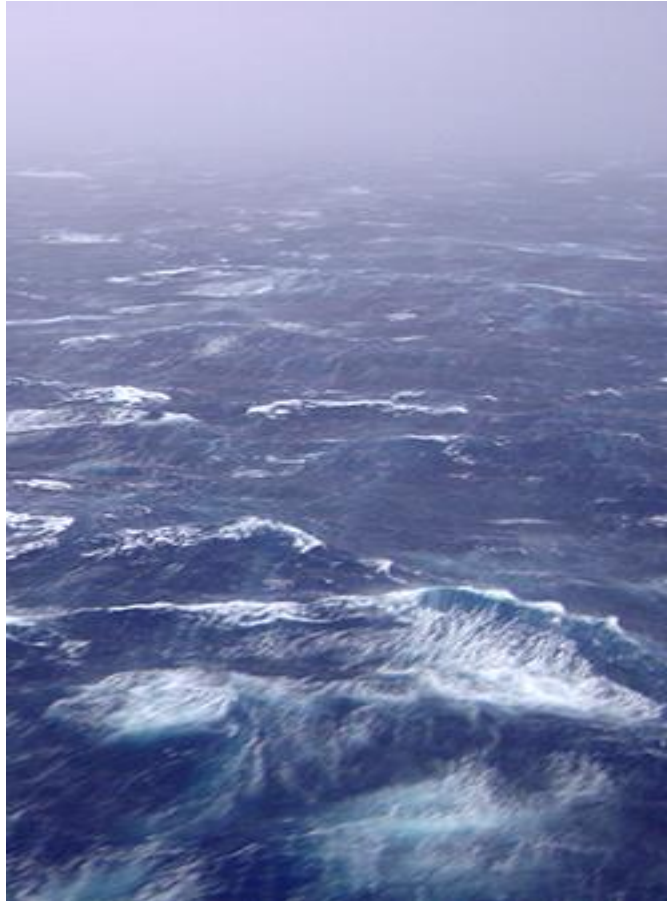


TCo1279+ORCA025 full coupling relative to uncoupled OSTIA SST

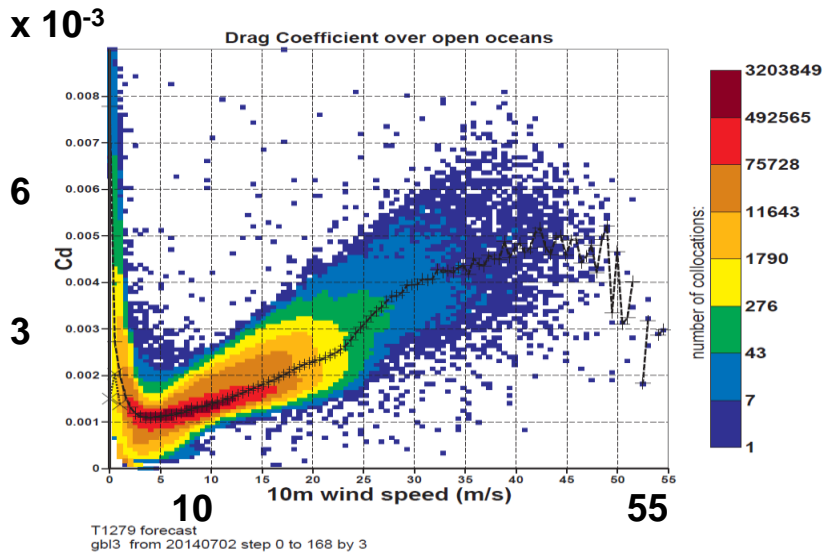
● Soulik ● Usagi ● Francisco ● Haiyan ● Neoguri ● Halong ● Vongfong ● Hagupit



Future developments:



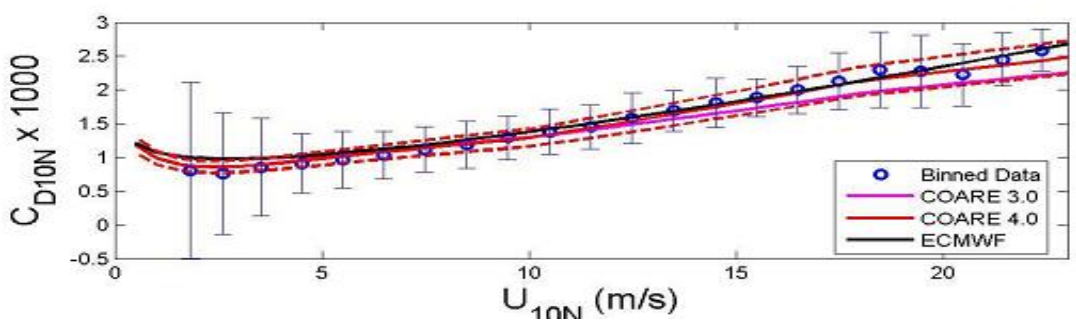
Impact of Coupling: revisit parameterisations?



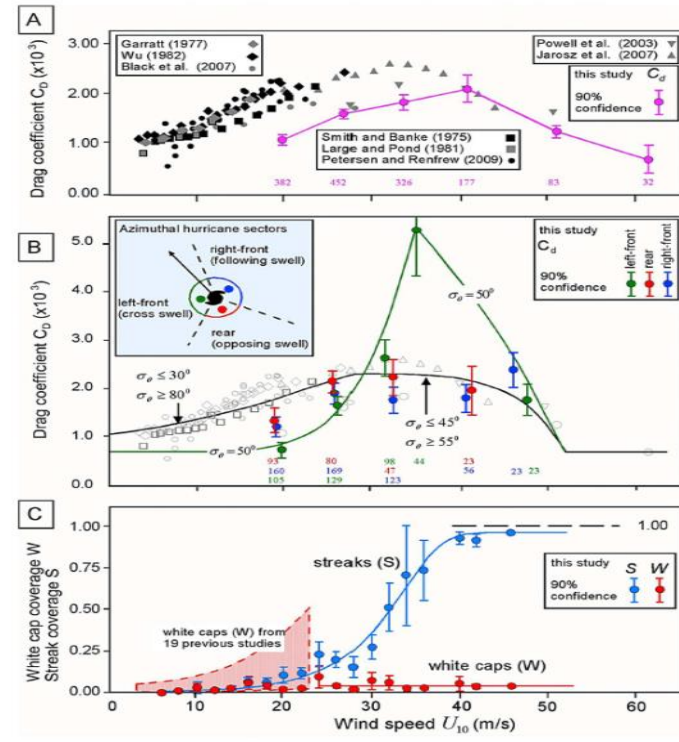
Exchange coefficients dependency on wind speed
Left: for momentum (C_d)

C_d fits well observations for winds up to 20m/s
But it might be too high for large winds

C_d is sea state dependent

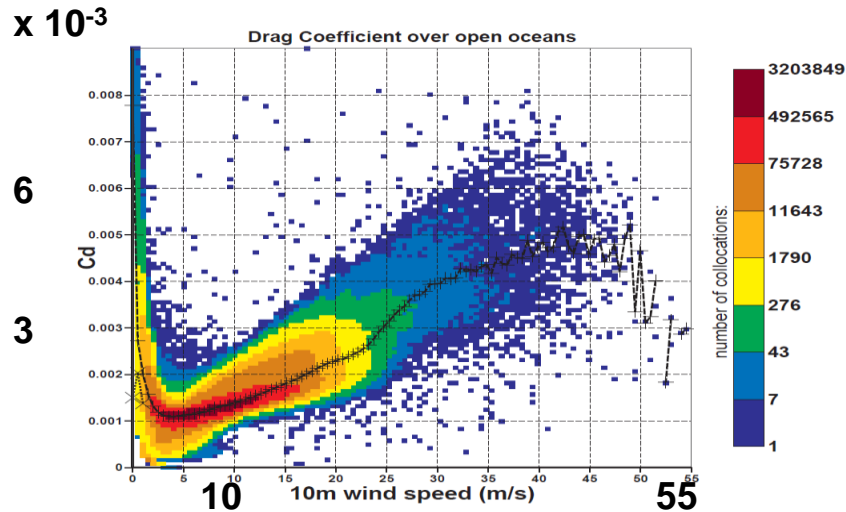


Edson et al., 2013

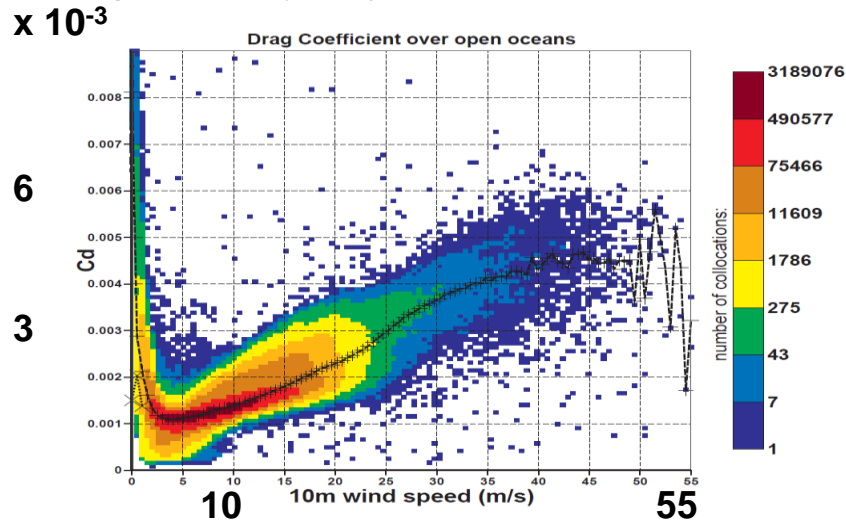


Holthuijsen et al., 2012

Impact of Coupling: revisit parameterisations?



T1279 forecast
gbl3 from 20140702 step 0 to 168 by 3



T1279 forecast
gbm2 from 20140702 step 0 to 168 by 3

In ECWAM, from about 1.3 times the peak frequency the model has an ω^{-4} spectrum which is caused by the nonlinear interactions pumping energy from the low frequency waves to the high frequency waves. In fact, we have the model spectra take the form of the Toba spectrum in that frequency range.

$$F(\omega) = \alpha_t g u_* \omega^{-4}$$

However, clearly for strong winds, hence large u_* , the Toba spectrum cannot hold because the waves in that frequency range become too steep and breaking should happen.

Therefore, we impose a limitation to the high frequency part of the spectrum based on a limiting Phillips spectrum. This is part of CY43R1.

$$F_{max}(f) = \alpha_{max} g^2 (2\pi)^{-4} f^{-5}$$

Impact of Coupling: revisit parameterisations?

Exchange coefficients
dependency on wind speed
Right: for heat (Ch)

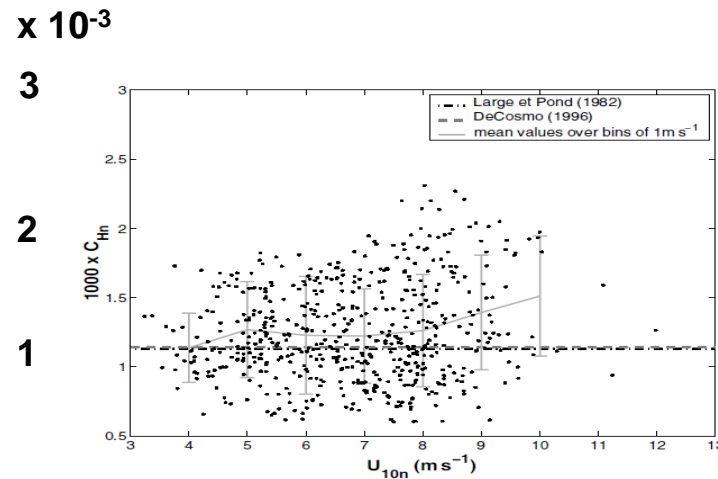
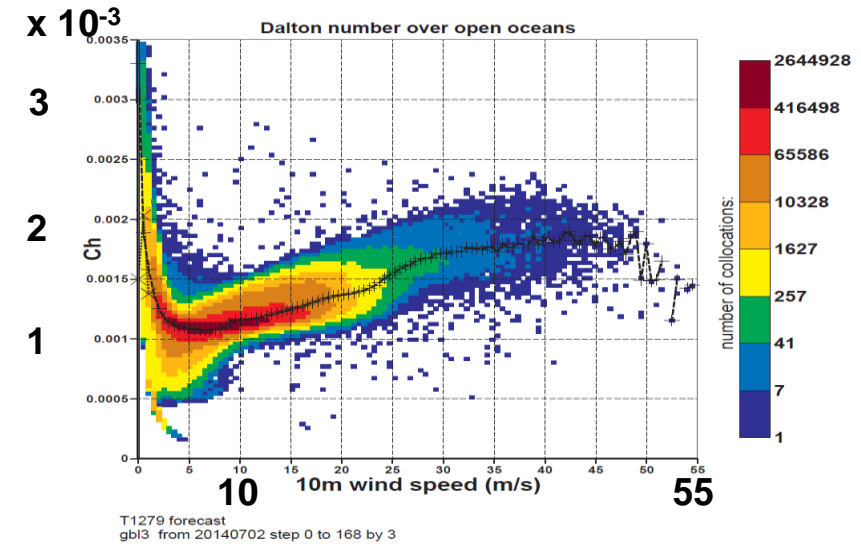


Figure 18. The exchange coefficient for temperature, C_{ht} , as a function of the neutral wind speed at 10 m, U_{10n} . The dots correspond to 30-minute samples. The solid line with error-bars represents the values averaged over wind speed bins of 1 m s^{-1} . The parameterizations proposed by Large and Pond (1982) and DeCosmo *et al.* (1996) are also plotted.

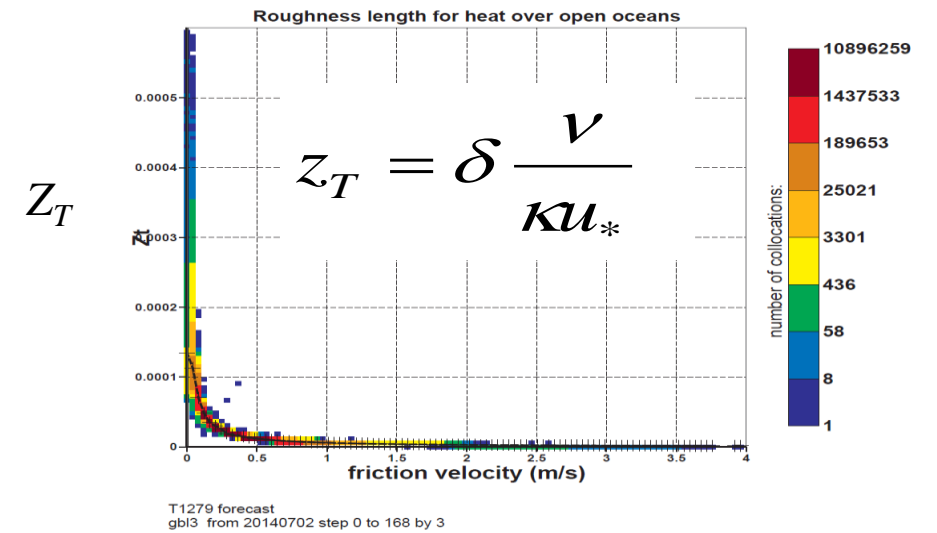
Brut et al. 2005



The current model
is underestimating a bit
the heat transfer from the
surface .

Effect of waves on heat flux :

Current operational :



Effect of waves on heat flux :

$$z_T = 10 \frac{\left(\frac{10+x_-}{x_-}\right)^{(z_1-x_-)}}{\left(\frac{10+x_+}{x_+}\right)^{(z_1-x_+)}}$$

$$x_{\pm} = (z_1 + \frac{1}{2} z_v) \mp \left\{ z_1^2 + \left(\frac{1}{2} z_v\right)^2 \right\}^{1/2}$$

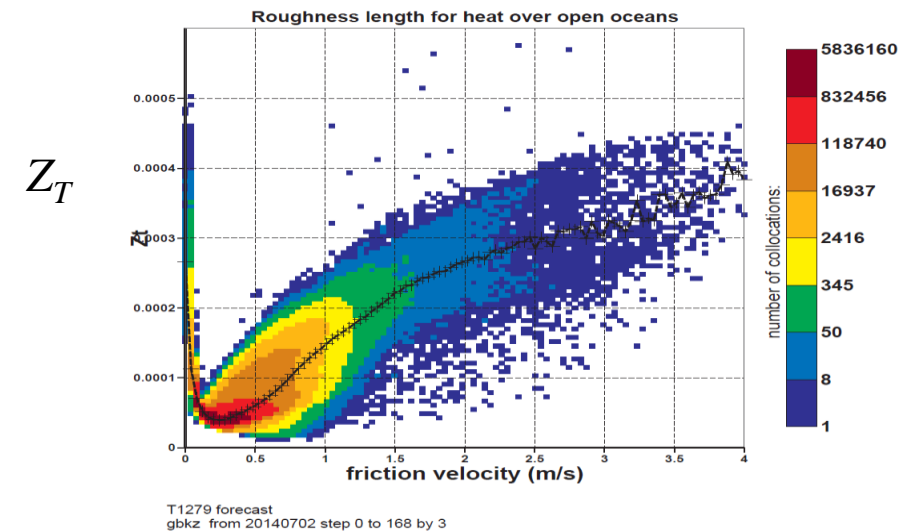
$$z_1 = \frac{\tilde{\alpha} u_*^2}{g} \left(\frac{1}{\left\{1 - \frac{\tau_w}{\tau}\right\}^{1/2}} - 1 \right) \quad z_v = \frac{\delta v}{\kappa u_*}$$

Wave induced stress:

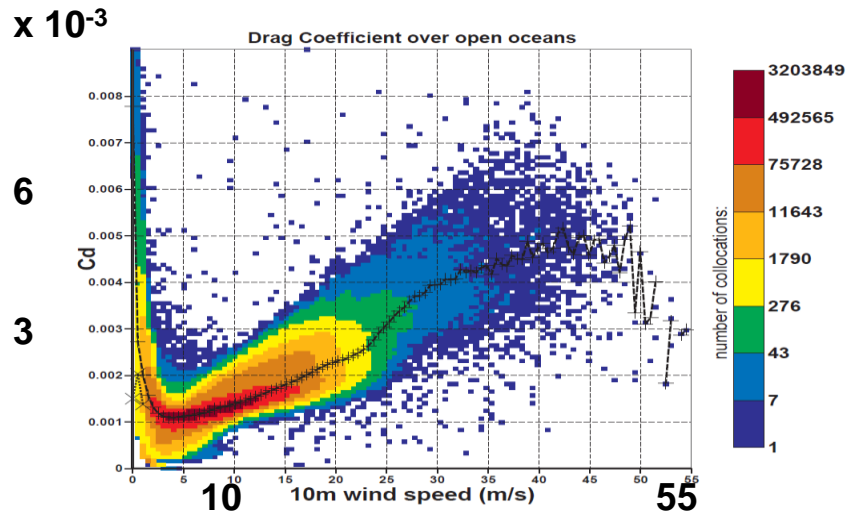
$$\tau = u_*^2 \quad \tau_w = \int d\omega d\theta \frac{k}{\omega} S_{wind}$$

Janssen, P.A.E.M., 1997: Effect of surface gravity waves on the heat flux. ECMWF Technical Memorandum 239. <http://www.ecmwf.int/en/elibrary/technical-memoranda>

Enhancing heat transfer:

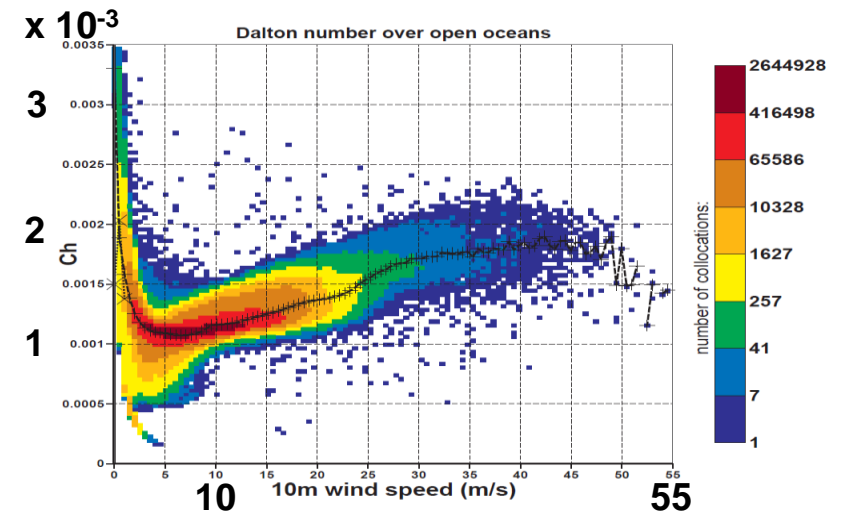


Impact of Coupling: revisit parameterisations?

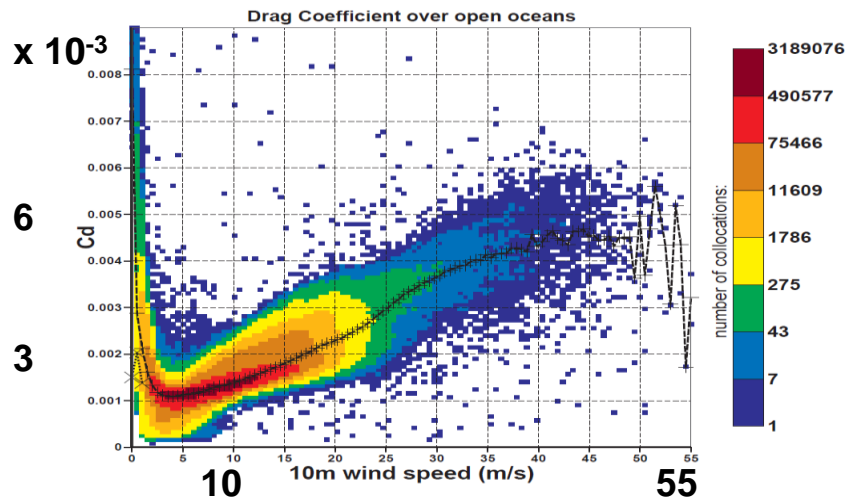


T1279 forecast
gbl3 from 20140702 step 0 to 168 by 3

Exchange coefficients
dependency on wind speed
Left: for momentum (C_d)
Right: for heat (C_h)
Operational version



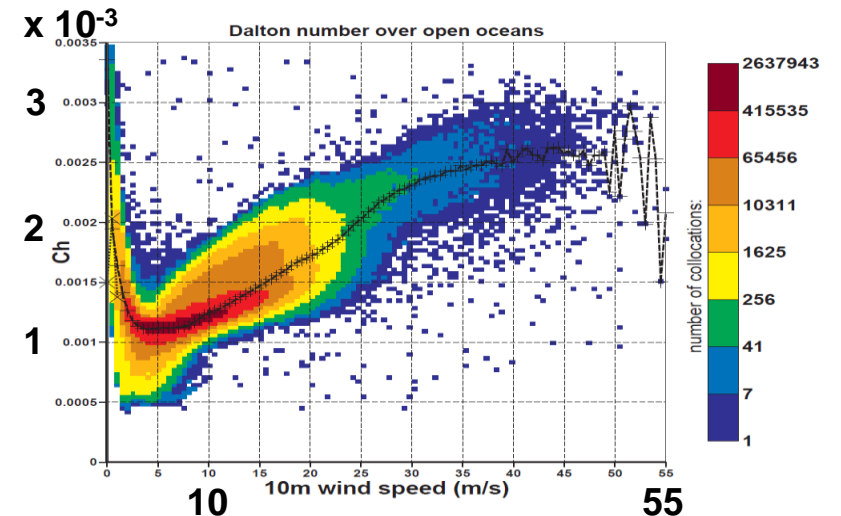
T1279 forecast
gbl3 from 20140702 step 0 to 168 by 3



T1279 forecast
gbm2 from 20140702 step 0 to 168 by 3

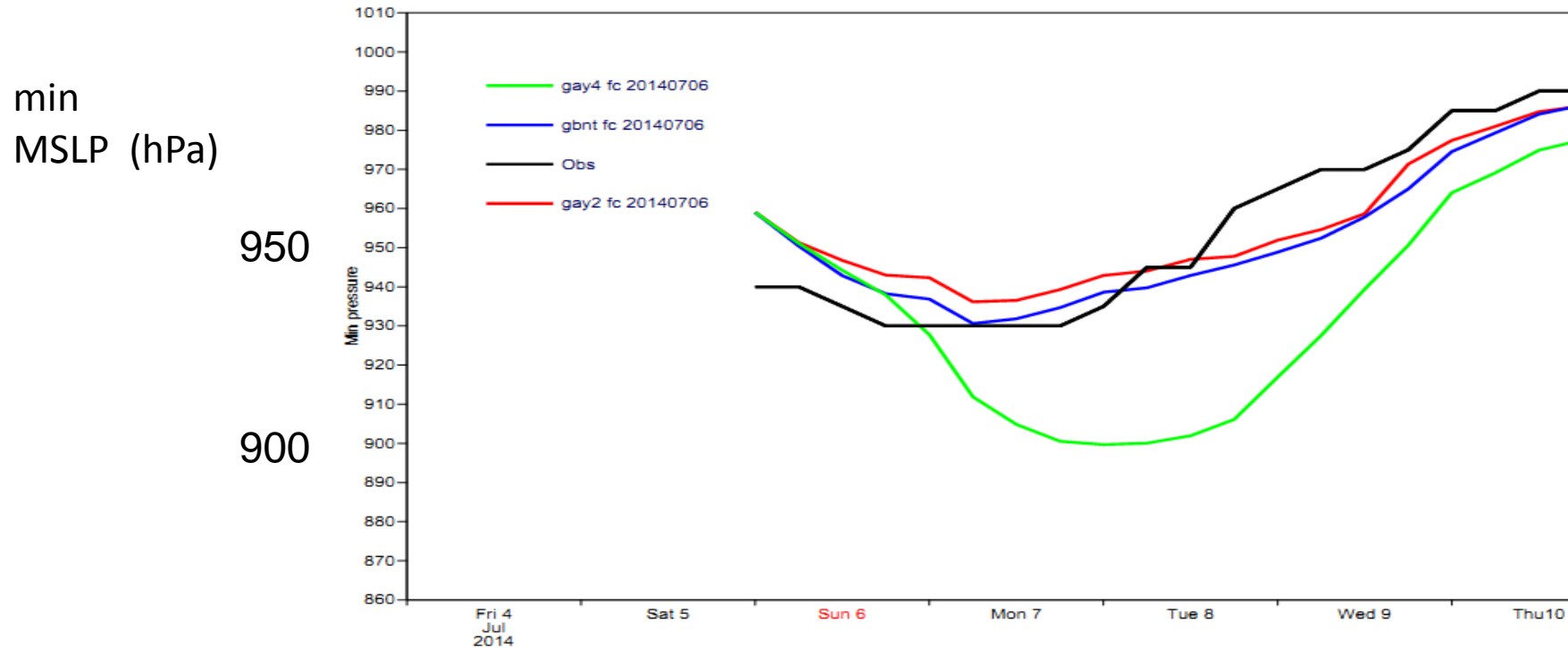
Experimental version

Sea state depend C_h
and
Maximum wave spectral
limitation.



T1279 forecast
gbm2 from 20140702 step 0 to 168 by 3

Impact of Coupling on tropical cyclone forecast



Black: estimated from observations

Green: operational HRES configuration (**uncoupled**) (16km)

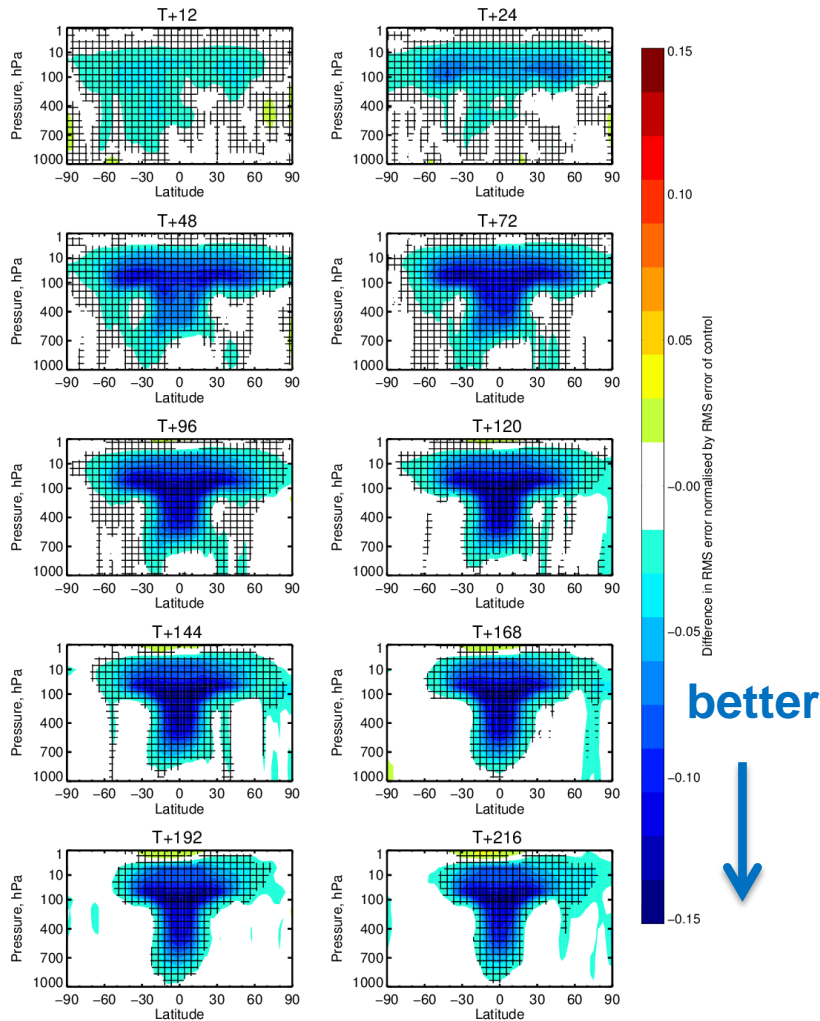
Red: 16km **coupled** to NEMO (ORCA025_Z75)

Blue: 16km **coupled to NEMO + new sea state dependant heat and moisture fluxes**

Sensitivity study: wave dependent heat and moisture fluxes

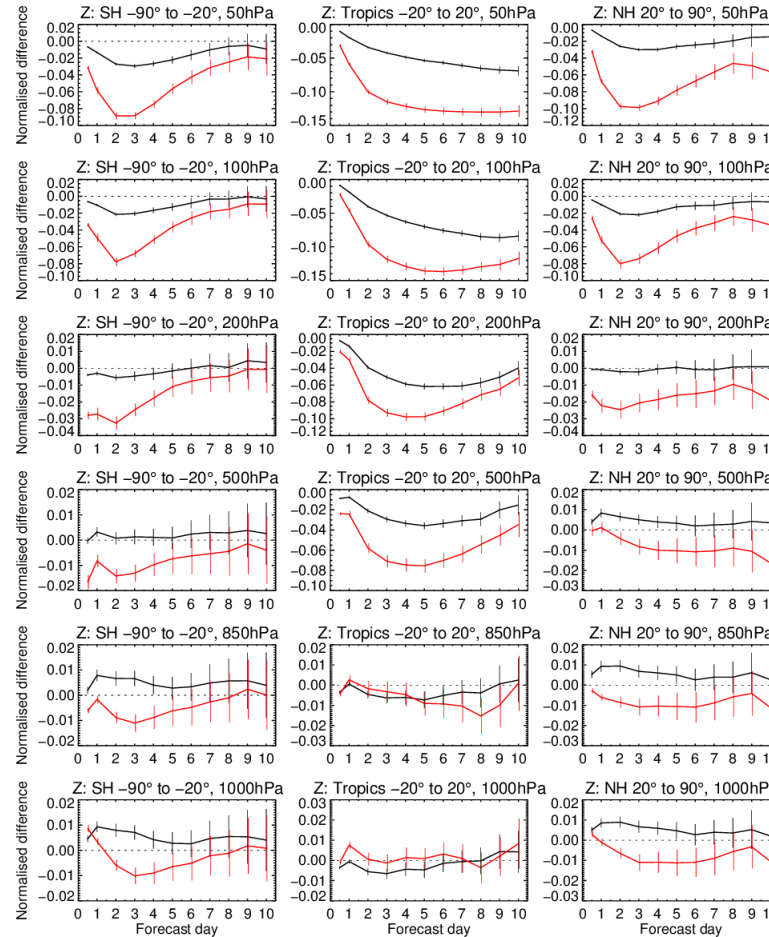
Change in error in Z (sea state dependent heatflux-Coupled_43r1 (partial coupling))

1-Jun-2015 to 30-May-2016 from 356 to 365 samples. Cross-hatching indicates 95% confidence. Verified against 0001.



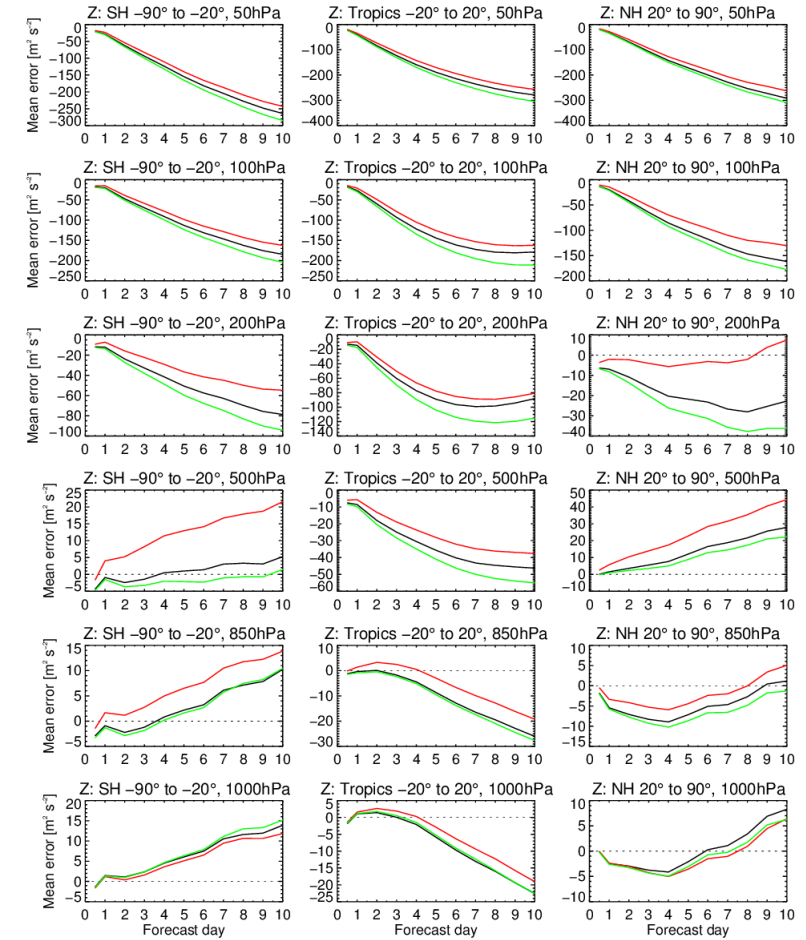
1-Jun-2015 to 30-May-2016 from 356 to 365 samples. Verified against 0001.

Confidence range 95% with AR(1) inflation and Sidak correction for 8 independent tests



— no WAM feedback to IFS - Coupled_43r1 (partial coupling)
 - - sea state dependent heatflux - Coupled_43r1 (partial coupling)

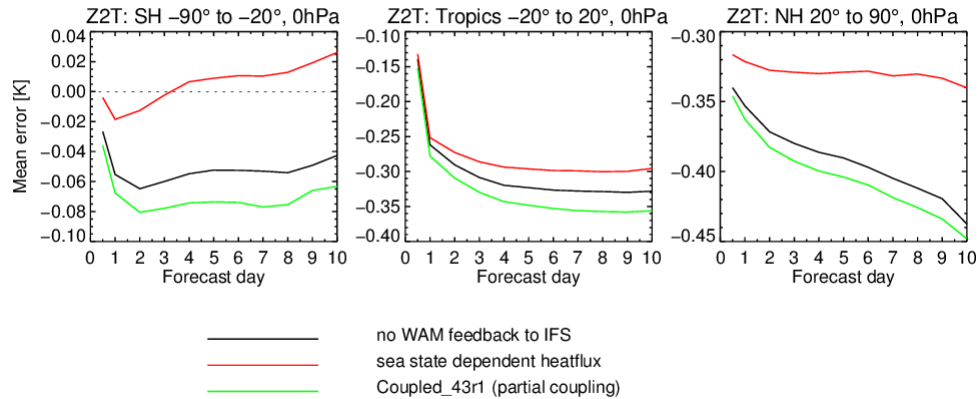
1-Jun-2015 to 30-May-2016 from 356 to 365 samples. Verified against 0001.



— no WAM feedback to IFS
 - - sea state dependent heatflux
 - - Coupled_43r1 (partial coupling)

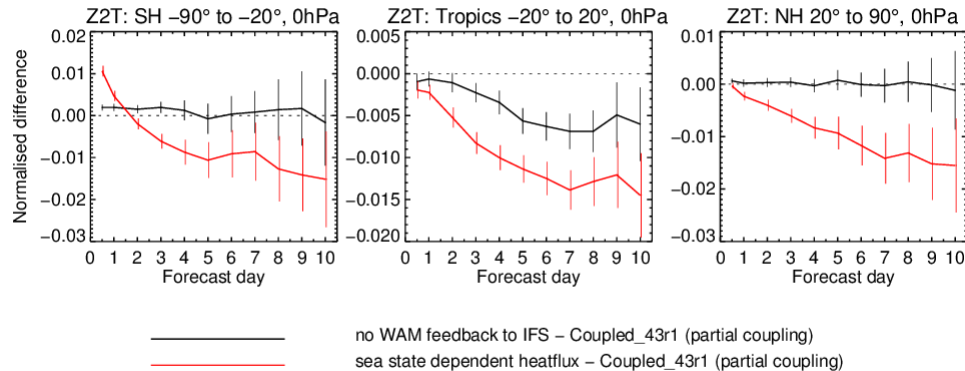
Sensitivity study: wave dependent heat and moisture fluxes

1-Jun-2015 to 30-May-2016 from 356 to 365 samples. Verified against 0001.



Mean forecast error for 2mT

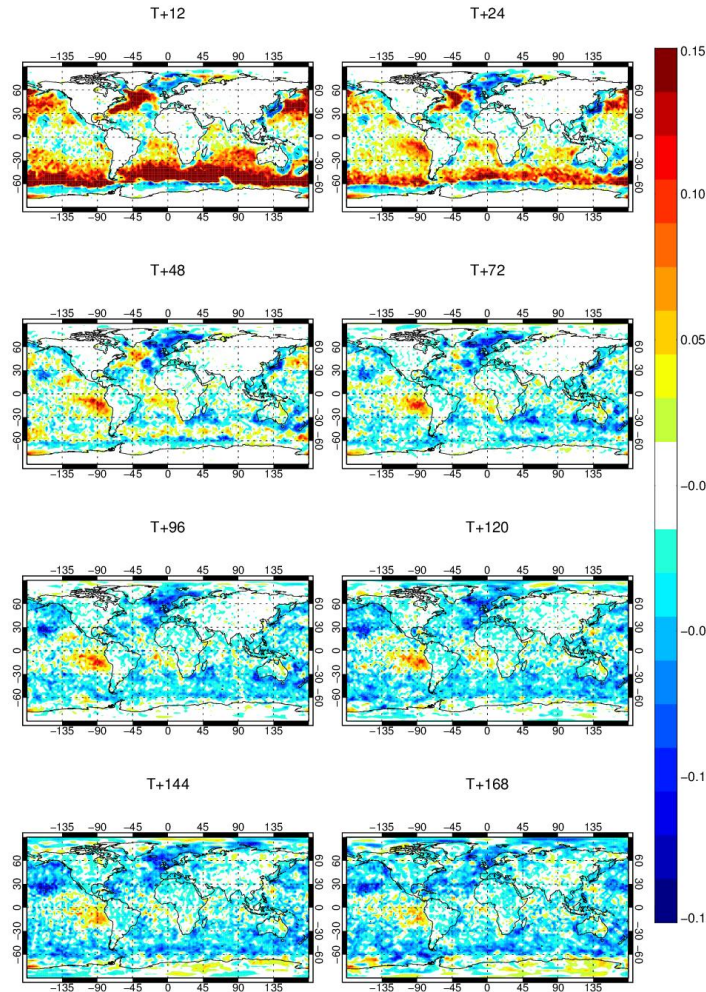
1-Jun-2015 to 30-May-2016 from 356 to 365 samples. Verified against 0001.
Confidence range 95% with AR(1) inflation and Sidak correction for 8 independent tests



Normalised difference in RMSE for 2mT

Change in error in Z2T (sea state dependent heatflux – Coupled_43r1 (partial coupling))

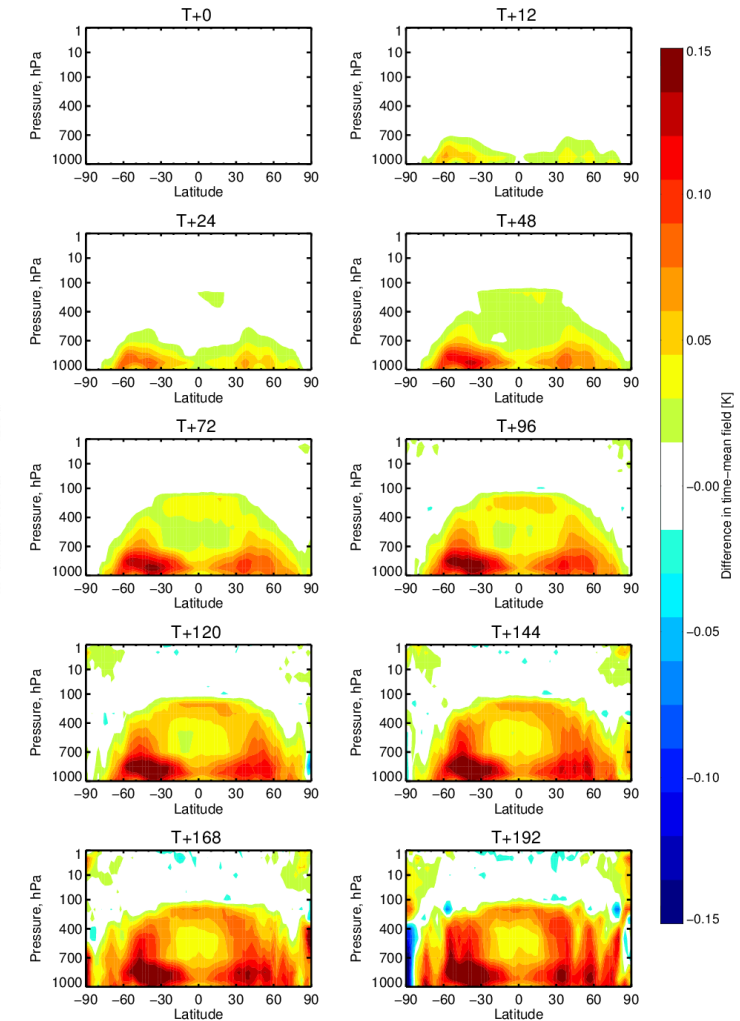
1-Jun-2015 to 30-May-2016 from 356 to 365 samples. Verified against 0001.



Normalised difference in RMSE for 2mT

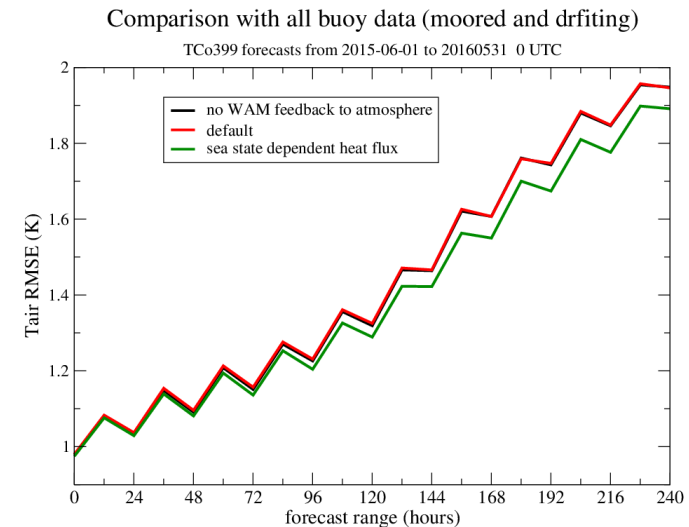
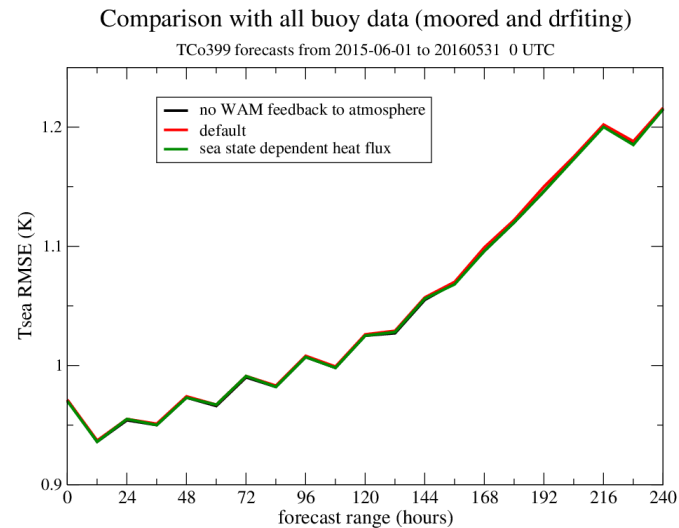
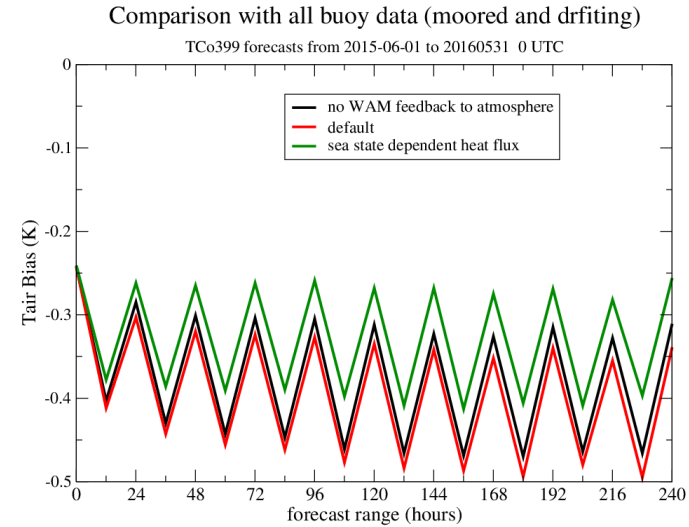
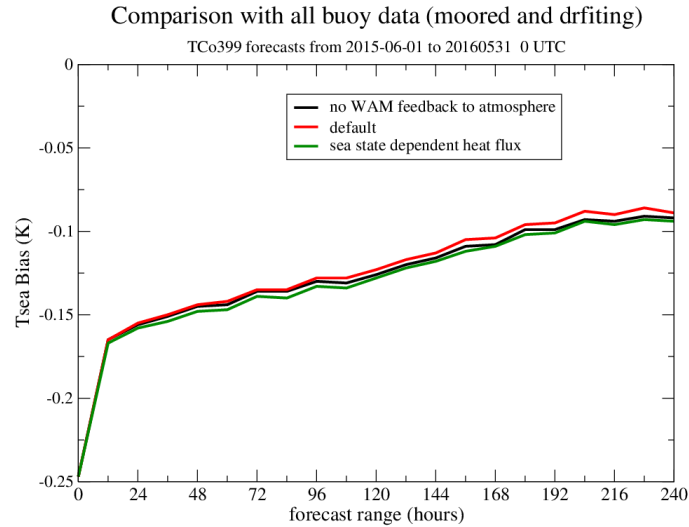
Difference in time-mean T (sea state dependent heatflux–Coupled_43r1 (partial coupling))

11-Jun-2015 to 31-May-2016 from 356 to 356 analyses.

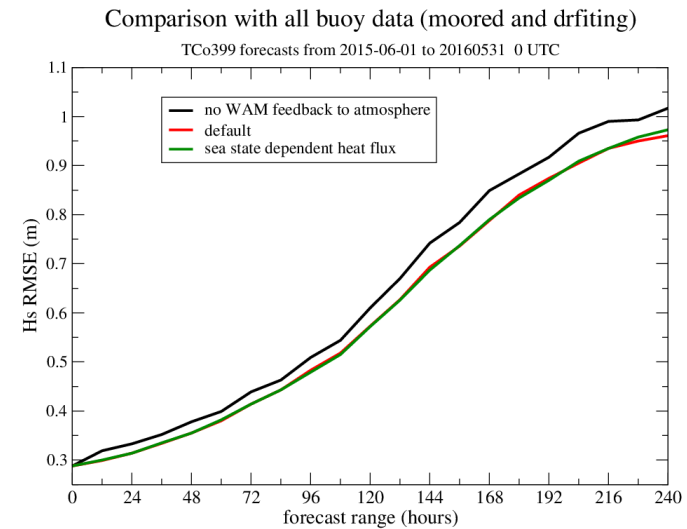
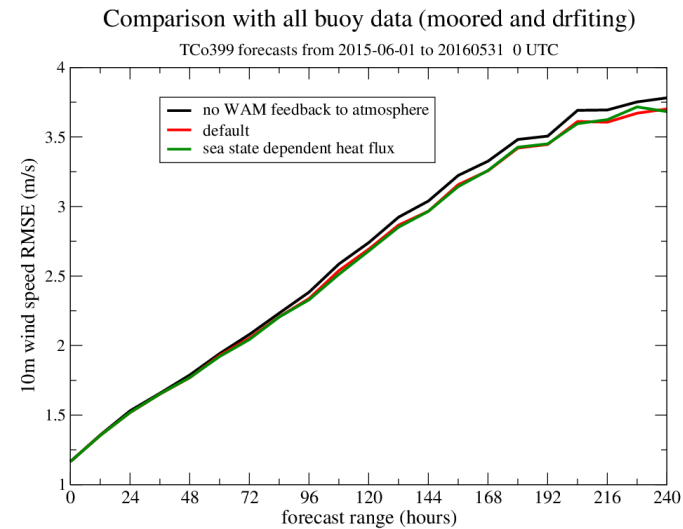
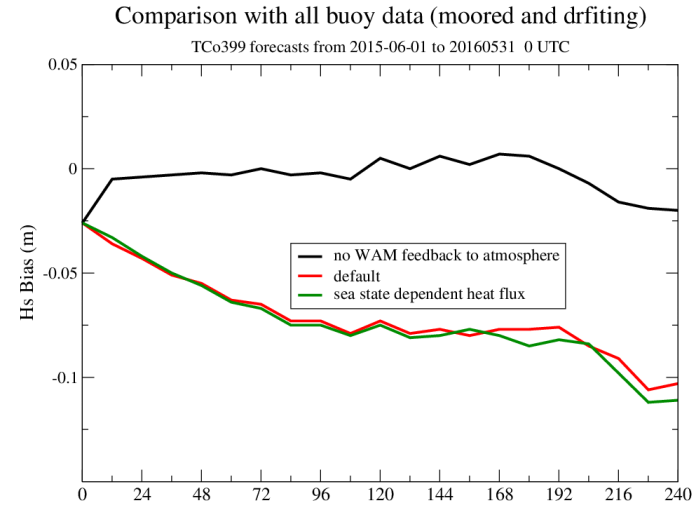
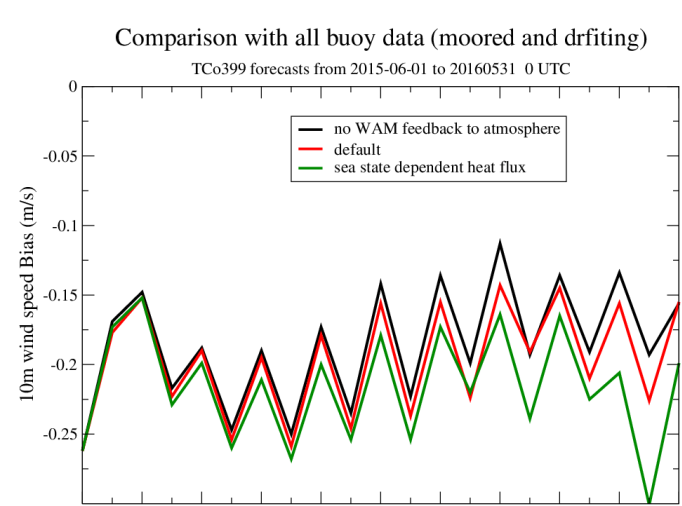


Mean forecast difference in T

Sensitivity study: wave dependent heat and moisture fluxes



Sensitivity study: wave dependent heat and moisture fluxes



Possible future developments: whitecap fraction W_F

Wave whitecap fraction is used in many parameterisations in air-sea interaction:

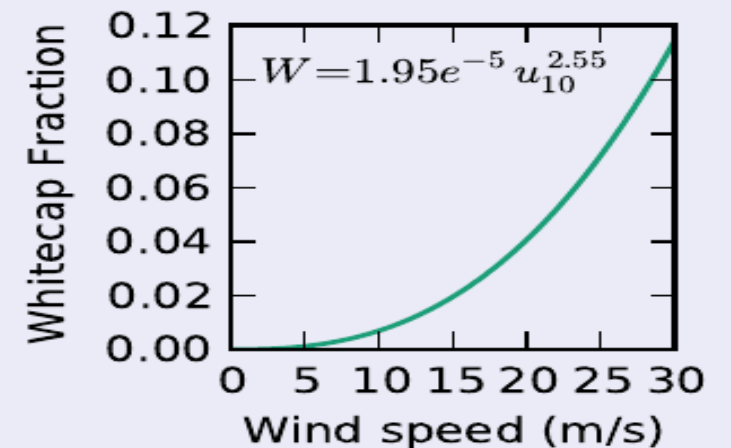
- sea spray production flux
- gas transfer velocity
- bubble production

It is also used to specify sea surface emissivity in satellite temperature radiances retrieval.

$$e = (1 - W) e_{foamfree} + W e_{foam}$$

Wave whitecap fraction is usually modelled in terms of wind speed:

[Monahan and O'Muircheartaigh, 1986]



Possible future developments: whitecap fraction W_F

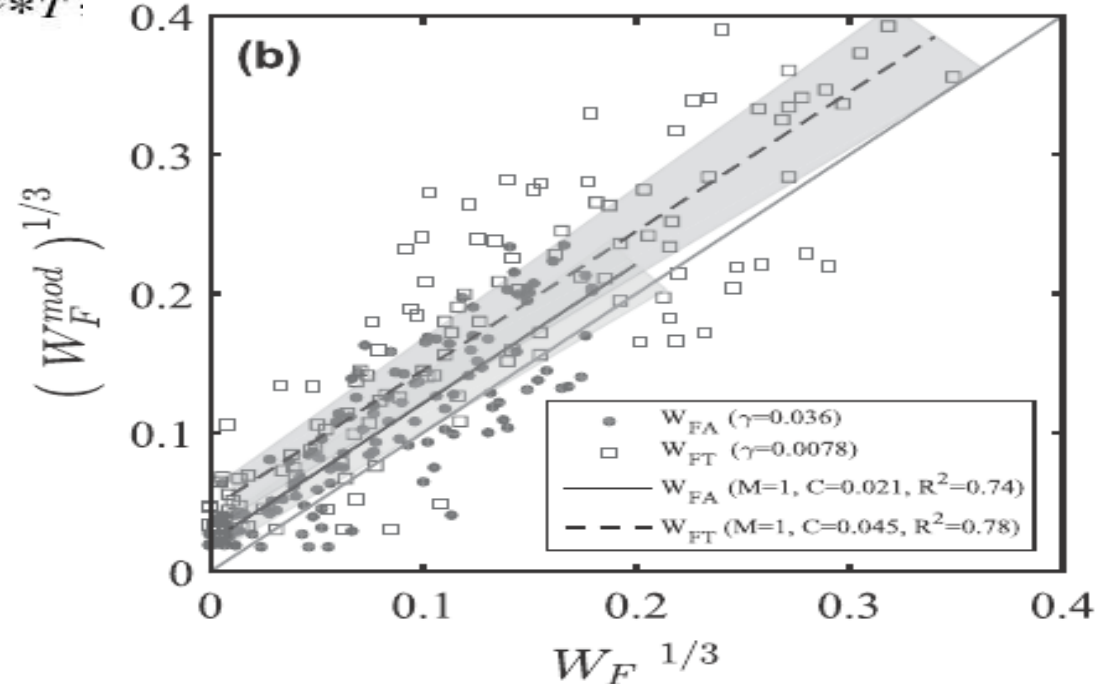
But, following work by Kraan et al. 1996, Scalon et al. (2016) showed that it can be modelled quite well using the wave model whitecap dissipation source term:

$$W_F^{\text{mod}} = \begin{cases} \frac{\Phi_{\text{oc}}}{\gamma \rho_w g \omega E} \left(\frac{u_* - u_{*T}}{u_*} \right)^3 & u_* > u_{*T} \\ 0 & u_* \leq u_{*T} \end{cases}$$

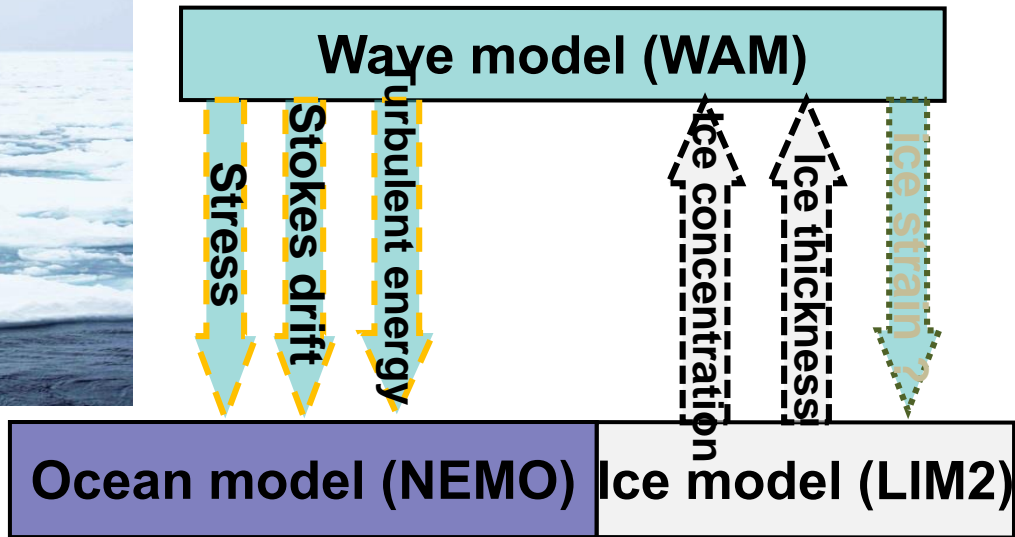
$$u_{*T} = 0.065 \text{ m s}^{-1}$$

$$E = (H_s/4)^2$$

$$\Phi_{\text{oc}} = \rho_w g \int_0^{2\pi} \int_0^\infty S_{\text{ds}} d\omega d\theta$$



Future developments: wave sea-ice interaction



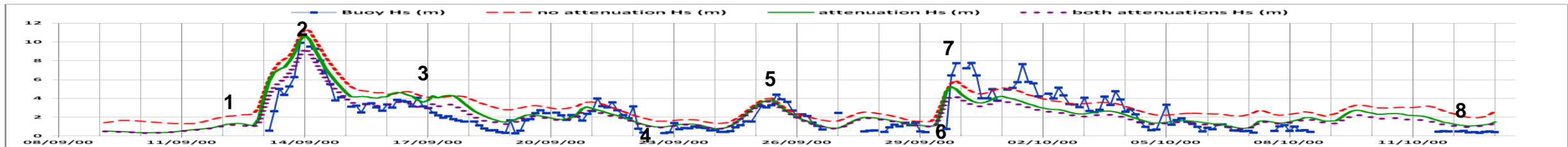
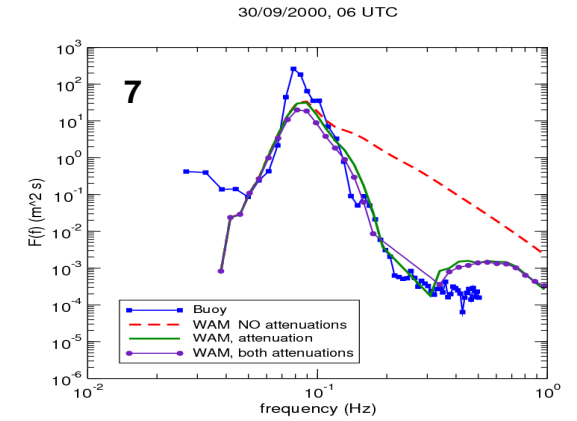
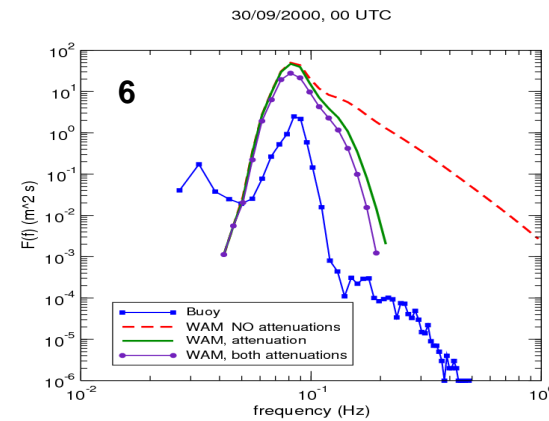
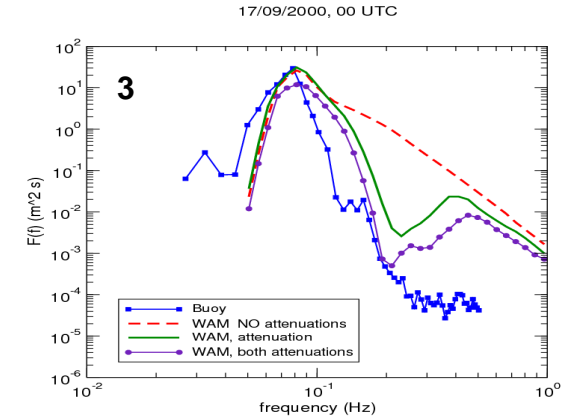
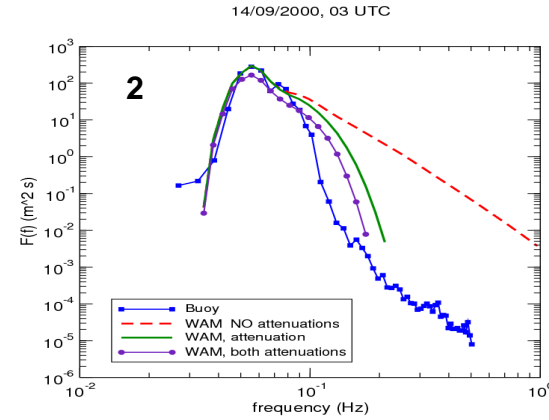
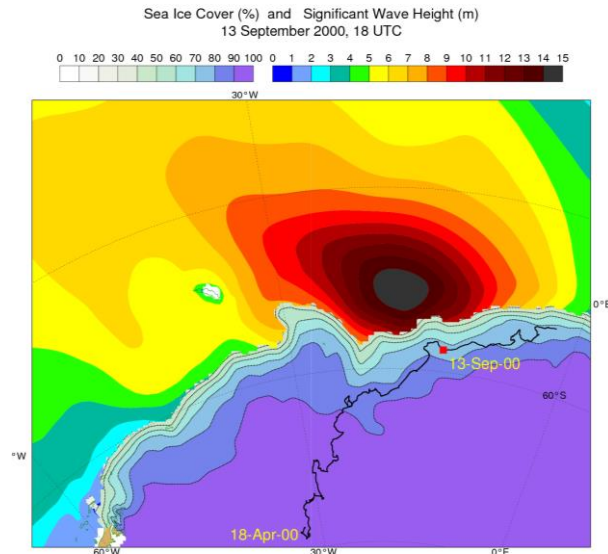
Sea ice attenuates waves,
and waves contribute to sea ice break-up and freeze-up.

Several parameterisations have been developed to deal with waves attenuation.

How waves affect sea ice is now an new field of research.

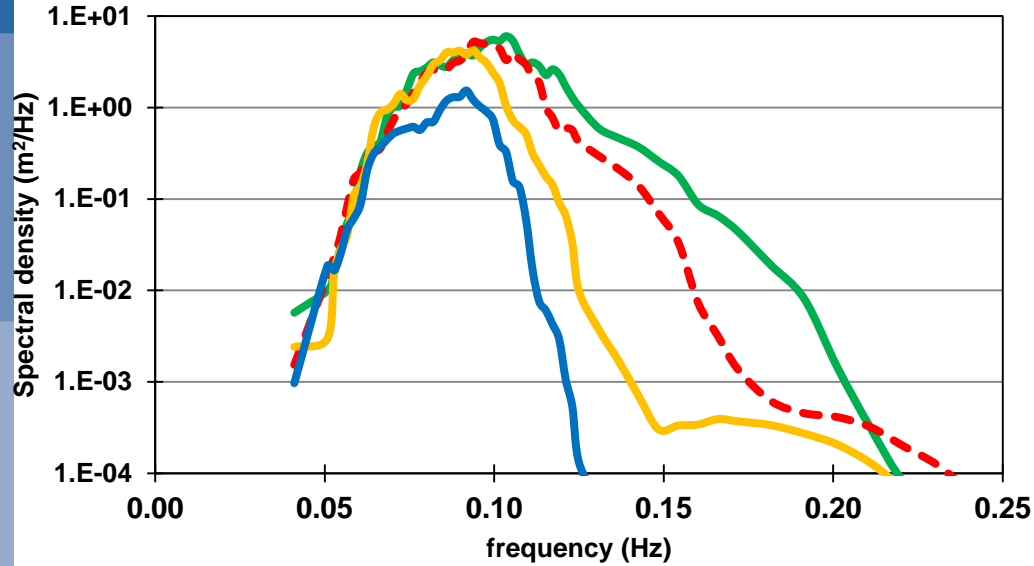
Sea ice damping modeling: simple scattering model in ECWAM

One buoy survive the winter in sea ice in the Weddell Sea and reported waves after being dislodged by a big storm.

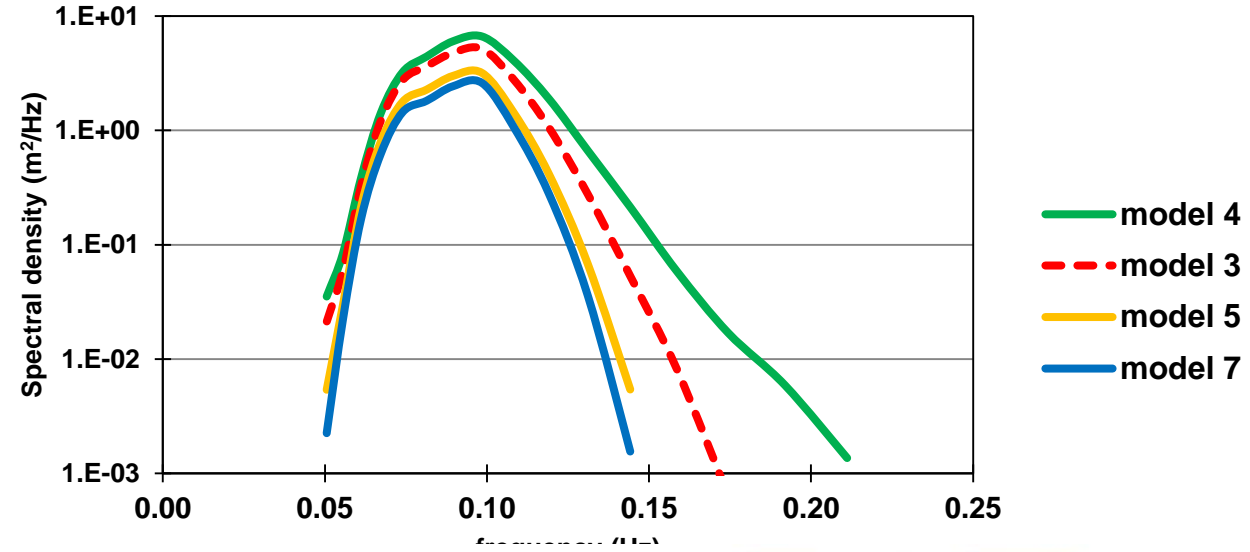


Sea ice damping modeling: simple scattering model in ECWAM

in-situ observations on 25/09/2012, 00 UTC



model on 25/09/2012, 00 UTC

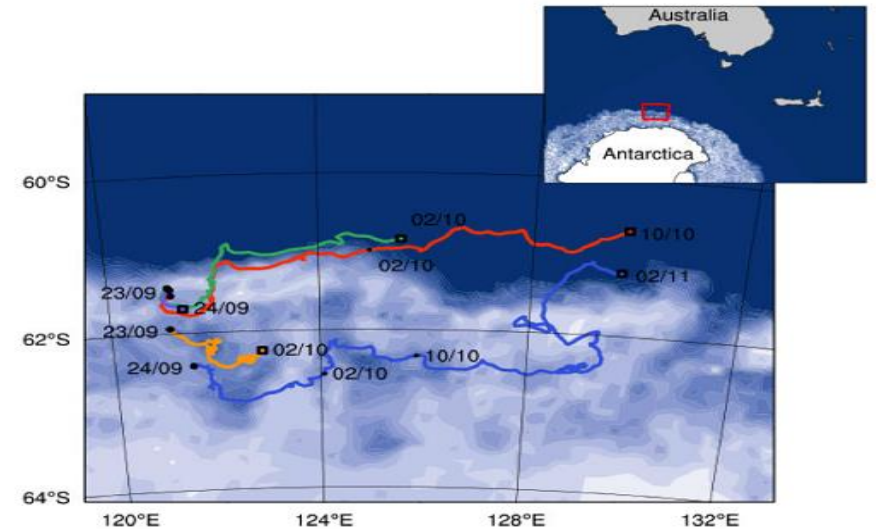


LETTER

doi:10.1038/nature13262

Storm-induced sea-ice breakup and the implications for ice extent

A. L. Kohout¹, M. J. M. Williams², S. M. Dean² & M. H. Meylan³



Sea ice damping modeling: simple viscoelastic model in WW3

From Rogers et al. 2016.
Data from the Sea State DRI
from the Beaufort Sea

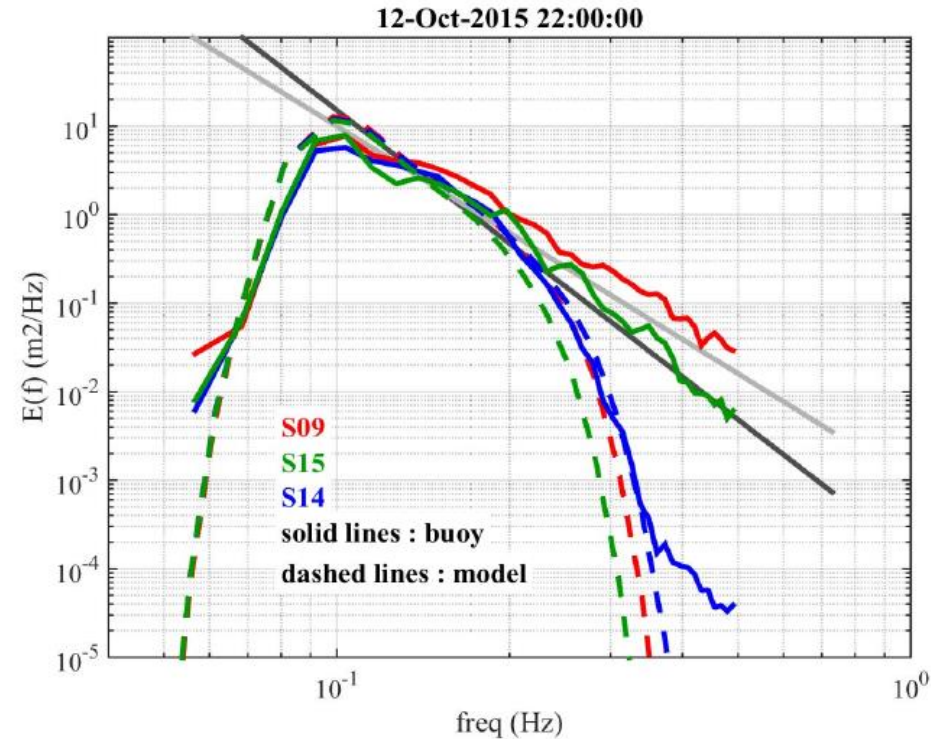


Figure 6. Example comparisons of 1-d spectrum, for three different SWIFT buoys, corresponding to the same time (2200 UTC 12 October). Dark and light gray lines correspond to an f^5 and f^4 tail slope, respectively. Solid red, dark green, and blue lines are measured spectra. Corresponding dashed lines are from the model hindcast.

All these modelling efforts are currently limited by the lack of detailed sea ice information, particularly affecting the tail of the spectrum

Conclusions:

ECMWF has a fully coupled atmosphere-wave-ocean circulation forecasting system, currently operational in the Ensemble Prediction System.

Work is ongoing on using a higher resolution ocean components (ORCA025z75) planned for end of 2016 in the Ensemble forecasts and later in the High resolution system.

There is a clear benefit in coupling the different models, but it creates new challenges as model parameterisations will need revisiting and new processes might need to be added.

Thank you for your attention ...

Øyvind Breivik, Kristian Mogensen, Jean-Raymond Bidlot, Magdalena Alonso Balmaseda, and Peter A.E.M. Janssen, 2015: Surface Wave Effects in the NEMO Ocean Model: Forced and Coupled Experiments. JGR, doi: 10.1002/2014JC010565

Janssen, P.A.E.M., 1997: Effect of surface gravity waves on the heat flux. ECMWF Technical Memorandum 239. <http://www.ecmwf.int/en/elibrary/technical-memoranda>

Rodwell et al., 2015: New Developments in the Diagnosis and Verification of High-Impact Weather Forecasts. ECMWF Technical Memorandum 759. <http://www.ecmwf.int/en/elibrary/technical-memoranda>

Brian Scanlon, Øyvind Breivik, Jean-Raymond Bidlot and Peter A. E. M. Janssen, Adrian H. Callaghan, Brian Ward, 2016: Modeling Whitecap Fraction with a Wave Model, J. Phys. Oceanogr., 46, 887-894. DOI: <http://dx.doi.org/10.1175/JPO-D-15-0158.1>

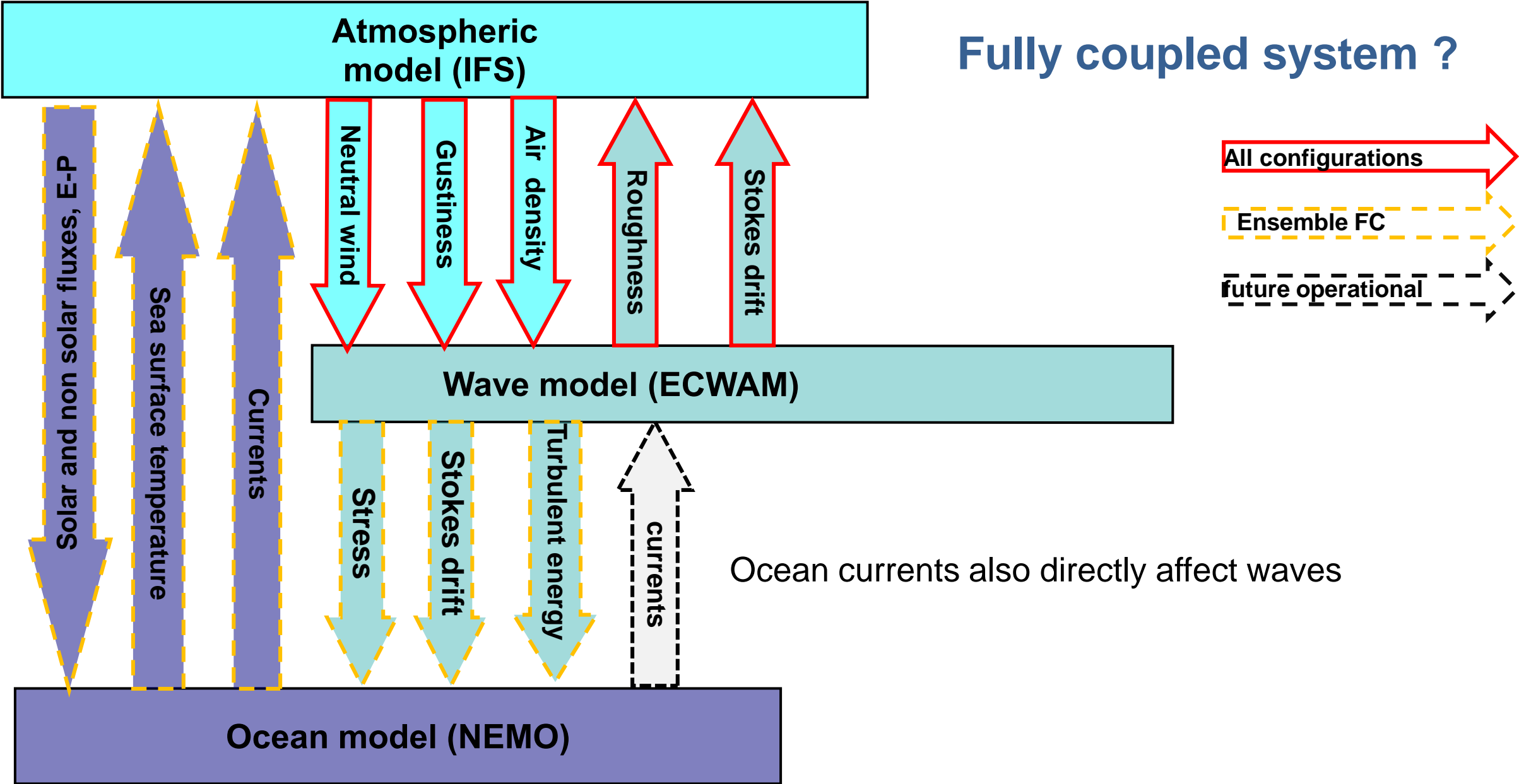
Extra slides

Partial coupling:

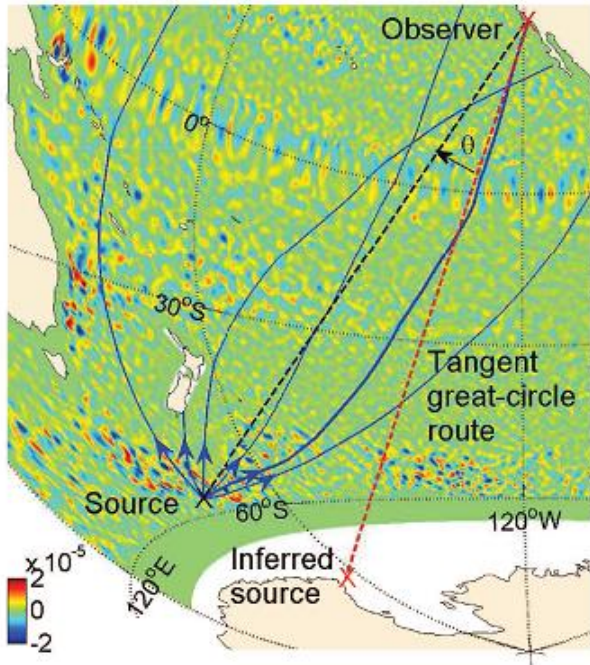


Figure 2: Partial coupling of the SST: At initial conditions the OSTIA SSTs at high resolution is evolving using the SST tendencies from the NEMO model applying an offset to ORAS SST. After 4-days of forecast integration the offset in temperatures between OSTIA and ORAS5 is progressively reduced towards 0 at day 8 when the SST is fully driven by NEMO model.

Fully coupled system ?



Ocean surface current impact on waves:



Gallet B. and Young W.R., 2014, JMR 72

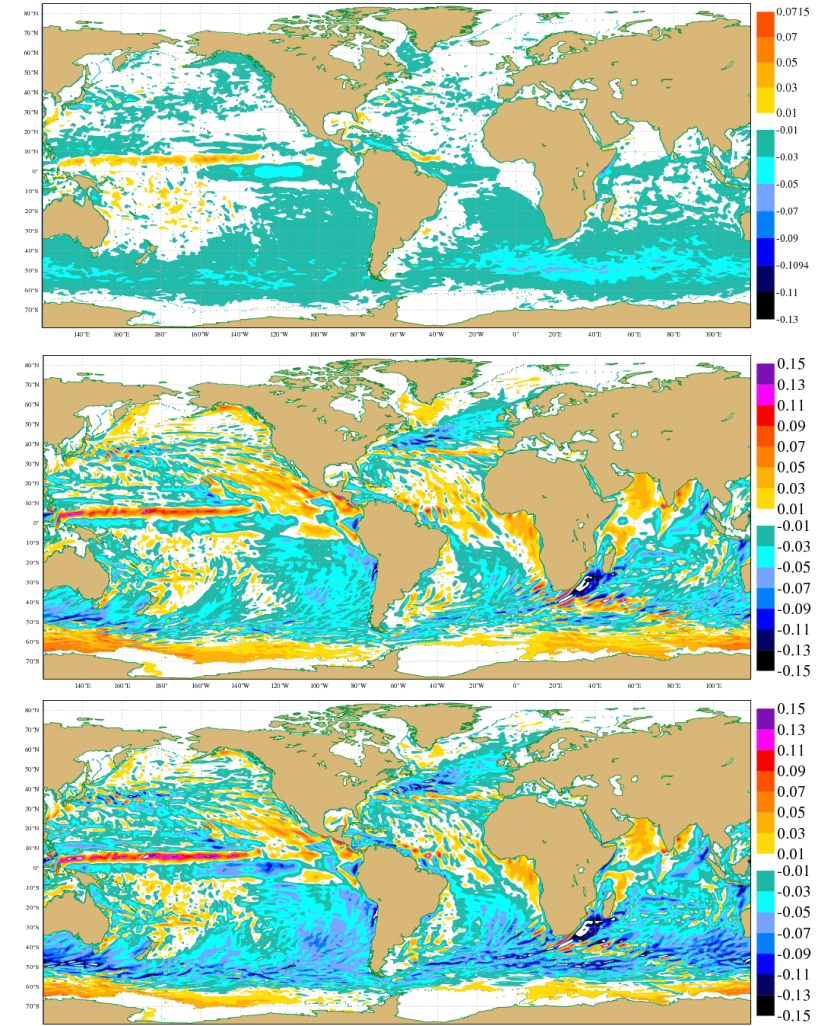
Impact of modified winds due to currents on waves

Direct impact of currents on waves

Combined impact of currents on waves

Currents – no currents

Mean wave height difference (ffxl wave - ffxd wave)
from 20091228 0Z to 20100228 18Z

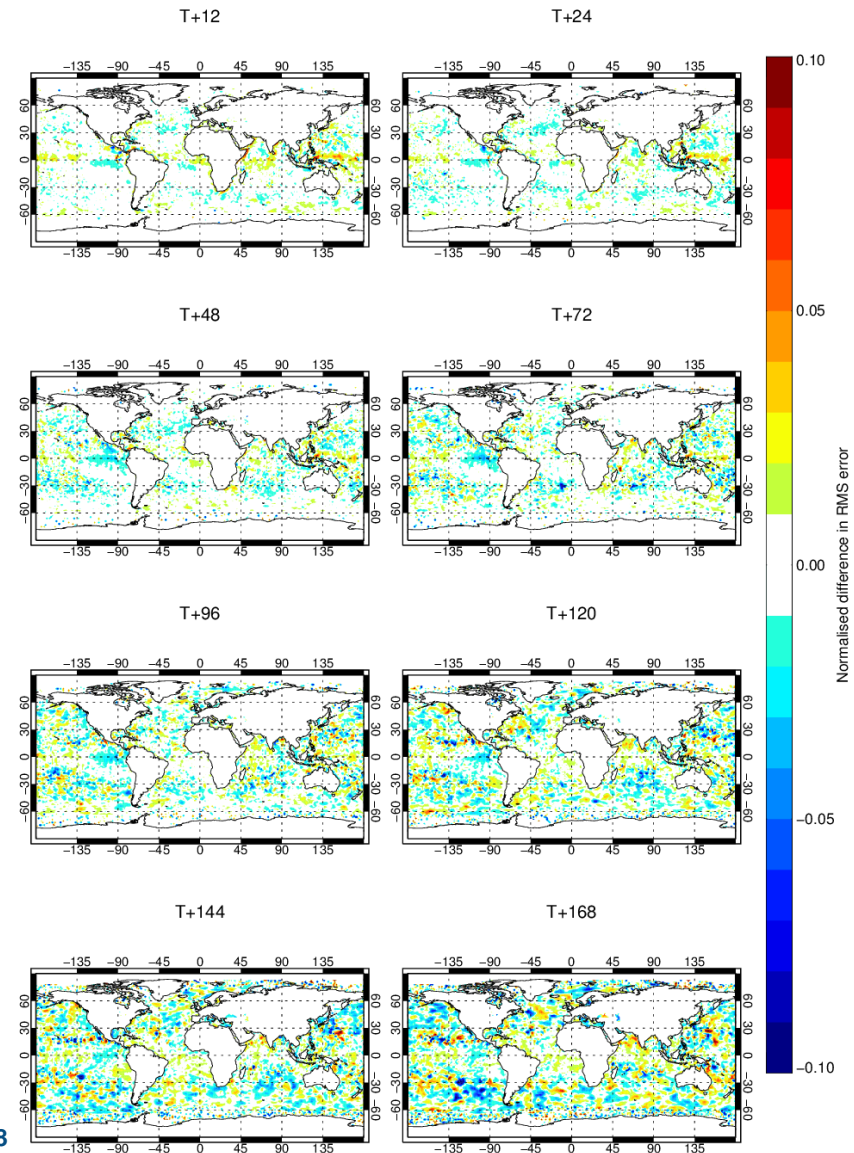


Bidlot J, 2012, ECMWF research memo

Sensitivity study:

Change in error in SWH (Partial Coupling with sfc currents in WAM – Coupled_43r1 (partial coupling))

1-Jun-2015 to 30-May-2016 from 356 to 365 samples. Verified against 0001.



Ocean Wave Modelling

The 2-D spectrum follows from the energy balance equation (in its simplest form: deep water case, no surface currents):

$$\frac{\partial F}{\partial t} + \vec{V}_g \cdot \nabla F = S_{in} + S_{nl} + S_{diss}$$

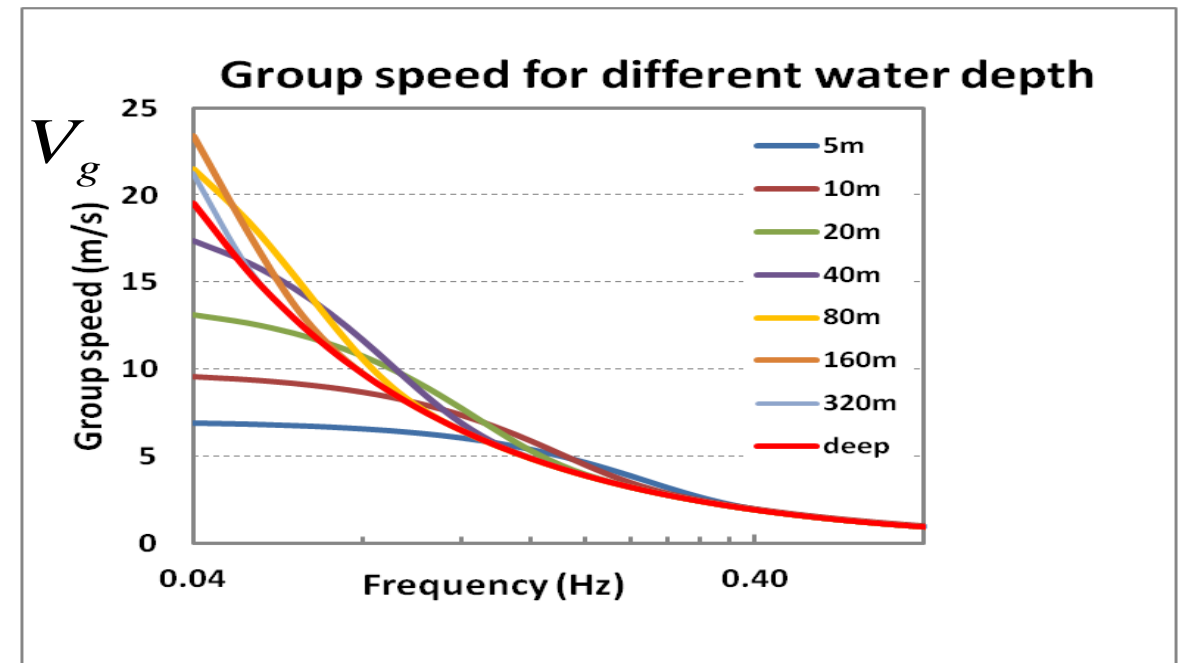
Where the group velocity \mathbf{V}_g is derived from the dispersion relationship which relates frequency (f) and wave number (k) for a given water depth (D).

$$\omega^2 = g k \tanh(k D)$$

$$V_g = \frac{\partial \omega}{\partial k}$$

$$\omega = 2\pi f$$

D: water depth



Sensitivity study: Stokes to IFS (double counting)?

ORCA025_Z75 has a much finer vertical resolution than ORCA1_Z42

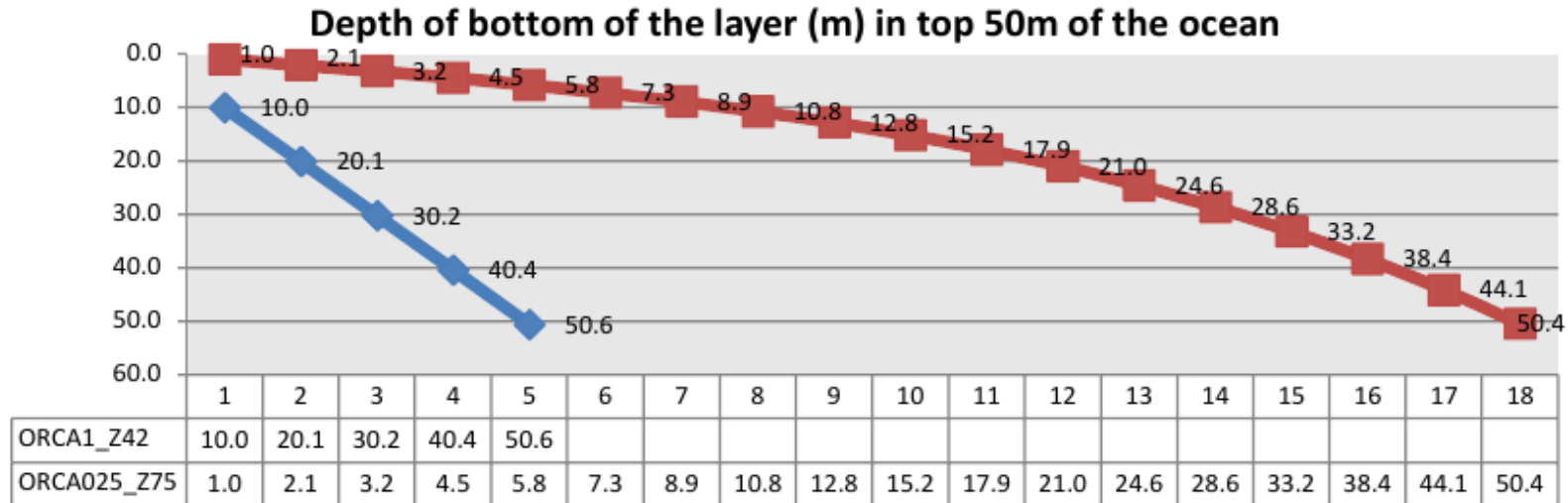


Figure 1: Vertical discretisation of the ocean layers in the top 50m below the surface in ORCA1_Z42 (blue) and ORCA025_Z75 (red).

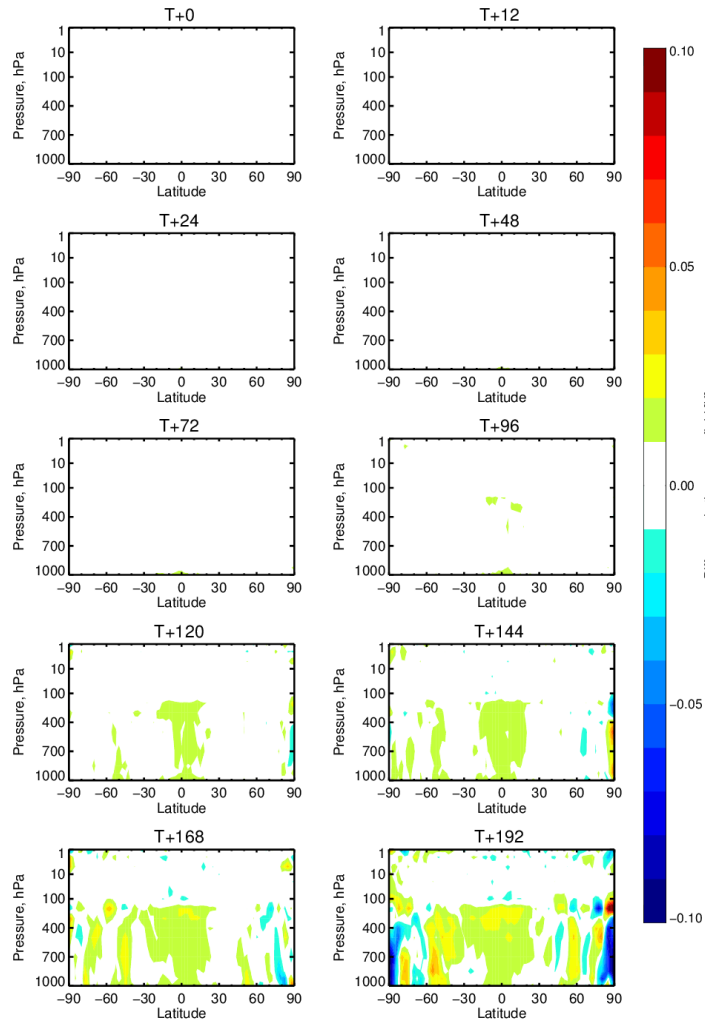
Wave effect on the upper ocean mixing is both passed to NEMO, but also to the atmospheric model.

The SST from NEMO is modified by the waves, there shouldn't be any need to also modify again (?)

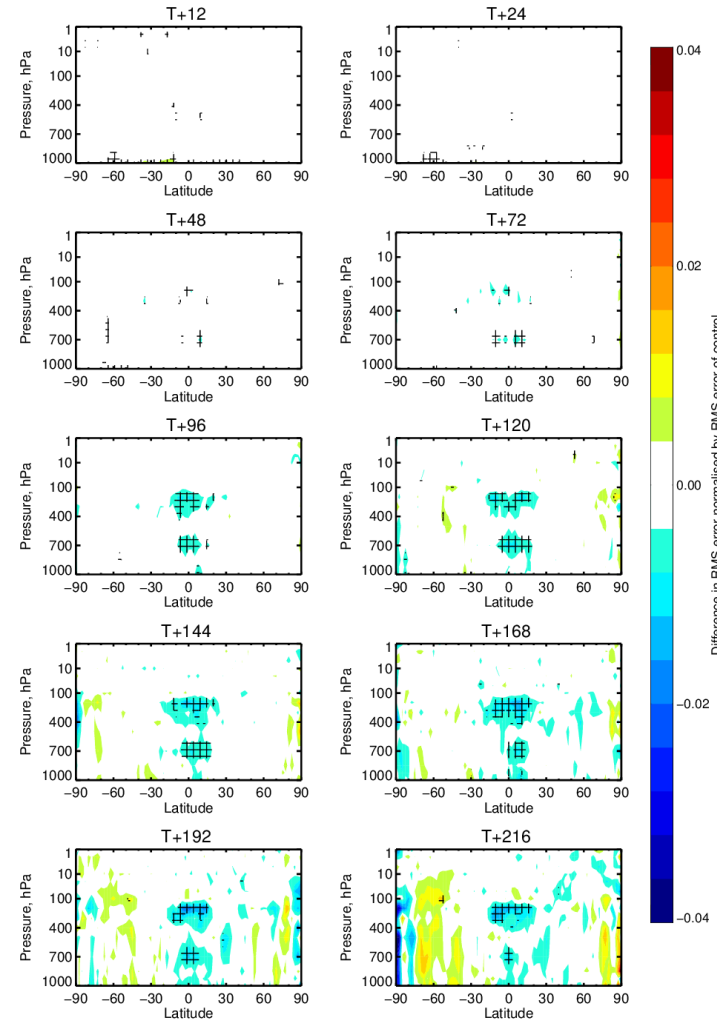
Sensitivity study: No Stokes to IFS

Normalised difference in RMSE for T

Difference in time-mean T (no Stokes from WAM to IFS-Coupled_43r1 (partial coupling))
11-Jun-2015 to 31-May-2016 from 356 to 356 analyses.



Change in error in T (no Stokes from WAM to IFS-Coupled_43r1 (partial coupling))
1-Jun-2015 to 30-May-2016 from 356 to 365 samples. Cross-hatching indicates 95% confidence. Verified against 0001.

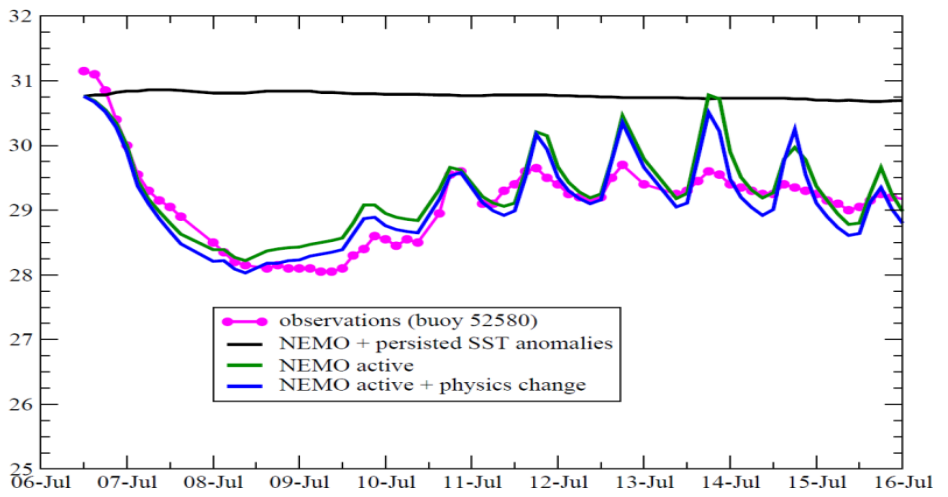
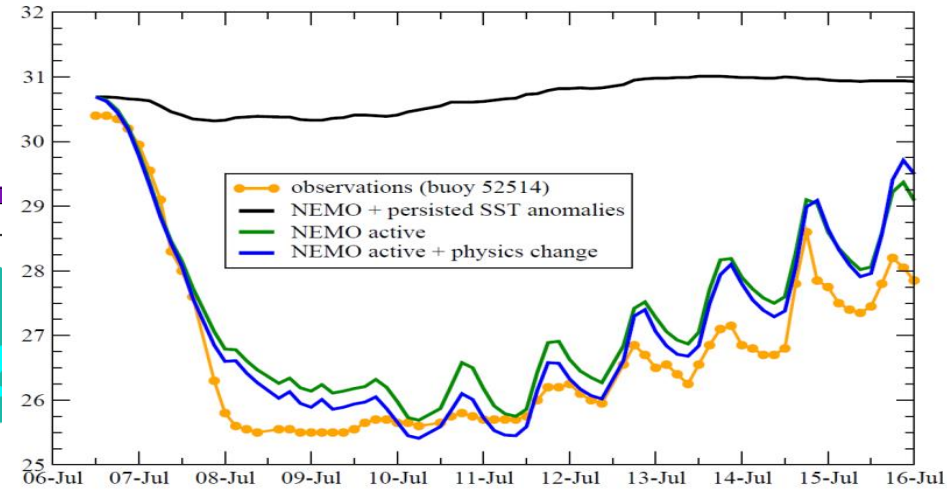
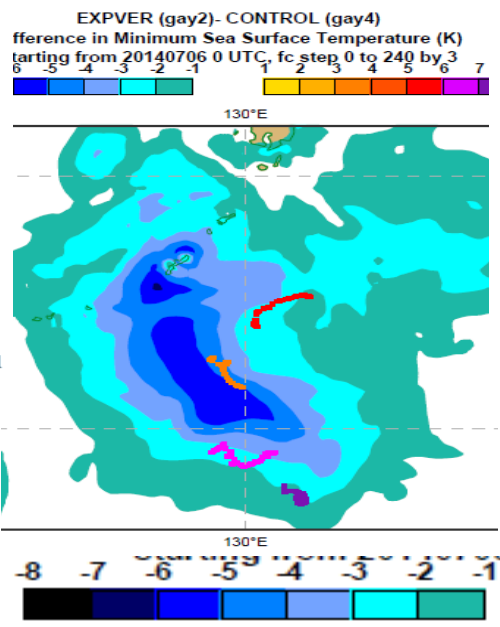
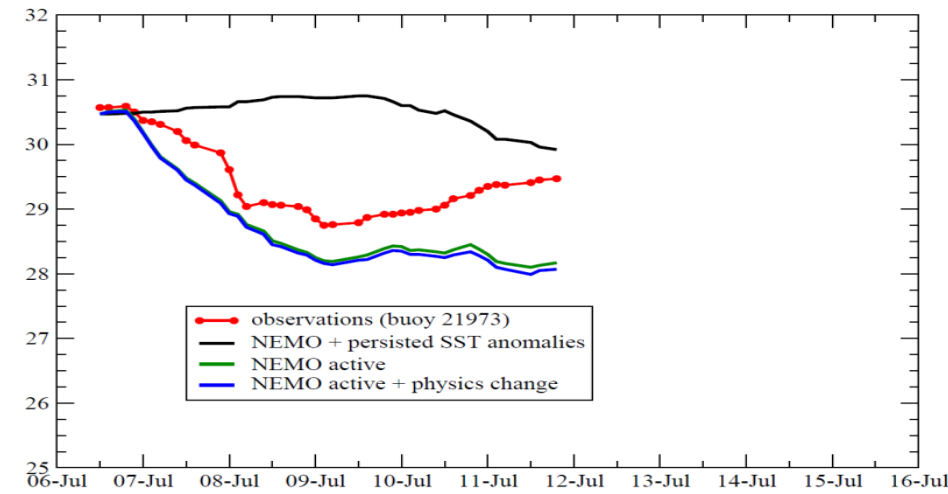


Mean forecast
difference in T

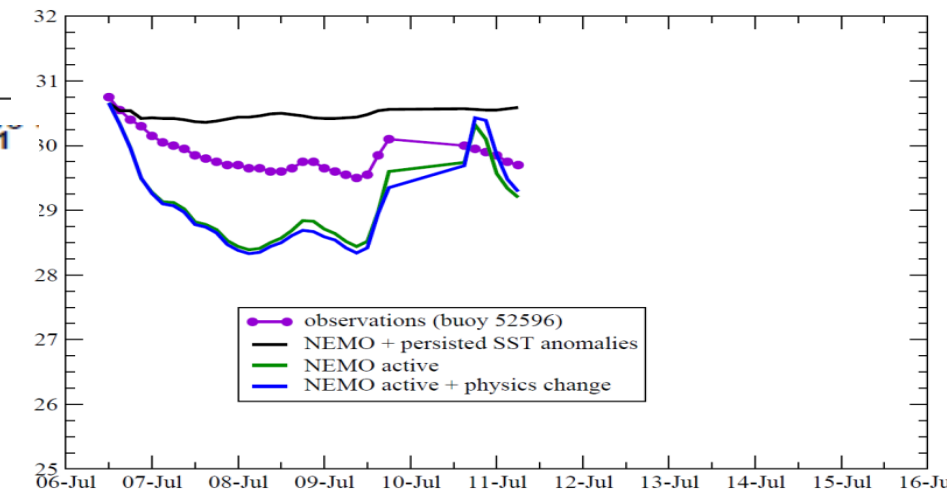
better



Impact of **Coupling** on tropical cyclone forecast

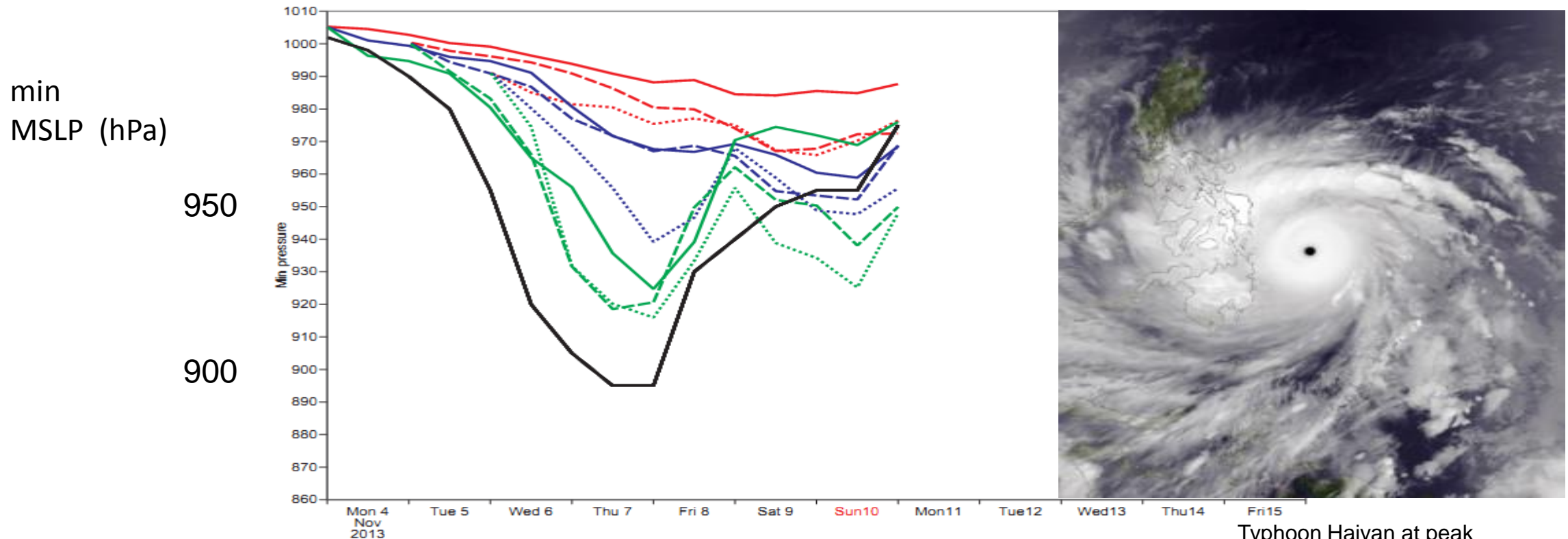


Data from drifting buoys



Impact of **Resolution** on tropical cyclone forecast

For instance Typhoon Haiyan: forecasts from 4th, 5th and 6th November 2013, 0 UTC all from operational analysis.

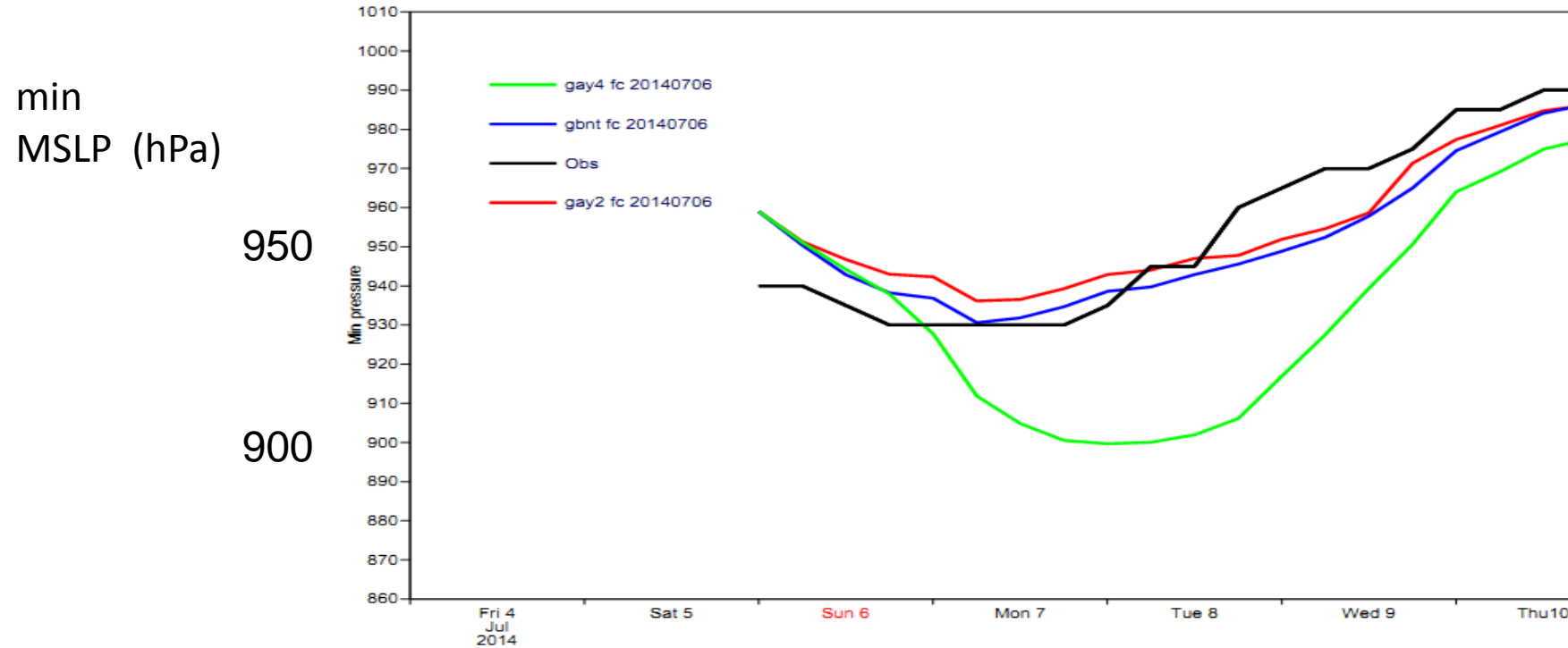


- Black:** estimated from observations
- Red:** old operational Ensemble resolution (**32 km**)
- Blue:** old operational HRES configuration (**16 km**)
- Green:** new HRES configuration (**10km**) (CY41R2)

Typhoon Haiyan at peak intensity on November 7, 2013

Impact of **Coupling** on tropical cyclone forecast

For instance Typhoon Neoguri: forecasts from 6 July 2014, 0 UTC



Black: estimated from observations

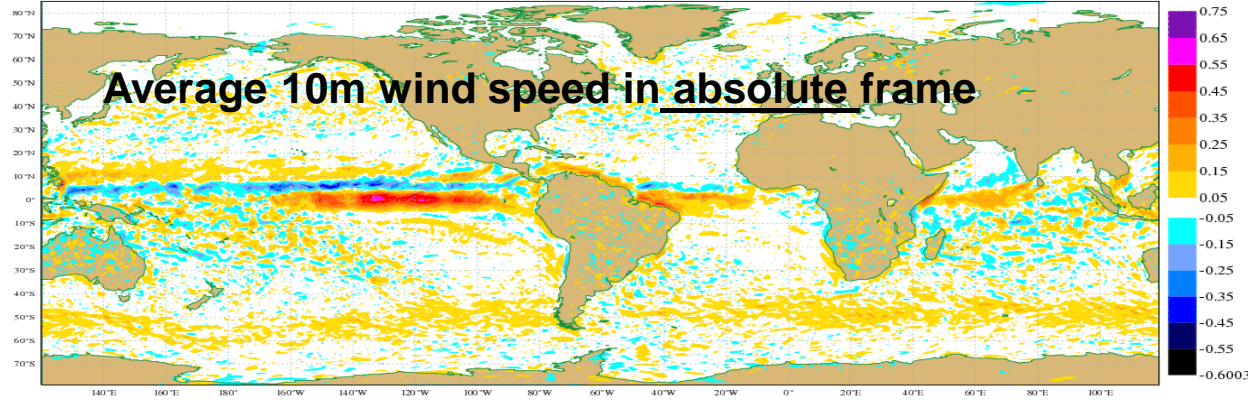
Green: old operational HRES configuration (**uncoupled**) (prescribed OSTIA SST) (16km)

Red: experimental: 16km **fully coupled** to NEMO (ORCA025_Z75)

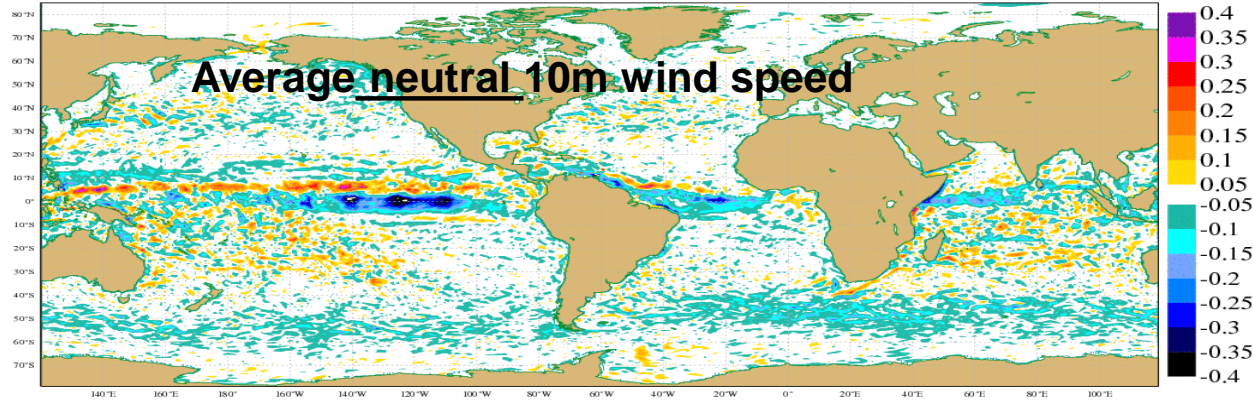
Blue: 16km coupled to NEMO + new physics

Surface current feedback on atmosphere

Mean analysis difference in 10m wind speed: rd feb8 dcda - rd febp dcda
from 20091221 to 20100228

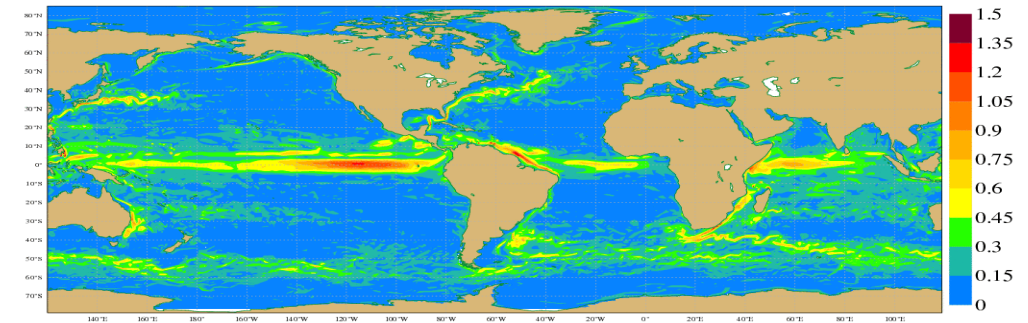


Mean neutral wind speed difference (feb8 dcwv - febp dcwv)
analysis from 20091221 0Z to 20100228 18Z



Currents – no currents

Mean analysis surface current speed: rd feb8 dcda
from 20091222 to 20100228



➤ **Absolute winds receive about 50% from ocean currents**